

**NASA CR-54905**  
**UNC-5148**



**ATHENA - A SYSTEM OF FORTRAN PROGRAMS FOR  
RADIATION TRANSPORT AND HEATING CALCULATIONS  
IN COMPLEX REACTOR GEOMETRIES**

**D. Spielberg**

**Prepared for**  
**NATIONAL AERONAUTICS AND SPACE ADMINISTRATION**  
**CONTRACT NAS 3-6200**  
**(UNC Project 2326)**

FACILITY FORM 608

**N66 27486**

(ACCESSION NUMBER)

**89**

(PAGES)

**CR-54905**

(NASA CR OR TMX OR AD NUMBER)

(THRU)

(CODE)

(CATEGORY)

#### NOTICE

This report was prepared as an account of Government sponsored work. Neither the United States, nor the National Aeronautics and Space Administration (NASA), nor any person acting on behalf of NASA:

- A.) Makes any warranty or representation, expressed or implied, with respect to the accuracy, completeness, or usefulness of the information contained in this report, or that the use of any information, apparatus, method, or process disclosed in this report may not infringe privately owned rights; or
- B.) Assumes any liabilities with respect to the use of, or for damages resulting from the use of any information, apparatus, method or process disclosed in this report.

As used above, "person acting on behalf of NASA" includes any employee or contractor of NASA, or employee of such contractor, to the extent that such employee or contractor of NASA, or employee of such contractor prepares, disseminates, or provides access to, any information pursuant to his employment or contract with NASA, or his employment with such contractor.

Requests for copies of this report should be referred to

**National Aeronautics and Space Administration**  
**Office of Scientific and Technical Information**  
**Attention: AFSS-A**  
**Washington, D.C. 20546**

NASA CR-54905  
UNC-5148

**FINAL REPORT**

**ATHENA - A SYSTEM OF FORTRAN PROGRAMS FOR  
RADIATION TRANSPORT AND HEATING CALCULATIONS  
IN COMPLEX REACTOR GEOMETRIES**

by

**D. Spielberg**

prepared for

**NATIONAL AERONAUTICS AND SPACE ADMINISTRATION**

**March 1966**

**Contract NAS 3-6200  
(UNC Project 2326)**

**Technical Management  
NASA Lewis Research Center  
Cleveland, Ohio  
Nuclear Systems Division  
Walter A. Paulson**

**UNITED NUCLEAR CORPORATION  
Research and Engineering Center  
Elmsford, New York**

## **ABSTRACT**

**ATHENA is a system of 11 coordinated programs, in FORTRAN IV for IBM-7094 and FORTRAN 63 for CDC-1604-A, for the solution of radiation transport and heating problems in complex three-dimensional geometries. Its geometry routines permit especially efficient representation of a reactor core possessing a vertical axis and hexagonal symmetry, such that any two adjacent 30-degree sectors are reflectionally symmetric with respect to the vertical plane separating them. The report describes the logic, functions, and interrelations of the component programs; in addition, operating instructions and details of the input and output for each program are given.**



## TABLE OF CONTENTS

<b>SUMMARY</b> . . . . .	<b>1</b>
<b>1. INTRODUCTION</b> . . . . .	<b>3</b>
<b>2. THE GENERATION OF DATA ROUTINE (GENDA)</b> . . . . .	<b>15</b>
2.1 Technical Description . . . . .	16
2.2 The Preparation of Input Data for GENDA . . . . .	22
2.3 GENDA Problem Input . . . . .	22
2.3.1 Title Card . . . . .	22
2.3.2 Problem Control Card . . . . .	23
2.3.3 Energy Input . . . . .	23
2.3.4 Weighting Function $\phi_c(E)$ (IPHI = 1). . . . .	23
2.3.5 Weighting Function $B_T(E_T)$ (IPHI = 1 and IDELP = 1). . . . .	24
2.4 GENDA Element Input. . . . .	24
2.4.1 Element Control Card . . . . .	24
2.4.2 Total Cross Section, $\sigma_T$ . . . . .	25
2.4.3 Elastic Scattering Cross Section, $\sigma_n$ . . . . .	26
2.4.4 Angular Distribution Data, $f_p$ . . . . .	26
2.4.5 Inelastic Scattering Data, Discrete, $\sigma_{nn',L}$ . . . . .	27
2.4.6 Excitation of the Continuum, $\sigma_{nn',c}$ (Includes $\sigma_{n,m}$ ) . . . . .	29
2.4.7 Cross Section for the Emission of Two Neutrons, $\sigma_{n,m}$ . . . . .	32
2.4.8 Other Cross Sections (Input Data as Described Above) . . . . .	33
2.5 GENDA Output . . . . .	33
<b>3. THE GENDA-PROCESSOR ROUTINE (GENPRO)</b> . . . . .	<b>34</b>
3.1 Technical Description. . . . .	35
3.2 GENPRO Input . . . . .	40
3.3 Format of the EDT . . . . .	40
<b>4. DESCRIPTION OF THE AVAILABLE PROBLEM     GEOMETRIES</b> . . . . .	<b>44</b>

4.1	360-Degree Geometry . . . . .	47
4.2	30-Degree Geometry . . . . .	49
5.	THE SOURCE-GENERATOR PROGRAM, VANGEN . . . . .	53
5.1	Spatial Selection . . . . .	54
5.1.1	360-Degree Geometry . . . . .	54
5.1.2	30-Degree Geometry. . . . .	60
5.2	Digression on Cylinder-Input for VANGEN and EZGEOM . . . . .	64
5.3	Energy Selection and Region Splitting . . . . .	68
5.3.1	Neutron Energy Selection - Energy Importance Sampling . . . . .	68
5.3.2	Gamma Energy Selection - Energy Importance Sampling. . . . .	72
5.4	Note on Energy-Bin Identification for Weight Assignments . . . . .	74
5.5	Transmission of Flux-at-a-Point Data to Common Dump Tape. . . . .	74
5.6	Description of the Input Data for VANGEN . . . . .	77
6.	THE INPUT SEQUENCER PROGRAM, MEZDA. . . . .	84
7.	THE ORGANIZATION OF THE GEOMETRY DATA (EZGEOM) . . . . .	86
7.1	Definitions and Notation . . . . .	86
7.2	Technical Description . . . . .	89
7.3	Description of the Input Data for EZGEOM . . . . .	96
7.4	EZGEOM Output . . . . .	99
8.	THE GEOMETRY TESTING ROUTINE, TESTG. . . . .	104
9.	THE DATA ORGANIZATION PROGRAM, DATORG . . . . .	107
9.1	Technical Description . . . . .	108
9.2	Description of the Input for DATORG . . . . .	110
10.	THE PARAMETER-INPUT PROGRAM, INPUTD . . . . .	114
10.1	Technical Description . . . . .	114
10.2	Description of the Input for INPUTD. . . . .	116
11.	THE MONTE CARLO TRACKING AND SCORING PROGRAM, ATHENA . . . . .	120
11.1	Importance Sampling . . . . .	120
11.2	Statistical Estimation . . . . .	121
11.3	The Main Tracking and Scoring Sequence . . . . .	121
11.4	The Data Retrieval and Interaction Routines . . . . .	128
11.4.1	ELAST Routine. . . . .	131
11.4.2	INELAS Routine . . . . .	134
11.4.3	The NIKI Routine . . . . .	134

11.4.4	The DIREC Routine . . . . .	136
11.5	The Flux-at-a-Point Routines . . . . .	137
11.5.1	Primary-Gamma Estimations . . . . .	137
11.5.2	Secondary-Gamma Estimations . . . . .	140
11.5.3	Tracking Phase . . . . .	147
11.5.4	Estimation Phase . . . . .	148
11.5.5	Adjoint Calculations . . . . .	151
11.6	Description of the ATHENA Input and Output . . . . .	151
11.6.1	Input . . . . .	151
11.6.2	ATHENA Output . . . . .	153
11.6.3	Error-Tracing Printout . . . . .	154
11.7	Operating Instructions for ATHENA, Restart	
	Option, Limits on Problem Size . . . . .	157
11.7.1	Restarting a Terminated ATHENA Problem . . . . .	158
11.7.2	Limitations on Problem Size . . . . .	159
12.	THE ATHENA-EDITING PROGRAM, STATC . . . . .	162
13.	THE SECONDARY-GAMMA SOURCE PROGRAM, GASP . . . . .	165
13.1	Real Interactions and Secondary Gammas . . . . .	165
13.2	Fake Interactions and Secondary Gammas . . . . .	166
13.3	Description of the GASP Input . . . . .	167
13.4	Limitation on GASP Problem Size . . . . .	168
14.	THE NEUTRON ABSORPTION TALLY PROGRAM, NATALE . . . . .	170
14.1	NATALE Options (1-4). . . . .	171
14.2	Description of the Input for NATALE . . . . .	171
14.3	NATALE Output . . . . .	173
14.4	Limitation on Problem Size . . . . .	173
15.	REFERENCES . . . . .	175

## TABLES

1.	Functions of the Data Retrieval (DR, N) Branches. . . . .	130
2.	Special Functions Referred to in the Flux-at-a-Point Flow Charts . . . . .	150
3.	Nuclide Identifiers (ATHENA Neutron Data Tapes) and Sizes of Neutron Data Arrays . . . . .	161

## FIGURES

1.	Macroscopic Flow Chart of ATHENA System . . . . .	7
2.	Representation of Reactor Core within a 360-Degree ATHENA Geometry . . . . .	45
3.	Horizontal Section ( $z = \text{Constant}$ ) Illustrating 30-Degree Geometry with Straddling and Sectorized Cylinders . . . . .	46
4.	Vertical Section through a Typical 360-Degree Configuration . . . . .	48
5.	Illustrating 360-Degree Type Reactor Geometry and Relationship between Implied Stages (here NSTAGE = 5) and Tracking Cylinders . . . . .	55
6.	Selection of Radius R within a Radial Bin . . . . .	59
7(a)	Fuel Stage with Four Fuel Cylinders . . . . .	62
7(b)	Top View . . . . .	62
7(c)	Illustrating Cobasal Macro Cylinders d, f, and g, Enclosing 1, 1, and 2 Micro Cylinders, Respectively . . . . .	62
7(d)	Macro Cylinders a, b, and c Enclose 4, 8, and 8 Micro Cylinders, Respectively (four cylinders/stage) . . . . .	63
7(e)	Macro Cylinders a, b, c, d, e Enclose 3, 1, 8, 2, and 6 Micro Cylinders, Respectively . . . . .	63
7(f)	Macro Cylinders a, b, and d Are Not Permitted . . . . .	63
8(a)	Subroutine BINLOC . . . . .	75
8(b)	Subroutine SEEK . . . . .	75
9.	Case where Regions 1 and $m$ Have a Face Lying in a Common Plane ( $x_{1,1}^{\alpha} = x_{1,m}^{\beta}$ ) with No Overlapping . . . . .	90
10.	Case where Regions 1 and $m$ Have a Face Lying in a Common Plane ( $x_{1,1}^{\alpha} = x_{1,m}^{\beta}$ ) . . . . .	91
11.	Illustration of the EZGEOM Decomposition of a Complex Surface . . . . .	94
12.	Cylinder Location Types . . . . .	115
13.	Illustrating Types of Events Occurring during Particle Tracking . . . . .	123
14.	Operation of Subroutine RSTRT (N,M) for Odd N; Tape Writing Operations on Logical M . . . . .	129
15.	Flux-at-a-Point - Tracking Phase and Estimation Phase . . . . .	141
16.	The ADJ Routine . . . . .	152

**ATHENA - A SYSTEM OF FORTRAN PROGRAMS FOR  
RADIATION TRANSPORT AND HEATING CALCULATIONS  
IN COMPLEX REACTOR GEOMETRIES**

By D. Spielberg  
United Nuclear Corporation

**SUMMARY**

**ATHENA** is a coordinated system of 11 computer programs for the Monte Carlo solution of neutron and gamma transport and gamma heating problems in complex three-dimensional geometries. The geometry routines, although fairly general, permit especially efficient representation of a reactor core possessing hexagonal symmetry. The entire system is available in FORTRAN IV for the IBM-7094 and FORTRAN 63 for the CDC-1604-A computers.

Deriving its basic structure from the UNC-SAM program, **ATHENA** embodies many generalizations and new features which greatly increase its usefulness.

These include:

1. A generalized neutron and gamma source-generator program which permits the automatic generation of a delayed-gamma spectrum following an arbitrary reactor operating history. This program permits the implementation of spatial and energy importance sampling for neutrons and/or gammas, and can represent an input specified spatial power pattern in great detail.

2. Several programs and routines to test the geometry input prior to the main Monte Carlo calculations.
3. Two basic geometries, denoted as 30-degree and 360-degree. The 30-degree representation permits highly detailed representation of a reactor core possessing 12-fold hexagonal symmetry.
4. Automatic generation and application of gamma-heating response functions, requiring no additional problem input.
5. New routines for computing gamma fluxes and heating at point detectors (in 360-degree geometry) as well as the corresponding volume-averaged quantities.
6. Several programs to interpret neutron-interaction records for the generation of secondary-gamma sources and the tallying of response-function-weighted neutron absorptions.

The report describes the logic, functions, and interrelations of the 11 component programs. In addition, operating instructions and details of the input and output for each program are given.

## 1. INTRODUCTION

The ATHENA\* system consists of a number of coordinated computer programs for the solution of radiation transport and heating problems in complex geometries, with special emphasis on the computation of gamma heating in reactor cores. The system recognizes two geometry types, designated as 360-degree and 30-degree.

The 360-degree option accepts a description of an essentially homogenized cylindrical reactor core, which can be subdivided radially and axially to permit variation of the composition within the core and to provide several in-core flux scoring regions.

The 30-degree option, designed to exploit the 12-fold symmetry of a hexagonal-lattice reactor core, permits a much closer approximation to the actual configuration of such a core. Within the space between vertical planes bounding a 30-degree sector of space, the configuration of individual fuel and poison rods may be defined, as well as that of the coaxial fuel cylinders within a fuel rod. In the Monte Carlo tracking of neutrons or gamma rays within this structure, particles striking the bounding planes are reflected optically, yielding, after many histories, the correct flux patterns in the representative 30-degree sector, without the need for describing explicitly (or tracking particles in) the other, congruent sectors of the reactor.

---

\*Attenuation, Tracking, and Heating for NASA.

The programs, written in FORTRAN 63 for the CDC-1604-A and FORTRAN IV for the IBM-7094 computers, are modeled after those in the UNC-SAM system;<sup>1</sup> both systems use essentially the same nuclear-data library, interaction routines, and source-tape formats. However, ATHENA embodies many generalizations and new features which greatly increase its usefulness. Among the new features of this system are:

1. A generalized and extremely versatile source-generator program, VANGEN;
2. New geometry-testing features, in program TESTG and in portions of the parameter-input routine, INPUTD;
3. The optional 30-degree-sector representation of a reactor;
4. Acceptability of "straddling" cylinders, each internal to several rectangular regions;
5. New high-efficiency cylinder and sphere tracking routines;
6. Sected-cylinder scoring;
7. Automatic generation of gamma-heating response functions;
8. New routines for primary- and secondary-gamma scoring at in-core and out-of-core point detectors;
9. Energy as well as spatial importance sampling in all pertinent programs;
10. A new GASP (secondary-gamma source production) program;
11. A neutron-absorption tally program, NATALE, for interpreting neutron interaction tapes.

The ATHENA system was developed over the period from December 1964 to January 1966. During this time the various component programs were debugged and tested exhaustively on a wide variety of problems. When the CDC-1604-A version of this system was debugged to a high confidence level, calculations were done on several full-scale gamma-heating problems, defined by Lewis Research



Center. Finally the IBM-7094 version was debugged on the Lewis Research Center computer.

Brief descriptions of the component programs of the ATHENA system are given below. A chart indicating the relationship of the programs, and the information flow, is given in Fig. 1.

### GENDA

The Generation of Data routine (GENDA) starts with a fundamental set of neutron or photon cross-section data tabulated as functions of energy. It allows for the basic tabulation of the total cross section, the scattering cross section, the Legendre expansion coefficients of the differential scattering cross section, and the inelastic scattering cross sections for both level and continuum scattering. These data are tabulated generally on differing energy meshes. GENDA processes the data to generate a set of cross-section data on a desired energy mesh. It includes the option of averaging with respect to a given weighting function, prescribed by input, if desired. Otherwise, it determines the desired cross-section set by either linear interpolation or by log-log interpolation. The spectrum of neutrons emitted in inelastic scattering, according to statistical theory, is used for heavier materials. For lighter materials, such as Li and Be, special treatments are available. The output of this routine is a tape which may be used as input to GENPRO.

### GENPRO

The GENDA Processor (GENPRO) routine uses the GENDA output to determine the tables of probabilities peculiar to a nuclide, required for a Monte Carlo code, at a prescribed energy mesh. For instance, the probability that a neutron suffers an elastic scattering is given by the ratio of elastic to total scattering at that energy. The probability of inelastic scattering from one energy to another is computed in this routine. At its conclusion, one has a library tape called the

Element Data Tape (EDT) on a given energy mesh to be used in subsequent processing.

The library Element Data Tapes available at present for the ATHENA system use 81-energy equal-lethargy meshes; the energy ranges are from 0.037137 ev to 18.017 Mev for neutrons, and from 10 kev to 10 Mev for photons.

For the generation of the Element Data Tapes, no problem-oriented input is needed. The functioning of all the later routines (VANGEN, EZGEOM, TESTG, DATORG, INPUTD, ATHENA, STATC, GASP, NATALE) will be dependent on problem-oriented data.

### VANGEN

The source input tapes for primary gamma or neutron ATHENA problems are generated by the VANGEN program.

This program writes, on separate output tapes, description of neutrons and/or photons whose spatial and energy distributions are consistent with detailed, input-specified reactor geometry, power pattern, and operating history. For either or both types of output particles, the a priori particle distributions may be modified according to importance-sampling parameters (region and energy weights) to be used in the ATHENA problem.

The spatial selection of source points follows the input power pattern as specified for either of the two general geometries available in this system; these are designated as 30° or 360°, pertaining to the mode of representation of the reactor. In the 30° geometry, the power pattern may be very detailed; the input allows arbitrary a priori source strengths for various fuel elements, and for the coaxial fuel cylinders within a fuel element. In addition, an arbitrary axial power pattern is permitted. In the 360° geometry, particles are selected in accordance with input-specified axial and radial power distributions; these are assumed to be separable.

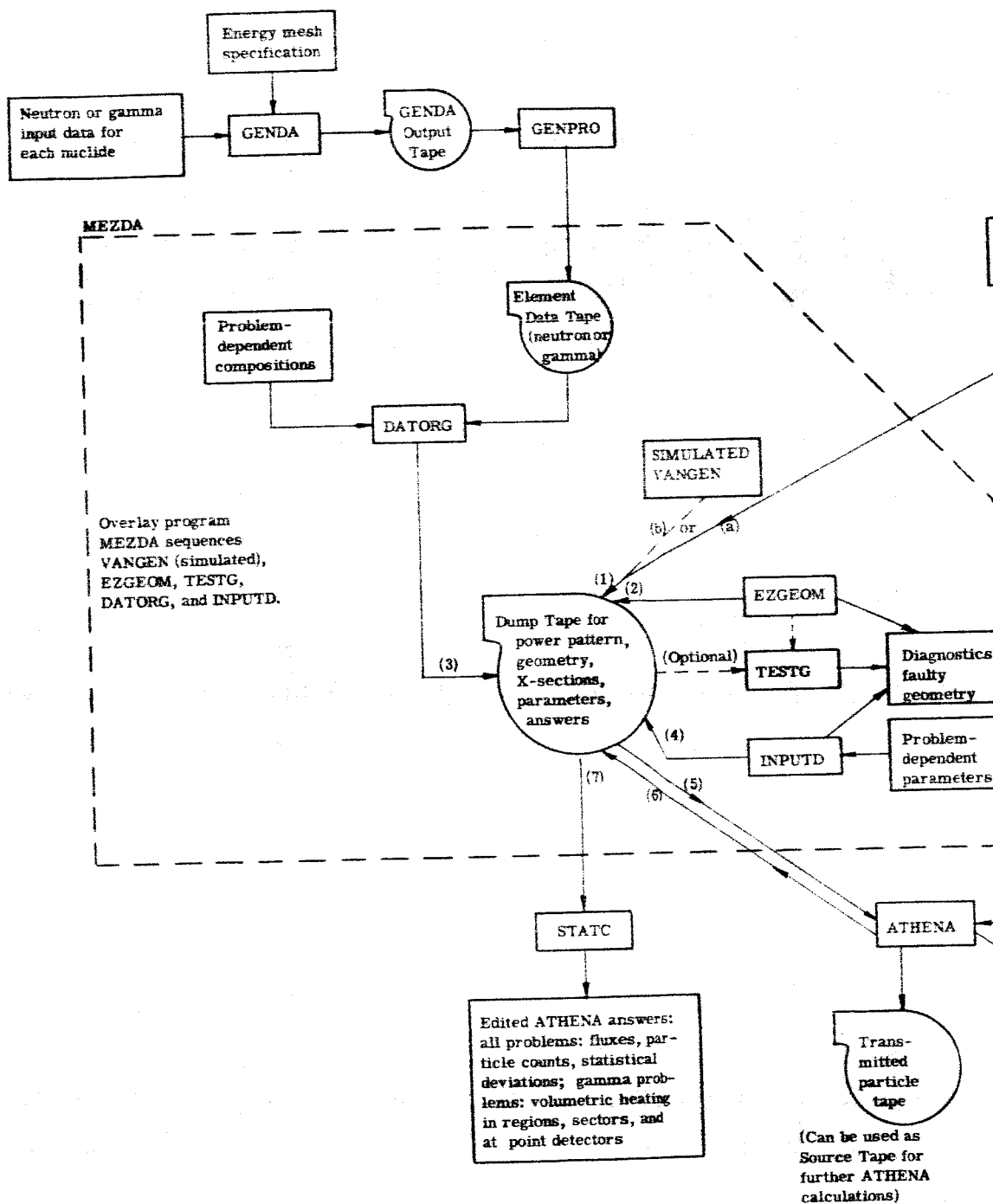
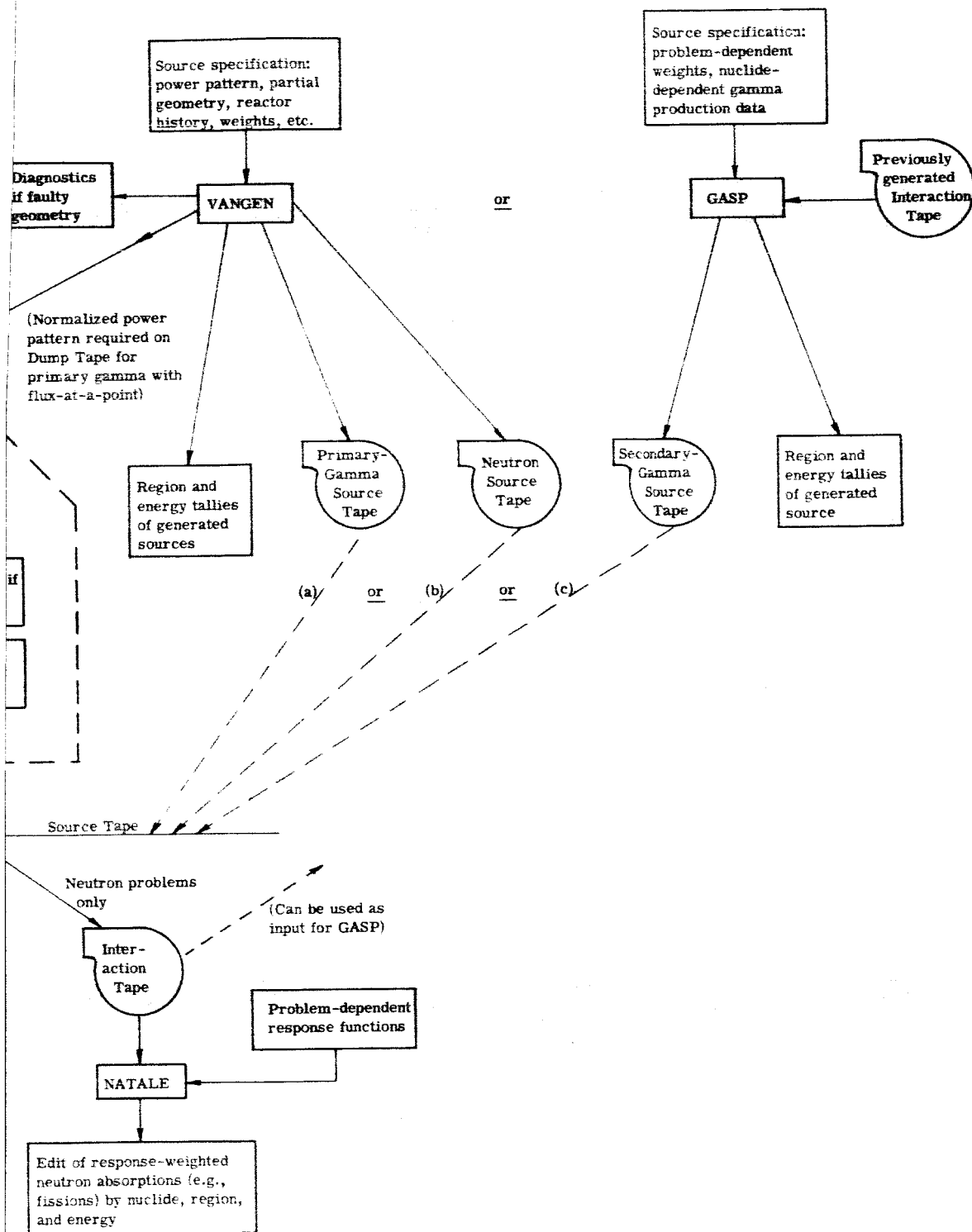


Fig. 1 — Macroscopic



Flow Chart of ATHENA System

For both 30° and 360° problems, the spatial resolution in the source generation may be finer than that of the tracking geometry; given the pertinent data for the tracking geometry, VANGEN assigns the proper region numbers to the selected source locations.

The angular distribution of all generated particles is isotropic.

The energy distribution may be monoenergetic, fission-spectrum, or a combination of up to 15 discrete-energy sources, the latter with arbitrary relative intensities, or with intensities (computed by VANGEN, from internal or supplied delayed-gamma data) corresponding to the post-fission gamma spectrum following an arbitrary reactor operating history. If energy importance sampling is to be used in the main tracking problem (ATHENA), the energy weights (piecewise constant, in specified energy bins) are used to modify the a priori spectrum; energies are then selected from the modified spectrum.

Spatial importance sampling is reflected in VANGEN, via splitting and Russian roulette on the source, based on the region-dependent weights to be used in the ATHENA problem.

The output of VANGEN is: a neutron and/or a gamma source tape; listings of all or a part of the generated sources; tables describing the normalized power pattern, transmitted (for flux-at-a-point) to the interprogram communications (dump) tape; and various optional printouts, including the results of the delayed-gamma integrations and of internal cylinder-scanning and partial geometry verification. VANGEN also prints out the integral of the input reactor operating history, which, together with the delayed-gamma integrals, provides sufficient information for the normalizations of the primary-gamma and secondary-gamma ATHENA results.

## MEZDA

This is an overlay program which can take input for all of the following programs and execute them in sequence: VANGEN (simulated); EZGEOM; TESTG; DATORG; INPUTD. The result of the operation of the final program, INPUTD, is a dump tape containing all the data needed by ATHENA, except for a particle source tape. The format of the dump tape calls for certain output tables from VANGEN, which, however, are actually needed only for primary-gamma flux-at-a-point. The dump tape for such an ATHENA problem, therefore, must be in communication with the real VANGEN program during the primary-gamma source-tape generation (Fig. 1). For all other ATHENA problems, these tables are irrelevant, and dummy tables can be set up by using a VANGEN program-calling card as the first item in the MEZDA input.

## EZGEOM

This program accepts a simplified geometric description of the physical system, as provided by the problem originator, and produces the complex set of data required by the transport program ATHENA.

The problem originator must decompose the space within a large rectangular volume into a set of boxes known as "ordinary regions." Inside these boxes may be placed various "nonordinary regions" consisting of spheres, cylinders, wedges, or other boxes. Nonordinary regions may enclose other nonordinary regions; in general, each nonordinary region must be completely contained in a single region (except for "straddling" cylinders, which may occupy parts of one, two, or four boxes), and must not touch any other region (exception: co-basal, coaxial cylinder-clusters are permitted).

In addition to arranging the geometry data into the formats needed for the tracking routines, EZGEOM checks the consistency of the ordinary-region input.

EZGEOM prints out a synopsis of its calculations, and communicates the processed geometry data to the common dump tape (see Fig. 1).

### TESTG

This routine takes the output of EZGEOM (assuming that no geometry input errors have been found by that program) and subjects the configuration to further testing. A subset of all the regions in the problem is considered, namely, the innermost regions, i.e., those which have no internal regions. For each such pair of regions (i,j), TESTG selects points at random within the volume of i and within j, computes the length and direction cosines of the vector connecting these points, and attempts to track from one to the other. Failure to end up at the required distance and/or final region leads to a diagnostic trace of the trajectory.

A complete set of trackings between points in each pair of innermost regions is called a pass through the geometry. Use of TESTG is optional. The desired numbers of complete passes to be executed (barring the discovery of an excessive number of errors) is specified in the input.

### DATORG

This routine combines the nuclide-dependent cross sections, as read from an Element Data Tape, according to the nuclide concentrations specified for each material composition needed in the tracking problem. For each composition, and at each energy in the mesh previously used in GENDA and GENPRO, DATORG computes and tabulates the total macroscopic cross section, and gamma-heat-ing response function (if a gamma problem); these are transmitted to the common dump tape, along with the nuclide- and energy-dependent microscopic scattering and absorption cross sections, and equal-probability-bin tables describing in-elastic and anisotropic elastic scattering (neutron problems).

## INPUTD

From punched-card input, this routine transmits to the dump tape a variety of problem parameters which complete the definition of the ATHENA problem to be run. These quantities include: geometry type ( $30^\circ$  or  $360^\circ$ ); region and energy weights; energy bins and regions for flux scoring; location of flux-at-a-point detectors; and composition identifiers for regions.

## ATHENA

This is the main tracking and scoring program in the system. Input to this program are the processed geometry, cross-section, power-pattern, and problem parameters as read from the dump tape, plus a neutron or gamma source tape produced by VANGEN or GASP.

ATHENA reads in source particles in sets of 100 from the source tape and processes each of these particles through its migrations and interactions until absorption, transmission, death by energy or spatial Russian roulette, or degradation below an energy cutoff occurs. (In neutron problems with a thermal-group option, particles below the cutoff energy are returned to a thermal energy, and tracking continues.) As the particle travels, a variety of information is recorded, including:

1. Fluxes in specified energy bins and regions, along with their standard deviations, in both gamma and neutron problems;
2. In gamma problems, total and volumetric heat deposition, and standard deviation thereof, for each region, and for equiangular sectors of specified cylinders;
3. A neutron-interaction tape for future calculation of secondary-gamma sources (via GASP) or other response-function calculations (via NATALE);
4. A transmitted-particle tape for future processing;



5. Counts of particle births, deaths, absorptions, and degradations by region, and of births and deaths by energy.

ATHENA permits the use of spatial and energy importance sampling through the specification of region weights (energy-independent) and energy weights, piecewise constant over arbitrary energy bins (one energy-weight mesh, region-independent). When a particle crosses a boundary between tracking regions, splitting or Russian roulette is done, based on the ratio of the pertinent region weights. Similar operations are performed after each collision, based on the energy weights before and after the collision. Heating and track-length scores are all computed taking into account the energy weight of the particle. In the final edit, answers pertinent to a given region are multiplied by the region weight.

Finally, there is the option of specifying a number of point detectors, at which primary-gamma and secondary-gamma fluxes and heating can be computed.

ATHENA sends back its answers to the common dump tape.

### STATC

This is an edit routine which reads back the ATHENA answers from the dump tape, and does the final computations of volumes, interpretations of fluxes, heating and statistical deviations, etc. All answers are printed out; fluxes and heating are expressed per primary-gamma or neutron history.

### GASP

This routine accepts as input the interaction tape produced in a neutron ATHENA calculation, plus nuclide-dependent data giving (as functions of neutron and secondary-gamma energy) probable numbers of secondary gammas produced per absorption and per inelastic scattering, plus problem-dependent neutron and gamma region and energy weights. GASP converts into appropriate entries on an output secondary-gamma source tape both the records of ordinary neutron

interactions, and those of so-called "fake" interactions, generated during a neutron problem for which secondary-gamma flux-at-a-point answers will be required.

### NATALE

This is another routine for editing a neutron interaction tape. The real absorptions recorded thereon can be counted and printed out by region, nuclide, and energy; weighting of absorptions by nuclide- and energy-dependent input response functions is also available. NATALE requires as input, and includes in the calculations, the neutron region and energy weights used in the ATHENA problem.

### Acknowledgments

The greater part of the programming of the UNC-SAM and ATHENA systems was done by Burton Eisenman and Walter Guber. The author is indebted to Malvin H. Kalos for much useful counsel, particularly regarding the routines for flux-at-a-point, importance sampling, and tracking in the 30-degree geometry.

The analysis for many of the specific geometry routines was done by Jeremiah Certainé and Henry Brysk.

Finally, the author acknowledges with thanks the considerable contributions of Walter A. Paulson, of the Nuclear Systems Division at NASA, toward the production of a version of ATHENA operable on the Lewis Operating System.

## **2. THE GENERATION OF DATA ROUTINE (GENDA)\***

Given experimental or theoretical microscopic cross-section data at arbitrary energies in a given range for elements of interest, it is often desirable to process these data into cross-section sets at specified energy point values.

The GENDA routine has been programmed in FORTRAN to accomplish this in the following manner:

1. The raw cross-section data are tabulated according to an established format which can be easily modified and updated. The point values of the input cross-section data are selected to give the best detailed representation of the cross-section variation with energy for the interpolation technique used.
2. For a given element and type of cross section, intermediate point values are obtained from these tables, using either linear or log-log interpolation techniques as directed by the input.
3. Weighted point values of cross sections in a specified energy mesh may be evaluated using a given weighting function. This input function is tabulated in a similar manner as the raw cross-section data and intermediate point values are obtained by interpolation.

---

\*This chapter is taken, with minor changes and additions, from Reference 1.

## 2.1 TECHNICAL DESCRIPTION

Let  $\sigma(E)$  denote generically a typical cross section at energy  $E$ . This might stand for the total cross section, the scattering cross section, the Legendre expansion coefficient ( $f_p$ ) of the differential scattering cross section, the inelastic scattering cross section for level or continuum scattering, etc. (the cross-section types included appear in the input instructions). Let  $\sigma_0(E)$  be the continuous portion of the typical cross section  $\sigma(E)$ . On occasion, where many resonances exist, a set of resonance parameters  $A_\nu(E_\nu)$  may be given for each generic cross-section type such that for the purpose of suitable averages,  $\sigma(E)$  is representable as:

$$\sigma(E) = \sigma_0(E) + \sum_{\nu=1}^{\nu_{\max}} A_\nu(E_\nu) \delta(E-E_\nu) \quad (1)$$

where  $\delta(E-E_\nu)$  is the Dirac delta function of argument  $E-E_\nu$ . This characterization of  $\sigma(E)$  is allowed only when the cross-section averaging routine (CAR) is used; otherwise, an infinitely narrow resonance peak is not physically reasonable, nor computationally manageable.

Let  $E_j^G$ ,  $j = 1, 2, \dots, J$  be a set of final energies in decreasing order at which the output data are to be tabulated. These may be tabulated either as input or computed given the highest energy,  $E_{\max}$ , the number of final energies,  $J$ , and the constant lethargy spacing,  $h$ , such that

$$h = \frac{1}{J-1} \ln \frac{E_{\max}}{E_J}, \quad (2)$$

where  $E_J$  is the lowest energy.

Let  $\phi(E)$  be an arbitrary weighting function supplied by an input table

$$\phi(E) = \phi_0(E) + \sum_{\tau=1}^{\tau_{\max}} B_\tau(E_\tau) \delta(E-E_\tau). \quad (3)$$

(The  $E_\tau$  must not have an energy value equal to any of the  $E_\nu$ .) Let  $\sigma_0(E)$  and  $\phi_0(E)$  be given as functions of energy such that between tabulated values these functions are either linear or exponential.

The GENDA code then provides for the following mutually exclusive options.

1. Find  $\sigma(E_j^G)$ ;  $j = 1, \dots, J_{\max}$  by linear interpolation
2. Find  $\sigma(E_j^G)$ ;  $j = 1, \dots, J_{\max}$  by log-log interpolation
3. Find  $\sigma(E_j^G)$ ;  $j = 2, \dots, J-1$  by

$$\sigma(E_j^G) = \frac{\int_{(E_j^G + E_{j+1}^G)/2}^{(E_j^G + E_{j-1}^G)/2} \sigma_0(E) \phi_0(E) dE + \sum A_\nu(E_\nu) \phi_0(E_\nu) + \sum B_\tau(E_\tau) \sigma_0(E_\tau)}{\int_{(E_j^G + E_{j+1}^G)/2}^{(E_j^G + E_{j-1}^G)/2} \phi_0(E) dE + \sum B_\tau(E_\tau)} \quad (4)$$

where the sums include those values of  $E_\nu$  and  $E_\tau$  falling within the integration interval.

For the purpose of CAR, the energy mesh used is made up of the set of all energies at which  $\sigma$  and  $\phi$  are given, plus the end points of the interval of integration. In the present program, the integration is carried out numerically, using the trapezoidal rule. Consequently, the richer the input mesh, the better the results. It should be noted that exact integration could be performed at the price of some modifications of the program.

The cross section at thermal energy may be included in GENDA. In that case, the lowest entry in the final energy mesh tabulation is the thermal energy.

In addition, GENDA can compute the synthesized differential scattering cross section

$$\sigma(E_j^G, \omega) = \frac{\sigma_n(E_j^G)}{4\pi} \sum_{l=0}^L (2l+1) f_l(E_j^G) P_l(\omega) \quad \text{for } \omega = -1 \quad (0.01) \quad 1 \quad (5)$$

where  $\sigma_n$  = the elastic scattering cross section

$P_l(\omega)$  = the Legendre polynomial of order  $l$  evaluated at the angle cosine  $\omega$

$f_l(E_j^G)$  = the Legendre expansion coefficient.

All negative values for  $\sigma(E_j^G, \omega)$  are printed out. An edit on the coarser mesh -1 (0.1) 1 is also available.

For the treatment of inelastic scattering, it is necessary to describe in greater detail the kernel  $g(E_j^G, E')$  which represents the probability that, following an inelastic scattering, a neutron at energy  $E_j^G$  will scatter into energy  $E'$ . The spacing of the discrete energy levels in the nucleus is known to decrease with increasing energy. At high energies, the levels are so close that they may be considered as a continuum of energy levels. Let  $E_{BC}$  be the energy at which the discrete level spectrum can be considered to pass over into a continuous spectrum. Then, for incident neutron energies less than or equal to  $E_{BC}$ , only discrete level inelastic scattering occurs. The kernel  $g(E_j^G, E')$  is representable as a sum of delta functions

$$g(E_j^G, E') = g_D(E_j^G, E') = \sum_{\text{all } \nu} a_\nu(E_j^G) \delta[E_j^G - (E' + E^\nu)] \quad E^\nu < E_j^G \leq E_{BC} \quad (6)$$

where  $\nu$  = the  $\nu^{\text{th}}$  energy level

$E^\nu$  = the energy of the  $\nu^{\text{th}}$  discrete level

$a_\nu(E_j^G)$  = the probability that a neutron at energy  $E_j^G$  will scatter into energy

$$E' = E_j^G - E^\nu.$$

From the definition of  $g_D$  it follows that

$$\int_0^{E_j^G} g_D(E_j^G, E') dE' = \sum_{\text{all } \nu} a_\nu(E_j^G) = 1 \quad (7)$$

for  $E_j^G \geq E'$ . If  $E_j^G < E'$ , the inelastic scattering cross section is zero and  $g_D(E_j^G, E')$  is undefined.

If the incident neutron energy is greater than  $E_{BC}$ , two cases must be considered.

1. If  $E_j^G$  is sufficiently large that the probability of discrete level scattering is zero, then only continuum level scattering occurs. Let  $E_{BD}$  be the energy above which all  $a_\nu$  are zero, then the kernel  $g(E_j^G, E')$  can be represented by a continuous probability distribution function,  $g_c(E_j^G, E')$  which satisfies the following condition.

$$\int_0^{E_j^G} g_c(E_j^G, E') dE' = 1. \quad (8)$$

2. If  $E_{BC} < E_j^G \leq E_{BD}$ , then both continuum and discrete level scattering occur. Both the continuum and discrete kernels,  $g_c$  and  $a_\nu$ 's are computed, satisfying the normalization given by Eqs. 7 and 8. Hence, the inelastic scattering kernel is

$$g(E_j^G, E') = \frac{\sigma_{nn',c}(E_j^G) g_c(E_j^G, E') + \sigma_{nn',D}(E_j^G) g_D(E_j^G, E')}{\sigma_{nn',c}(E_j^G) + \sigma_{nn',D}(E_j^G)} \quad (9)$$

where  $\sigma_{nn',c}$  and  $\sigma_{nn',D}$  are the cross sections for the excitation of the continuum and of the discrete levels, respectively.

The continuum energy spectrum of neutrons emitted per inelastic scattering at energy  $E$  is obtained using a routine called ASPIC which computes the probabili-

ty  $g(E, E')$  according to a statistical theory.\*

$$g^{(i)}(E, E') = \frac{E' \sigma_c^{(i)}(E') \rho^{(i)}(E-E')}{\int_0^E E' \sigma_c^{(i)}(E') \rho^{(i)}(E-E') dE'} \quad (10)$$

where  $\sigma_c^{(i)}(E)$  is the cross section for compound nucleus formation and  $\rho^{(i)}(E)$  is the level density in the nucleus  $i$  ( $i = 1$  refers to the target nucleus).

The following form is assumed for the level density:

$$\begin{aligned} \rho^{(i)}(E) &= 0 & \text{for } E < E_1^{(i)} \\ \rho^{(i)}(E) &= \rho_0 & \text{for } E_1^{(i)} < E < E_0^{(i)} \\ \rho^{(i)}(E) &= \rho_0 \exp [2\sqrt{a^{(i)}E} - 2\sqrt{a^{(i)}E_0^{(i)}}] & \text{for } E > E_0^{(i)}. \end{aligned} \quad (11)$$

For the treatment of  $(n, 2n)$  reactions, it is assumed that the first neutron has the distribution (Eq. 10) where  $i = 1$ . After the emission of the first neutron, the target nucleus is left at excited states  $E^+$  with a population density:

$$R(E, E^+) = g^{(i)}(E, E-E^+). \quad (12)$$

$R(E^+)$  has a maximum at  $E^+ = E - \sqrt{E/a^{(1)}}$ ; [ $\sqrt{E/a^{(1)}}$  is the nuclear temperature]. We make the simplifying assumption that all secondary neutrons are emitted from the states  $E^+ = E - \sqrt{E/a^{(1)}}$ . Applying statistical theory, the spectrum of secondary neutrons per  $(n, 2n)$  collision is given by

$$g^{(2)}[E - \sqrt{E/a^{(1)}} - E_t, E'] \quad (13)$$

where  $E_t$  is the threshold for the  $(n, 2n)$  reaction,  $g^{(2)}$  is given by Eq. 10, and the superscript (2) refers to the nucleus left after the  $(n, 2n)$  reaction on the target.

---

\*See terminology and definitions at the end of this section.



In order to account for the neutrons leading to the ground state of this final nucleus, one should set  $E_1^{(2)} \approx 0$  [choose  $E_1^{(2)} = 0.01$ ]. Hence, the composite spectrum of neutrons emitted per  $(nn'; n, 2n)$  reaction is given by

$$g(E, E') = g^{(1)}(E, E') + \frac{\sigma_{n, n}(E)}{\sigma_{nn', c}(E)} g^{(2)}(E, E') \quad (14)$$

where  $\sigma_{n, n}(E)$  is included into  $\sigma_{nn', c}(E)$  in GENDA.

In the event that the core storage requires more than 18,000 words for  $g(E, E')$ , the code determines a lowest value for  $E'$  (which will be higher than the lowest energy of the problem) so that  $g(E, E')$  fits in storage. The portion of  $g(E, E')$  neglected is generally negligible.

The above description of the calculation of the probability  $g(E, E')$  is not adequate for light nuclei. Special treatments for lithium and beryllium are available at the user's option.

The GENDA lithium option will compute  $g(E, E')$  by means of a built-in routine based on the assumptions of a continuous spectrum for  $E_j^G > 3.95$  Mev, and inelastic scattering for  $E < 3.95$  Mev arising only from the excitation of the 0.477-Mev level.<sup>2</sup> There is also a built-in routine<sup>3,4,5</sup> in GENDA for computing the  $g(E, E')$  of beryllium. Details of these special Li and Be routines can be found in Reference 1, pp. 15 through 19.

### Terminology for Section 2.1

$E_t$	the threshold of the $(n, 2n)$ reaction
$a^{(1)}, E_1^{(1)}$	level density parameters for the target nucleus
$a^{(2)}, E_1^{(2)}$	level density parameters for the nucleus
$E_1^{(1)}$	energy at which the continuum starts
$E_1^{(2)}$	should be set equal to 0.01

$\sigma_c^{(1)}$  cross section for compound nucleus formation of the target nucleus  
 $\sigma_c^{(2)}$  cross section for compound nucleus left over after the (n,2n) reaction.

## 2.2 THE PREPARATION OF INPUT DATA FOR GENDA

Unless otherwise stated, all data for this code are in standard FORTRAN E format. The data are punched in six fields of 10 columns each (i.e., 6E10.4). For the general data decks, it is in the order of energy followed by its cross section; energies are in Mev, entered in decreasing order,  $E_i > E_{i+1}$ .

### Example

Column

1-10	$E_1$
11-20	$\sigma(E_1)$
21-30	$E_2$
31-40	$\sigma(E_2)$
41-50	$E_3$
51-60	$\sigma(E_3)$

10	20	30	40	50	60
$E_1$	$\sigma(E_1)$	$E_2$	$\sigma(E_2)$	$E_3$	$\sigma(E_3)$

All energies must span the range from  $E_{\max}$  to  $E_{J\max}^G$  (the minimum energy) with the exception of the discrete inelastic scattering cross section ( $\sigma_{nn',L}$ ).

The data control information is in integer format, with the exception of the true mass number which is in F format.

## 2.3 GENDA PROBLEM INPUT

### 2.3.1 Title Card

Any 80 Hollerith characters (e.g., user's name, element name, date, etc.)

### 2.3.2 Problem Control Card

Column	Item
1-3	Number of elements (NEL)
4-7	Number of final energies (JMAX) ( $\leq 450$ )
8	IEN = 0 - compute final energy table with fixed lethargy IEN = 1 - final energy table is input
9	IPHI = 0 - weighting function $\phi_c(E)$ is not present IPHI = 1 - weighting function $\phi_c(E)$ is present
10	IDELP = 0 - table of $B_T(E_T)$ is not present IDELP = 1 - table of $B_T(E_T)$ is present

#### Note:

IDELP must = 0 if IPHI = 0.

### 2.3.3 Energy Input

For IEN = 0

Column	Item	
1-10	$E_{\max}$ - maximum energy (Mev)	Floating
11-20	H, fixed lethargy step	Floating
	$\frac{1}{JMAX - 1} \ln \frac{E_{\max}}{E_{J\max}}$	

For IEN = 1

Energy table  $E_j^G$ ,  $j = 1, 2, \dots, JMAX$ ;  $E_j^G > E_{j+1}^G$

Format (6E10.4)

### 2.3.4 Weighting Function $\phi_c(E)$ (IPHI = 1)

#### Identification Card

Column	Item
1-6	Any six Hollerith characters for identification
8	= 1 - linear = 2 - linear on log-log paper
9-12	Number of $\phi_c(E)$ tabulated ( $\leq 300$ )

## $E^\phi, \phi_c(E^\phi)$ Data Deck

### Note:

The  $\phi_c(E^\phi)$  must be included if CAR-type group averaging is to be used.

## 2.3.5 Weighting Function $B_T(E_T)$ (IPHI = 1 and IDELP = 1)

### Identification Card

Column	Item
1-6	Any six Hollerith characters
7-8	Number of $B_T$ tabulated ( $\leq 99$ entries)

## $E_T, B_T(E_T)$ Data Deck

## 2.4 GENDA ELEMENT INPUT

### 2.4.1 Element Control Card

Column	Item
1-6	Element name, Hollerith format
7-13	True mass (F format)
14-17	Arbitrary problem label (integer)
18	Blank
19-23	Nuclide identifier ZZABC, where ZZ = atomic number, and ABC are arbitrary digits (see DATORG, Chapter 9)
ZZABC	ZZ = atomic number
19 23	ABC = arbitrary digits to complete nuclide identification ABC = 000 if natural element
24-50	Control for the following: Data = 1 - data are present Data = 0 - data are not present
24	Blank
25	Total cross section, $\sigma_T$
26	Elastic scattering cross section, $\sigma_n$
27, 28	The order of expansion ( $T^N \leq 20$ , $f_p$ , $p = 1, 2, \dots, T^N$ ) if the elastic scattering is anisotropic
29	Excitation of discrete levels, $\sigma_{nn',L}$
30, 31	Not used; reserved for future application
32	Excitation of the continuum, $\sigma_{nn',c}$ (includes $\sigma_{n,2n}$ )
33, 34	Not used; reserved for future application

Column	Item
35	Cross section for the emission of two neutrons, $\sigma_{n,2n}$
36	Fission cross section, $\sigma_f$
37	Absorption cross section, $\sigma_{abs}$
38	Transport cross section, $\sigma_{tr}$
39	Cross section for the emission of an $\alpha$ particle, $\sigma_\alpha$
40	Cross section for the emission of a proton, $\sigma_p$
41	Cross section for the emission of $H_2$ , $\sigma_{H_2}$
42	Cross section for the emission of $H_3$ , $\sigma_{H_3}$
43	Radiative capture cross section, $\sigma_{n,\gamma}$
44-48	Not used; reserved for future applications
49	Edit synthesized $f_p$ data
50	Thermal data
51	Enter 1, 2, or 3 for following output. 1: punch out, in standard GENDA (E, $\sigma$ ) (6E10.4) format, $\sigma_T - \Sigma\sigma$ ( $\approx 0$ ). 2: same, for $\sigma_T$ , $\sigma_S$ , $\sigma_{nn',L}$ , and $\sigma_{nn',c}$ , these decks intermixed as follows: highest three energies, one card for each for four cross-section types, then next three energies (four cards), etc., 3: punch out all data of options 1 and 2.
52	1: omit printout of $g(E,E')$ 0: print $g(E,E')$ .

#### 2.4.2 Total Cross Section, $\sigma_T$

##### Identification Card

Column	Item
1-6	Any six Hollerith characters
7	= 1 - linear = 2 - linear on log-log paper
10	= 0 - $\sigma(E_j^G)$ found by interpolation = 1 - $\sigma(E_j^G)$ found by CAR-type averaging
11-14	Number of $\sigma(E)$ tabulated ( $\leq 1100$ )
15	= 0 - no resonance parameters = 1 - resonance parameters, $A_\nu$ for $\sigma_T$

##### E, $\sigma_T(E)$ Data Deck

##### Thermal Value of $\sigma_T$ (Format E10.4)

### Identification Card for $A_\nu$

Column	Item
1-6	Any six Hollerith characters
7-8	Number of $A_\nu$ tabulated ( $\leq 99$ )

### $E_\nu, A_\nu(E_\nu)$ Data Deck

### 2.4.3 Elastic Scattering Cross Section, $\sigma_n$

#### Identification Card

Column	Item
1-6	Any six Hollerith characters
7	= 1 - linear
	= 2 - linear on log-log paper
10	= 0 - $\sigma(E_j^G)$ found by interpolation
	= 1 - $\sigma(E_j^G)$ found by CAR-type averaging
11-14	Number of $\sigma(E)$ tabulated ( $\leq 1100$ )
15	= 0 - no resonance parameters
	= 1 - resonance parameters, $A_\nu$ for $\sigma_n$

### $E, \sigma_n(E)$ Data Deck

Thermal Value for  $\sigma_n$  (Format E10.4)

### Identification Card for $A_\nu$

Column	Item
1-6	Any six Hollerith characters
7-8	Number of $A_\nu$ tabulated ( $\leq 99$ )

### $E_\nu, A_\nu(E_\nu)$ Data Deck

### 2.4.4 Angular Distribution Data, $f_p$

Anisotropic elastic scattering for each  $f_p$ ,  $p = 1, 2, \dots, T^N$  ( $T^N \leq 20$ ).

### Identification Card (One for each $f_p$ data deck)

Column	Item
1-6	Any six Hollerith characters
7	= 1 - linear = 2 - linear on log-log paper
10	= 0 - $f_p(E_j^G)$ found by interpolation = 1 - $f_p(E_j^G)$ found by CAR-type averaging
11-14	Number of $f_p(E)$ tabulated ( $\leq 1100$ )

### 2.4.5 Inelastic Scattering Data, Discrete, $\sigma_{nn',L}$

#### Inelastic Scattering Data, Discrete, Control Card

Column	Item
1-10	$E_{BD}$ , energy at which the discrete spectrum begins. This value should be less than $E_{max}$ (e.g., $E_{max} = 18.01739$ Mev, $E_{BD} = 7.93$ Mev)
11-13	NU, number of level parameters, $a_{\nu}\sigma_{nn',L}$ ( $\leq 20$ )

### Excitation of Discrete Levels, $\sigma_{nn',L}$

#### Identification Card

Column	Item
1-6	Any six Hollerith characters
7	= 1 - linear = 2 - linear on log-log paper
10	= 0 - $\sigma(E_j^G)$ found by interpolation = 1 - $\sigma(E_j^G)$ found by CAR-type averaging
11-14	Number of $\sigma(E)$ tabulated ( $\leq 1100$ )
15	= 0 - no resonance parameters = 1 - resonance parameters, $A_{\nu}$ , for $\sigma_{nn',L}$

E,  $\sigma_{nn',L}(E)$  Data Deck from  $E_{BD}$  to  $E_j^G_{max}$

Thermal Value of  $\sigma_{nn',L}$  (Format E10.4)

Identification Card for  $A_\nu$

Column	Item
1-6	Any six Hollerith characters
7-8	Number of $A_\nu$ tabulated ( $\leq 99$ )

$E_\nu, A_\nu(E_\nu)$  Data Deck

$E_\nu$  Deck

$\nu = 1, 2, \dots, NU$      $E_1 < E_2 < \dots < E_{NU}$  (Format 6E10.4)

Level Parameters  $a_\nu \sigma_{nn',L}$

Identification Card (one for each deck of  $A_\nu \sigma_{nn',L}$ , as  $\nu = 1, 2, \dots, NU$ )

Column	Item
1-6	Any six Hollerith characters
7	= 1 - linear
	= 2 - linear on log-log paper
10	= 0 - $a_\nu \sigma_{nn',L}(E_j^G)$ found by interpolation
	= 1 - $a_\nu \sigma_{nn',L}(E_j^G)$ found by CAR-type averaging
11-14	Number of $a_\nu \sigma_{nn',L}$ tabulated ( $\leq 1100$ )

$E, a_\nu \sigma_{nn',L}(E)$  Data Deck from  $E_{BD}$  to  $E_j^G \max$

Thermal Value of  $a_\nu \sigma_{nn',L}$  (Format E10.4)

Identification Card for  $A_\nu$

Column	Item
1-6	Any six Hollerith characters
7-8	Number of $A_\nu$ tabulated ( $\leq 99$ )

$E_\nu, A_\nu(E_\nu)$  Data Deck



#### 2.4.6 Excitation of the Continuum, $\sigma_{nn',c}$ (Includes $\sigma_{n,2n}$ )

##### Inelastic Scattering Data, Continuous, Control Card

Column	Item
1-10	EBC
13	IGOP: Option to compute $G(E,E')$ IGOP = 1 - ASPIC IGOP = 2 - lithium special code IGOP = 3 - beryllium special code

##### Excitation of the Continuum, $\sigma_{nn',c}$

##### Identification Card

Column	Item
1-6	Any six Hollerith characters
7	= 1 - linear = 2 - linear on log-log paper
10	= 0 - $\sigma(E_j^G)$ found by interpolation = 1 - $\sigma(E_j^G)$ found by CAR-type group averaging
11-14	Number of $\sigma(E)$ tabulated ( $\leq 1100$ )
15	= 0 - no resonance parameters = 1 - resonance parameters, $A_\nu$ for $\sigma_{nn',c}$

##### $E, \sigma_{nn',c}(E)$ Data Deck ( $E_{\max} = E_{\min}$ )

##### Thermal Value of $\sigma_{nn',c}$ (Format E10.4)

##### Identification Card for $A_\nu$

Column	Item
1-6	Any six Hollerith characters
7-8	Number of $A_\nu$ tabulated ( $\leq 99$ )

##### $E_\nu, A_\nu(E_\nu)$ Data Deck

IGOP = 1

Parameters for the Temperature Model of the Nucleus

Column	Item
1-10	$E_t$ , the threshold energy of the (n,2n) reaction
11-20	$a^{(1)}$ - level density parameter for the target nucleus
21-30	$a^{(2)}$ - level density parameter for the nucleus after an (n,2n) reaction
31-40	$E_0^{(1)}$ - level density parameter for the target nucleus
41-50	$E_0^{(2)}$ - level density parameter for the nucleus after an (n,2n) reaction
51-60	$E_1^{(1)}$ - first excited state
61-70	$E_1^{(2)}$ - should be set equal to 0.01

Cross Section for the Emission of Two Neutrons,  $\sigma_{n,2n}$

Identification Card

Column	Item
1-6	Any six Hollerith characters
7	= 1 - linear
	= 2 - linear on log-log paper
10	= 0 - $\sigma(E_j^G)$ found by interpolation
	= 1 - $\sigma(E_j^G)$ found by CAR-type group averaging
11-14	Number of $\sigma(E)$ tabulated ( $\leq 1100$ )
15	= 0 - no resonance parameters
	= 1 - resonance parameters, $A_\nu$ for $\sigma_{n,2n}$

E,  $\sigma_{n,2n}(E)$  Data Deck

Thermal Value of  $\sigma_{n,2n}$  (Format E10.4)

Identification Card for  $A_\nu$

Column	Item
1-6	Any six Hollerith characters
7-8	Number of $A_\nu$ tabulated ( $\leq 99$ )

$E_\nu$ ,  $A_\nu(E_\nu)$  Data Deck

Cross Section for Compound Nucleus Formation of the Target Nucleus,  $\sigma_c^{(1)}$

Identification Card

Column	Item
1-6	Any six Hollerith characters
7	= 1 - linear
	= 2 - linear on log-log paper
10	= 0 - $\sigma(E_j^G)$ found by interpolation
	= 1 - $\sigma(E_j^G)$ found by CAR-type group averaging
11-14	Number of $\sigma(E)$ tabulated ( $\leq 1100$ )

E,  $\sigma_c^{(1)}(E)$  Data Deck

Cross Section for Compound Nucleus Left Over After the (n,2n) Reaction,  $\sigma_c^{(2)}$

Identification Card

Column	Item
1-6	Any six Hollerith characters
7	= 1 - linear
	= 2 - linear on log-log paper
10	= 0 - $\sigma(E_j^G)$ found by interpolation
	= 1 - $\sigma(E_j^G)$ found by CAR-type group averaging
11-14	Number of $\sigma(E)$ tabulated ( $\leq 1100$ )

E,  $\sigma_c^{(2)}(E)$  Data Deck

IGOP = 2 (Lithium Special Code)

No input required.

IGOP = 3 (Beryllium Special Code)

Identification Card

Column	Item
1-6	Any six Hollerith characters
7	= 1 - linear
	= 2 - linear on log-log paper
10	= 0 - $\epsilon(E_j^G)$ found by interpolation
	= 1 - $\epsilon(E_j^G)$ found by CAR-type group averaging
11-14	Number of $\epsilon(E)$ tabulated ( $\leq 1100$ )

E,  $\epsilon(E)$  Data Deck

#### 2.4.7 Cross Section for the Emission of Two Neutrons, $\sigma_{n,2n}$

(If  $\sigma_{n,2n}$  has been supplied for the ASPIC routine do not input again and do not flag  $\sigma_{n,2n}$  on the element control card.)

##### Identification Card

Column	Item
1-6	Any six Hollerith characters
7	= 1 - linear
	= 2 - linear on log-log paper
10	= 0 - $\sigma(E_j^G)$ found by interpolation
	= 1 - $\sigma(E_j^G)$ found by CAR-type group averaging
11-14	Number of $\sigma(E)$ tabulated ( $\leq 1100$ )
	= 0 - no resonance parameters
	= 1 - resonance parameters, $A_\nu$ for $\sigma_{n,2n}$

##### E, $\sigma_{n,2n}(E)$ Data Deck

##### Thermal Value of $\sigma_{n,2n}$ (Format E10.4)

##### Identification Card for $A_\nu$

Column	Item
1-6	Any six Hollerith characters
7-8	Number of $A_\nu$ tabulated ( $\leq 99$ )

##### $E_\nu$ , $A_\nu(E_\nu)$ Data Deck

For the following eight cross sections (see Section 2.4.8) the following general format is to be used in the order of the cross sections listed.

##### Identification Card

Column	Item
1-6	Any six Hollerith characters
7	= 1 - linear
	= 2 - linear on log-log paper
10	= 0 - $\sigma(E_j^G)$ found by interpolation
	= 1 - $\sigma(E_j^G)$ found by CAR-type group averaging

Column	Item
11-14	Number of $\sigma(E)$ tabulated ( $\leq 1100$ )
15	= 0 - no resonance parameters = 1 - resonance parameters, $A_\nu$ for $\sigma$

#### E, $\sigma(E)$ Data Deck

#### Thermal Value of $\sigma$ (Format E10.4)

#### Identification Card for $A_\nu$

Column	Item
1-6	Any six Hollerith characters
7-8	Number of $A_\nu$ tabulated ( $\leq 99$ )

#### $E_\nu$ , $A_\nu(E_\nu)$ Data Deck

#### 2.4.8 Other Cross Sections (Input Data as Described Above)

1. Fission Cross Section,  $\sigma_f$
2. Absorption Cross Section,  $\sigma_{abs}$
3. Transport Cross Section,  $\sigma_{tr}$
4. Cross Section for the Emission of an  $\alpha$  Particle,  $\sigma_\alpha$
5. Cross Section for the Emission of a Proton,  $\sigma_p$
6. Cross Section for the Emission of  $H_2$ ,  $\sigma_{H_2}$
7. Cross Section for the Emission of  $H_3$ ,  $\sigma_{H_3}$
8. Radiative Capture Cross Section,  $\sigma_{n,\gamma}$

If the program control card specifies more than one element, repeat Section 2.4 of the above input preparation for each element.

### 2.5 GENDA OUTPUT

The GENDA output consists of two edits. The first edit tabulates the input data in the same order as they appear in the input cards. The second edit tabulates the cross-section data at the output mesh energies, as described in Section 2.1, and arranges them in an easily readable manner.

### 3. THE GENDA-PROCESSOR ROUTINE (GENPRO)\*

The cross-section data generated by GENDA may be used in various ways. However, in Monte Carlo type calculations, what has to be determined once a collision occurs, is

1. The type of event which takes place
2. The energy and direction angle of the emerging particle, if any.

The GENPRO program processes the GENDA output to tabulate probabilities peculiar to a nuclide at a prescribed energy mesh as follows.

1. It computes the probability of elastic scattering, inelastic scattering, and absorption.
2. In case of anisotropic elastic scattering, it tabulates the cosines of angles between which scattering is equi-probable.
3. In case of inelastic scattering, two possibilities exist.
  - a. If the spectrum has a continuous part, it computes energies to which the particle scatters with equal probability.
  - b. If the spectrum is representable by  $\nu$  distinct levels, it tabulates the probability that the particle will scatter to the level  $E_\nu$ .

It is important to note at this point that the maximum number of output energies is different for GENDA, GENPRO, and the subsequent Monte Carlo programs.

---

\*This chapter is taken, with minor changes and additions, from Reference 1.

Indeed, because of the need of fine tabulation of particular cross sections, GENDA was expanded to handle 450 output energy points. On the other hand, GENPRO can only handle 401 energy points (201 in the IBM-7094 version) due to core storage limitations. The UNC Monte Carlo programs are further restricted to a maximum energy mesh of 81 points. Therefore, in any Monte Carlo type calculations, input to GENDA must be consistent with the above restrictions.

Also, the output energy mesh for GENDA is variable. However, if it is used in connection with GENPRO, a fixed lethargy interval must be used.

### 3.1 TECHNICAL DESCRIPTION

The cross-section data for each element provided by GENDA are written on a magnetic tape called the Genda Output Tape (GOT).

GENPRO uses GOT to create an Element Data Tape (EDT) which contains the following information:

1. The number of energy points,  $J$
2. The set of final energies in increasing order  $E_j^G$  (using the given constant lethargy step).

Then, for each element,

1. The total cross section at each final energy,  $\sigma_T(E_j^G)$ , is transmitted to the EDT
2. The probabilities of elastic and inelastic scattering and absorption are computed.

$$P_S(E_j^G) = \frac{\sigma_S(E_j^G)}{\sigma_T(E_j^G)} \quad (15)$$

$$P_{nn'}(E_j^G) = \frac{\sigma_{nn'}(E_j^G)}{\sigma_T(E_j^G)} \quad (16)$$

$$P_A(E_j^G) = 1 - P_S(E_j^G) - P_{nn'}(E_j^G) \quad (17)$$

$P_S$  and  $P_A$  tables are then transmitted to the EDT.

It should be noted that for neutron absorption,  $P_A$  contains both fission and capture probabilities.

3. In the event of elastic scattering, the following calculation is performed to decide whether or not the scattering is isotropic.

The angular distribution data supplied by GOT in the form of Legendre expansion coefficients  $f_\ell$ 's are tested for each energy point. Let

$$\sigma(\omega=1) = \sum_{\ell=0}^L (2\ell + 1) f_\ell(E_j^G) \quad (18)$$

$$\sigma(\omega=-1) = \sum_{\ell=0}^L (2\ell + 1) f_\ell(E_j^G) (-1)^\ell \quad (19)$$

$$\sigma(\omega=0) = \sum_{\text{even } \ell \text{'s}} (2\ell + 1) f_\ell(E_j^G) P_\ell(0) \quad (20)$$

where the notation used is given in the GENDA section.

The largest and smallest of these are selected and referred to as  $M$  and  $m$ , respectively.



Then if

$$\frac{M - m}{0.5(M+m)} \leq 0.05, \quad (21)$$

the angular distribution is taken as isotropic and no further tabulated data are required. (See Section 11.4.)

Otherwise, the scattering is treated as anisotropic and GENPRO proceeds to compute the angles  $\theta$  through which it is equally probable to scatter.

Since the differential scattering cross section is given by

$$\sigma(E_j^G, \mu) = \frac{\sigma_n(E_j^G)}{4\pi} \sum_{\ell=0}^L (2\ell + 1) f_{\ell}(E_j^G) P_{\ell}(\mu) \quad (22)$$

where  $\mu = \cos \theta$  varies from  $-1$  to  $+1$ , GENPRO computes

$$F(\mu, E_j^G) = \frac{2\pi}{\sigma_n(E_j^G)} \int_{-1}^{\mu} \sigma(E_j^G, \mu) d\mu \quad (23)$$

which gives the  $\mu$  probability distribution. The integration of Eq. 22 yields

$$F(\mu, E_j^G) = \sum_{\ell=0}^L \frac{1}{2} f_{\ell}(E_j^G) [P_{\ell+1}(\mu) - P_{\ell-1}(\mu)] \quad (24)$$

with the convention that  $P_{-1} = -1$ .

$F(\mu, E_j^G)$  is computed for  $-1 \leq \mu \leq +1$  in steps of 0.01. Then GENPRO locates  $\mu_n$  such that

$$F(\mu_n) = \frac{n}{N} \text{ for } n = 0, 1, 2 \dots, N. \quad (25)$$

$N$  is usually 10 for the Monte Carlo programs.

For statistical considerations, it is desirable to use a new variable  $\chi$  which is related to  $\mu$  by

$$\mu = \cos \theta = 1 - 2\chi \quad (26)$$

where now  $\chi$  varies from 0 to 1.

Hence,

$$\chi_n = \frac{1 - \mu_n}{2}, \quad n = 0, 1, 2 \dots N \quad (27)$$

is tabulated and transmitted to the EDT as Table CHI.

4. In the event of continuum inelastic scattering (which is determined by the threshold energy supplied by GOT), the probability that a neutron entering collision at energy  $E_j^G$  will emerge from an inelastic scattering collision at energy  $E'$  has been computed by GENDA and entered into GOT in the form of  $g_c(E_j^G, E')$  with  $E_j^G > E_{BD}$ .

To obtain the energies to which it is equally probable to scatter, GENPRO calculates

$$G(E_j^G, E) = \int_0^E g_c(E_j^G, E') dE', \quad E \leq E_j^G \quad (28)$$

where the integral is evaluated by the trapezoidal rule.

Note that if one considers the spectrum of neutrons emitted by (nn') reactions, the integral (Eq. 28) is normalized to 1.

Indeed,

$$G(E_j^G, E_j^G) = 1.$$

However, GENDA considers the composite spectrum of neutrons emitted by  $(nn'; n, 2n)$  reactions and hence,  $G(E_j^G, E_j^G)$  may be different from 1 and GENPRO proceeds to compute:

$$\mathcal{G}(E_j^G, E) = \frac{G(E_j^G, E)}{G(E_j^G, E_j^G)}.$$

Then it locates  $E_n$  such that

$$\mathcal{G}(E_j^G, E_n) = \frac{n}{N} \text{ for } n = 0, 1, 2, \dots, N.$$

$N$  is usually 10 for the Monte Carlo programs. The  $E_n$  are tabulated and transmitted to the EDT as Table ENN.

5. In the event of discrete level inelastic scattering, GOT supplies the  $a_\nu$ 's. The  $a_\nu^j$ 's are tabulated and transmitted to the EDT as Table PLEV  $(\nu, j)$ . The corresponding values of the excitation level energies are tabulated and transmitted to the EDT as Table ELEV  $(\nu, j)$ .
6. If both continuum and discrete level inelastic scattering occur, i.e.,  $E_{BC} < E_j^G \leq E_{BD}$ , GOT supplies information on the kernels  $g_c(E_j^G, E')$  and  $g_D(E_j^G, E')$  and the continuum and discrete level inelastic scattering cross sections,  $\sigma_{nn',c}(E_j^G)$  and  $\sigma_{nn',D}(E_j^G)$ .

To obtain the energies to which it is equally probable to scatter, the GENPRO program calculates the probability  $G(E_j^G, E)$  that a neutron at  $E_j^G$  scatters to an energy below  $E$  as follows:

$$G(E_j^G, E) = \frac{\sigma_{nn',c}(E_j^G) \int_0^E g_c(E_j^G, E') dE' + \sigma_{nn',D}(E_j^G) \int_0^E g_D(E_j^G, E') dE'}{\sigma_{nn',c}(E_j^G) + \sigma_{nn',D}(E_j^G)} \quad (29)$$

where  $G(E_j^G, 0) = 0$  and  $G(E_j^G, E_j^G) = 1$ , and the probability distribution functions  $g_c$  and  $g_D$  have been discussed in the GENDA section.

Then, GENPRO proceeds to locate the energies,  $E_n$ , to which it is equally probable to scatter as if the level spectrum were continuous only. The method used is similar to that of determining the cosines of the angles through which it is equally probable to scatter. The  $E_n$  are tabulated and transmitted to the EDT as Table ENN.

### 3.2 GENPRO INPUT

The input to GENPRO consists of the GENDA Output Tape (GOT) (Logical tape 9 for the CDC-1604-A; logical tape 1 for the IBM-7094) and one card denoting the number of values of  $\chi$  needed to define the equally probable angular bins in anisotropic elastic scattering, and the (same) number of energy values defining the equally probable energy bins in continuum inelastic scattering. This number is usually 11; the format is I10.

### 3.3 FORMAT OF THE EDT

A description of the format of the EDT follows. Since the EDT is made up of card images, the description is in terms of card images.

<u>Item No.</u>	<u>No. of Entries</u>	<u>Card Description</u>	<u>Format</u>
1	1	NENERG NENERG is the number of energies in the energy table.	I10

<u>Item No.</u>	<u>No. of Entries</u>	<u>Card Description</u>	<u>Format</u>
2	NENERG	ETABLE(1), ETABLE(2), ETABLE(3), ETABLE(4), ETABLE(5), ... ETABLE (NENERG). ETABLE is the energy mesh for all elements. ETABLE(1) is the lowest energy and ETABLE(NENERG) is the highest energy.	5E14.5
3	3	ATWT, IATWT, J ATWT is the floating point atomic weight. IATWT a 5-digit nuclide identifier. J is an end of data flag. J≠0 means this card is the last card of the EDT.	E16.8, 2I6
4	5	OF, NOW, NFI, ISI, IPIN OF≠0 means this is last card of ele- ment. NOW is the number of words in the next group of data. NFI is a file number used for identifica- tion only. ISI≠0 means the next group of data is the scatter index. IPIN≠0 means this element has no inelastic scattering.	E16.8, 4I6
5	NOW	SIGMA(1), SIGMA(2), SIGMA(3), SIGMA(4), etc. SIGMA is the microscopic total cross section. Note that NOW must equal NENERG and that OF, ISI, IPIN must all be zero.	5E14.5
6	5	Repeat item 4	E16.8, 4I6
7	NOW	PSCAT(1), PSCAT(2), PSCAT(3), PSCAT(4), PSCAT(5), ..., PSCAT(NENERG). PSCAT is the probability of elastic scattering. PSCAT(1) corresponds to ETABLE(1) and PSCAT(NENERG) corresponds to ETABLE(NENERG).	5E14.5
8	5	Repeat item 4.	E16.8, 4I6

<u>Item No.</u>	<u>No. of Entries</u>	<u>Card Description</u>	<u>Format</u>
9	NOW	PABS(1), PABS(2), PABS(3), PABS(4), PABS(5), ..., PABS(NENERG).	5E14.5
10	5	OF, NOW, NFI, ISI, IPIN ISI must equal 1 because the next data group is the scatter index. If this element has no inelastic scattering, then IPIN must equal 1.	E16.8, 4I6
11	NENERG	IP, ID, IT, IA There are NENERG cards in this data group. Each card has the quan- tities IP, ID, IT, IA defined as follows:  IP = 1 for inelastic discrete scattering = 2 for inelastic continuum scatter- ing ID = the location of an ENN or PLEV table relative to the first word of the SIGMA table IT = 1 for isotropic scattering in cen- ter of mass = 2 for scattering in hydrogen = 3 for anisotropic scattering in center of mass = 4 isotropic scattering in the lab system ID = location of a $\chi$ Table if IT = 3.	4I10
12	5	Repeat item 4 with NOW = 11.	E16.8, 4I6
13	11	CHI(1), CHI(2), CHI(3), CHI(4), CHI(5), etc. CHI is a table of 11 entries. CHI(1) = 1.0, CHI(11) = 0. Items 12, 13 are repeated for each energy at which 'TT' of item 11 is 3.	5E14.5
14	5	Repeat item 4 with NOW = 11.	E16.8, 4I6
15	11	ENN(1), ENN(2), ENN(3), ENN(4), ENN(5), etc. The ENN table is used to determine the energy after scattering for an in- elastic continuum interaction. Items 14 and 15 are repeated for each energy	5E14.5

<u>Item No.</u>	<u>No. of Entries</u>	<u>Card Description</u>	<u>Format</u>
15	11 (Cont.)	at which 'IP' of item 11 is 2. If the element has no continuum scattering, items 14 and 15 are omitted.	5E14.5
16	5	Repeat item 4 with NOW = number of excitation levels for discrete scattering.	E16.8, 416
17	NOW	ELEV(1), ELEV(2), ELEV(3), ELEV(4), ELEV(5), ..., ELEV(NOW). The ELEV table is a list of possible excitation levels; each entry corresponds to a probability in a PLEV table.	5E14.5
18	5	Repeat item 16.	E16.8, 416
19	NOW	PLEV(1), PLEV(2), PLEV(3), PLEV(4), PLEV(5), ..., PLEV(NOW). The PLEV tables are tables of probabilities of scattering from the current energy to the excitation levels. Items 18 and 19 are repeated for each energy at which inelastic discrete scattering occurs (IP=1).	5E14.5
20	5	OF, NOW, NFI, ISI, IPIN OF = 1.0. Other quantities 0. Item 20 is the last card of an element.	E16.8, 416
21	3	ATWT, IATWT, J If there are no more elements ATWT and IATWT = 0, J = 1. If there are more elements repeat from item 3.	E16.8, 216

#### **4. DESCRIPTION OF THE AVAILABLE PROBLEM GEOMETRIES**

The ATHENA system recognizes problems of two geometry types, namely those of 30-degree and 360-degree descriptions. Various geometry-dependent routines, in particular VANGEN, TESTG, ATHENA, and STATC, are provided with the necessary information indicating which type of geometry is being considered.

The 360-degree geometry (Fig. 2) represents an essentially homogenized reactor core, which can be subdivided radially and axially to permit variation of the composition within the core, and to provide several in-core flux scoring regions.

The 30-degree geometry (Fig. 3) permits a much closer approximation to the configuration of an actual reactor core which contains a hexagonal lattice. The geometry data for a very detailed and extensive structure may require large amounts of machine storage, and much of the data may be repetitious for a symmetric configuration. The 30-degree geometry option was devised to exploit the 12-fold symmetry of a hexagonal-lattice reactor core, and thereby permit relatively detailed geometrical descriptions of a limited portion of the structure. For example, the source-generator or tracking routines (or both) may recognize individual fuel rods, axial divisions of these rods, and the presence of coaxial fuel cylinders within a fuel rod.



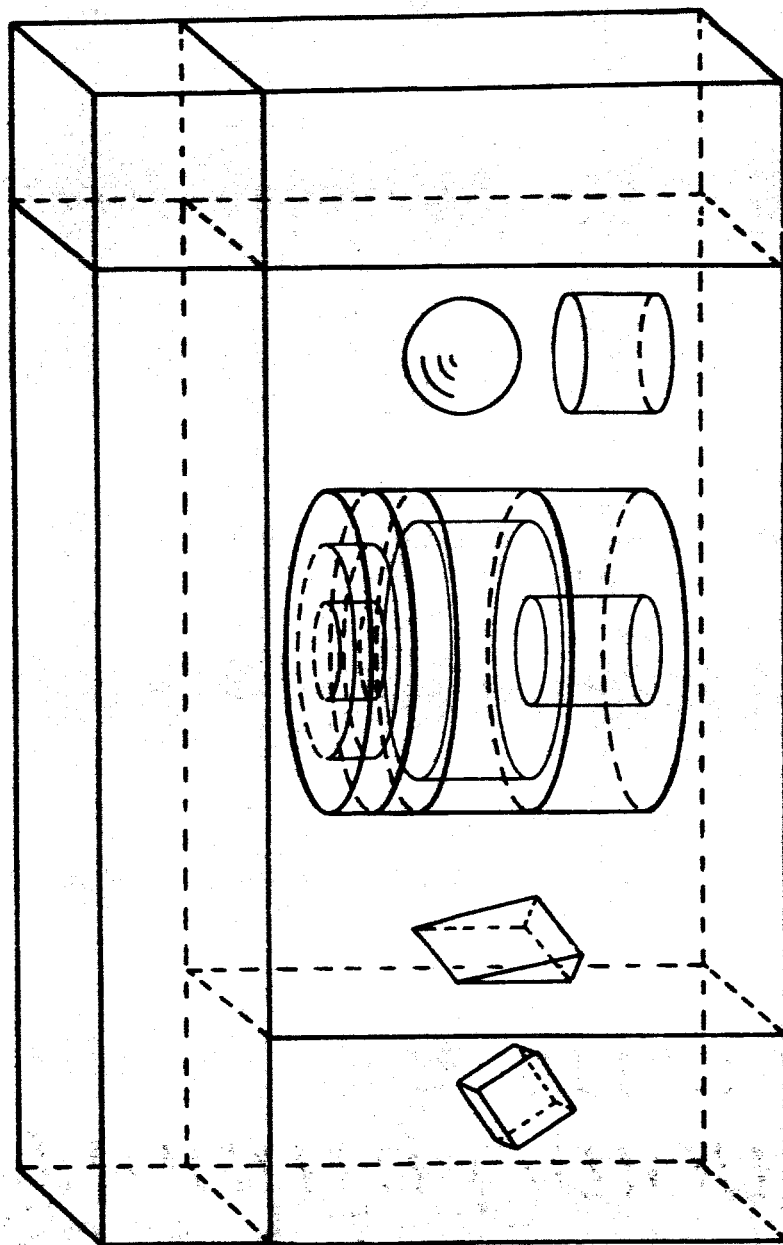
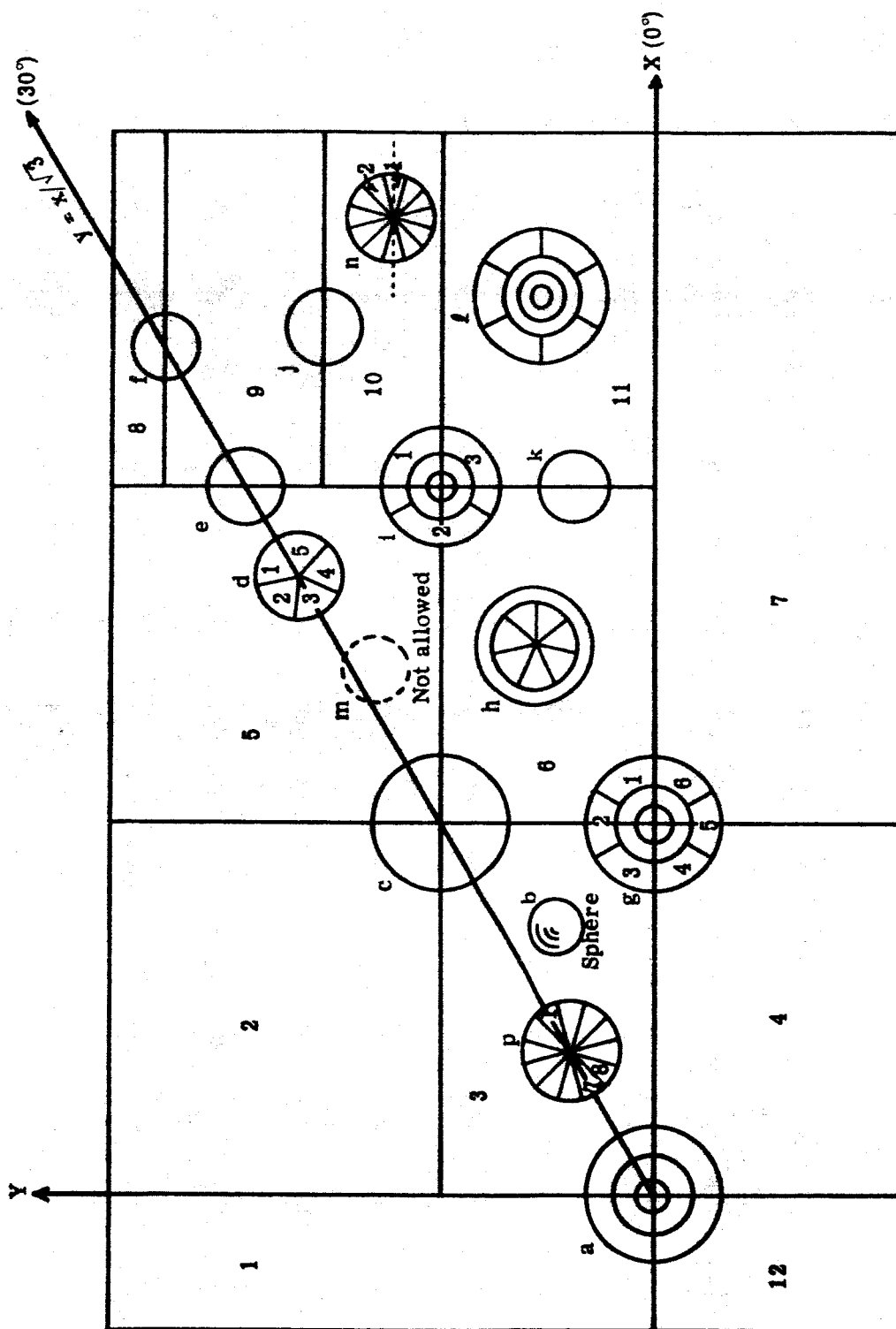


Fig. 2 — Representation of Reactor Core within a 360-Degree ATHENA Geometry. The Core May Be Subdivided into Several Axial Zones within Each of which an Arbitrary Subdivision into Coaxial Cylinders Is Permitted. Outside the Core, There May Be Cylinders, Spheres, and Arbitrarily Oriented Boxes and Wedges.



**Fig. 3 — Horizontal Section ( $z = \text{Constant}$ ) Illustrating 30-Degree Geometry with Straddling and Sected Cylinders**

A common feature of both geometries is the requirement that the region of three-space to be considered be bounded by a finite rectangular solid whose bounding planes are parallel to the coordinate planes of a right-handed coordinate system. This solid is decomposed, according to the problem input, into a number of ordinary boxes (rectangular solids with xyz orientation) which may, in turn, contain various numbers of nonordinary regions, e.g., cylinders, spheres, wedges, or nonordinary (arbitrarily oriented) boxes.

The geometry type specified affects principally the operation of VANGEN and ATHENA. A very useful feature of the programs is that, in both geometries, the spatial variation of the neutron or gamma sources may be considerably more detailed than the structure specified for tracking and scoring. There are, however, certain restrictions placed upon the reactor core specifications. Brief descriptions are given below of the capabilities and restrictions of each geometry type; further details are given in the discussion of the VANGEN program (Chapter 5).

#### 4.1 360-DEGREE GEOMETRY

The general requirements for the geometry input to a 360-degree problem are listed below. These are illustrated by Fig. 4.

1. The over-all volume is subdivided into  $\leq 80$  ordinary regions (boxes).

In the example (Fig. 4), there are seven ordinary regions, of which regions 6 and 7 are not shown; box 3 in this example contains cylinders 10, 13, 15, and 17 which together with their internal regions 9, 12, 14, and 16 and their internal regions, etc., make up the active core; there are other assorted figures (18-21) outside of the core.

2. The core axis must coincide with the z-axis.

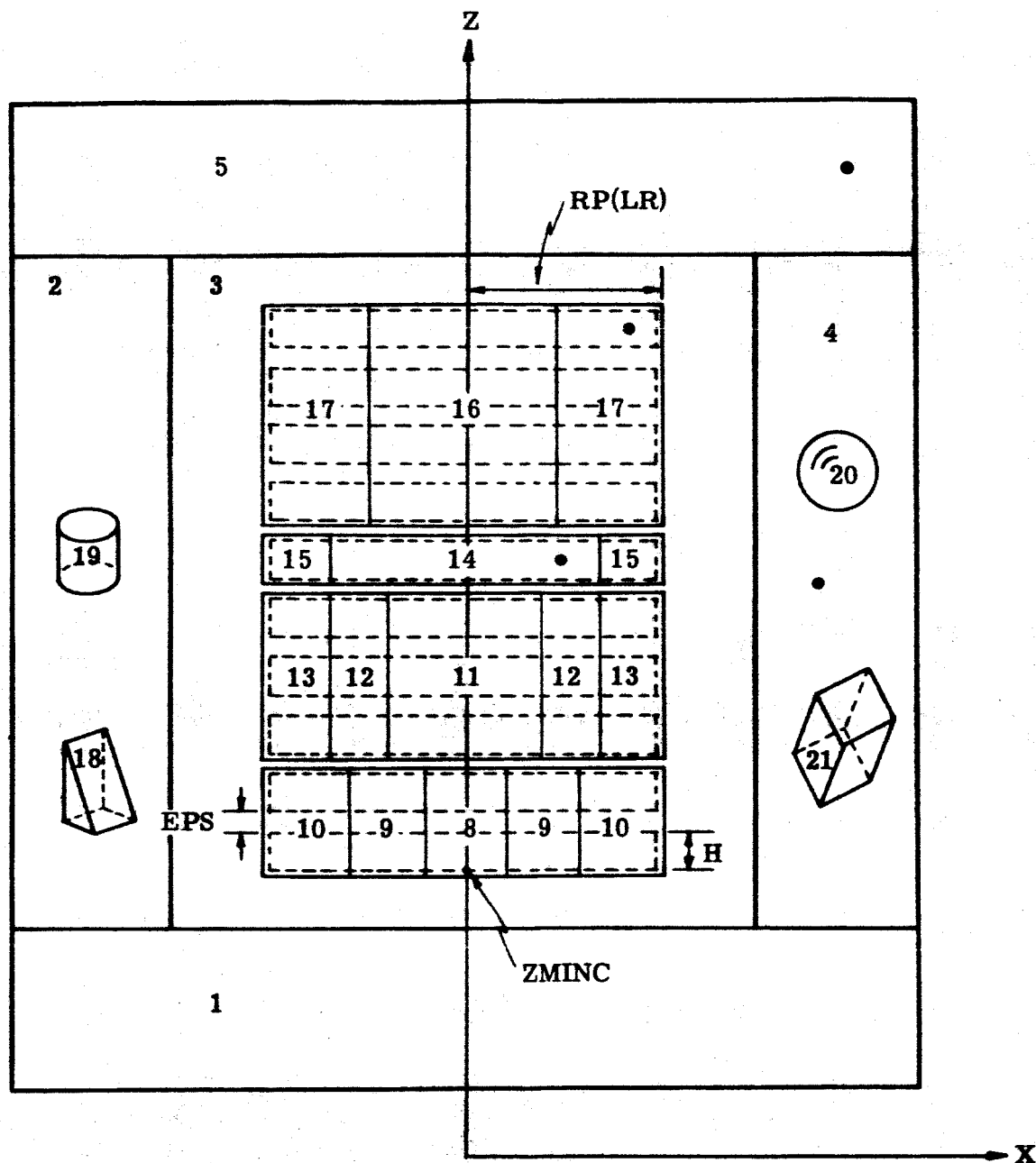


Fig. 4 — Vertical Section through a Typical 360-Degree Configuration. In this Example,  $NSTAGE = 10$ ,  $NAXZON = 4$ , and the Minimum Stage Indices (KSMIN) of the Four Zones are 1, 3, 6, and 7, Respectively.

3. The core is divided axially into NSTAGE ( $\leq 26$ ) stages; in the example, NSTAGE = 10. The stages represent the axial sections in which source particles may be generated.
4. Each stage is of height H; there are separations (gaps) of height  $\epsilon$  between stages, within which no sources are generated.
5. A grouping of consecutive stages is called an axial zone; there may be up to 26 zones in the core. In the example (Fig. 4), there are four axial zones, encompassing 2, 3, 1, and 4 stages, respectively.
6. The tracking cylinders occupying a given axial zone (for example, 11, 12, 13 in zone 2 of Fig. 4) must be cobasal at top and bottom and coaxial.
7. Each part of the active core space [defined in (8) below], apart from gaps ( $1/2 \epsilon$ ) between zones, must be assignable to one or the other of the core cylinders.
8. The axial extent of the active core is defined on input by ZMINC, the minimum  $z$  of stage 1; H, the height of one stage; EPS, the gap between stages; and NSTAGE, the number of stages. The radial extent is from  $R = 0$  to  $R = RP(LR)$ , where  $RP(LR)$  is the largest radius listed in the input radial power pattern (cf. VANGEN, Chapter 5).
9. In 360-degree problems only, one may specify point detectors for gamma heating and flux scoring. The present example shows four such detectors, located in regions 4, 5, 14, and 17.

## 4.2 30-DEGREE GEOMETRY

In this geometry option, the basic framework is retained of a set of ordinary boxes filling up all space within specified limits on  $x$ ,  $y$ ,  $z$ . There is the further restriction (on the source-generator, tracking, and all other pertinent routines) that particles are to be confined to the space in the first quadrant between the planes  $y = 0$  and  $y = x/\sqrt{3}$  (Fig. 3).

Fig. 3 shows the required orientation of the geometry for a 30-degree problem. Several important features of this geometry (which depart from previous restrictions and specifications for EZGEOM) are as follows.

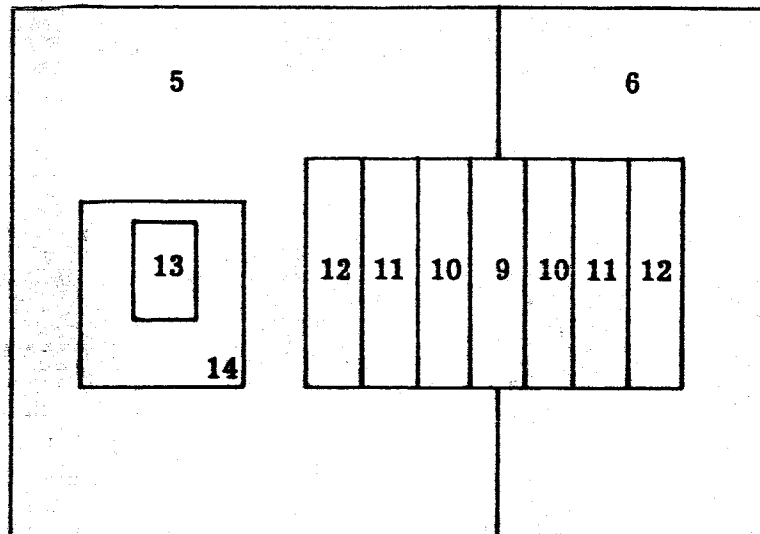
1. All cylinder axes must be vertical, parallel to the z-axis (this restriction may be removed for nonfuel cylinders in later versions of the program).
2. A cylinder vertex (x,y location of its axis) may lie at (0,0); in one of the reflection planes ( $y = 0$  or  $y = x/\sqrt{3}$ ); on the intersection plane of two ordinary boxes (e.g., cylinder f or j) or four ordinary boxes (e.g., cylinder i); or elsewhere (e.g., cylinder h). with the restriction that no plane may intersect a cylinder unless the cylinder axis is on that plane (e.g., a cylinder such as m is not allowed). Corollary: straddling [cf. (3) below] may occur only in the x-y plane.
3. Cylinders may have one external region (e.g., h is internal to 6) or may straddle two or four (but not three) ordinary regions (e.g., j is internal to 9 and 10; g is internal to 3, 4, 6, and 7).
4. Cylinders may be sectored into  $\leq 12$  equiangular sectors for purposes of azimuth-dependent gamma heating scoring. A cylindrical region (such as g) containing a coaxial, cobasal cylinder may also be sectored.
5. Cylinder sectors are oriented and numbered (by the programs) as follows. Sector identifiers increase counterclockwise, with the minimum azimuth of sector 1 being  $0^\circ$  for all cylinders except those on the  $30^\circ$  plane (but not on the origin). For such cylinders (e.g., c, d, e, f) sector 1 originates at  $30^\circ$ . Exceptions: for a cylinder with 12 sectors (e.g., n or p), the respective minimum azimuths are  $-15^\circ$  (instead of  $0^\circ$ ) and  $+15^\circ$  (instead of  $+30^\circ$ ). This convention (which is recognized in the tracking and volume computations) was adopted so that the nearest

points on nearest-neighbor 12-sectored cylinders in a hexagonal array would correspond to midpoints of sectors rather than boundaries thereof.

6. Nonzero heating gamma scores are accumulated only in trackable sectors (e.g., sectors 3, 4, and 5 of cylinder d). In this example, the computed volume of sector 3 is one-tenth rather than one-fifth that of cylinder d.
7. There may be  $\leq 15$  fuel-rod centers (vertices) within a fuel rod. There may be  $\leq 10$  fuel cylinders (defined by  $\leq 20$  radii). Arbitrary relative source strengths can be assigned to the fuel rods and to the fuel cylinders within a rod (cf. Chapter 5).
8. No other nonordinary objects (e.g., the sphere, region b) may straddle boxes or extend beyond the reflection planes (automatic tests are made for illegal locations of sphere centers or cylinder vertices).
9. Ordinary regions may be intersected arbitrarily by the  $30^\circ$  reflection plane; it is permitted (but not required) that certain ordinary regions be bounded by the  $0^\circ$  plane.

#### Concluding Remarks on Cobasal Cylinders and External Regions

The only nonordinary regions which may touch other regions without geometric clearance are the cylinders which make up a cobasal array. These must be coaxial and cobasal at both bases. In the sketch below, a cluster of cobasal cylinders 9, 10, 11, 12 is shown in vertical section; cylinder 12 is straddling regions 5 and 6; cylinders 13 and 14 are noncobasal. The external region numbers to be assigned to the various cylinders are:



<u>Cylinder</u>	<u>External Region</u>
9	10
10	11
11	12
12	(none); 5 and 6; (for exact format of spe- cification see VANGEN or EZGEOM input lists)
13	14
14	5

Note that cylinders 9 through 11 are not classified as straddling cylinders, since each has a single external region.



## **5. THE SOURCE-GENERATOR PROGRAM, VANGEN**

The source-generator program developed for the ATHENA system is designed to provide source tapes for use in conjunction with problems of 30-degree or 360-degree geometry. Its component routines perform the following functions.

1. Integrate over an arbitrary reactor power history to find:
  - a. delayed fission-gamma intensity and spectrum at a specified final instant; and
  - b. time-integral of the power.
2. Compute fission fractions in several neutron energy bins.
3. Generate modified gamma and/or neutron spectra for the source tapes, based on the results of (1) and (2) and input-specified energy weights.
4. Select source-particle locations within a reactor core geometry of 30-degree or 360-degree type (see Figs. 2, 3, and 4) at random from a detailed spatial distribution appropriate to the geometry type.
5. Perform splitting or Russian roulette on the source particles to reflect region-dependent weighting in the tracking program.
6. Assign source-particle locations to appropriate tracking-geometry regions, and label the particles on the source tape with these region numbers.

7. Normalize the input spatial power pattern and transmit the normalized power tables to an inter-program dump tape.
8. Perform validating tests on the cylindrical-region input for the source-generator, and edit the results of these tests.
9. Print out descriptions of input-specified numbers of source particles.
10. Generate a neutron tape, a gamma tape, or both, in a single problem, with arbitrary numbers of histories.
11. Read back the source tape or tapes and tally the particles recorded thereon, by region and by energy.

## 5.1 SPATIAL SELECTION

The spatial selection and associated geometry and power-pattern input will be described first.

### 5.1.1 360-Degree Geometry

The particles are generated within a core, or a cylindrical volume which extends axially from a minimum position ZMINC (see Fig. 5) to a maximum position which is the upper limit of the highest stage ( $NSTAGE \leq 26$ ). The implied stages are all of equal height ( $H$ ) and separation ( $\epsilon, EPS$ ). The regions which occupy the core must be cylinders, with bases offset by  $\epsilon/4$  from the bases of the uppermost and lowermost enclosed stages (a special cylinder-input format is available to facilitate these specifications). Thus, cylinder  $c$  of Fig. 5 would be described as having a base location of type  $-2$  [signifying that its base is  $(1/4)\epsilon$  below the second stage] and height type  $-2$  [signifying that its height is such as to enclose two stages, plus  $(1/4)\epsilon$  at the top]. Explicitly, if a cylinder is of negative height type,  $-N$ , its height is computed as

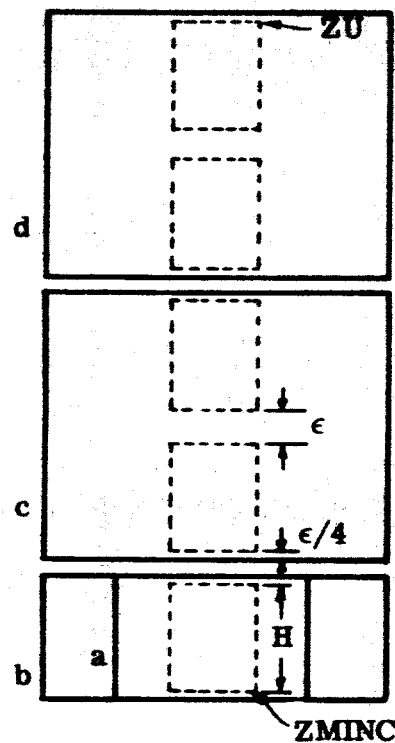


**Fig. 5 — Illustrating 360-Degree Type Reactor Geometry and Relationship between Implied Stages (here NSTAGE = 5) and Tracking Cylinders**

$$\begin{aligned}
 ht &= NH + (N - 1)\epsilon + \frac{1}{2}\epsilon \\
 &= NH + (N - \frac{1}{2})\epsilon.
 \end{aligned}
 \tag{30}$$

The axial distribution of the source particles is controlled by an input table of LZ ( $\leq 50$ ) pairs of numbers, PZ(K) and ZP(K), representing the relative fissioning density as a function of axial position from a minimum Z ( $\leq Z_{\text{MINC}}$ ) to a maximum Z

$$Z_{\text{max}} \geq Z_{\text{MINC}} + \text{NSTAGE} \cdot H + (\text{NSTAGE} - 1) \cdot \epsilon. \tag{31}$$

It is assumed in the program that linear interpolation is permissible for the PZ vs ZP table, and further (overriding the results of this interpolation) that the gaps (of height  $\epsilon$ ) between stages are "dead spaces," i.e., that no source particles are to be generated there.

The axial table is integrated in a pre-processing subroutine PWRPAT, which (inter alia) sets up a table of

$$PDZ = \int_{Z_{\text{min}}}^Z P(z) dz$$

as a function of Z, the entries for the latter consisting of all of the input values of ZP, plus all of the Z-boundaries of the implied NSTAGE stages.

The selection of all the parameters describing a source particle is done in subroutine TAPGEN. In particular, the axial coordinate Z is chosen as the Z satisfying

$$\frac{\int_{Z_{\min}}^Z P(z) dz}{\int_{Z_{\min}}^{Z_{\max}} P(z) dz} = \xi \quad (32)$$

(excluding  $\epsilon$ 's)

where  $0 \leq \xi \leq 1$ , chosen in subroutine RANDM. The  $Z$  thus chosen cannot lie in one of the "dead spaces"  $\epsilon$ , because of the manner of setting up the table of PDZ. The stage containing the selected  $Z$  is then determined, and finally the axial zone (KAX) containing this stage.

Next a radial location is selected, as follows. The radial distribution of the volumetric fissioning is described by means of an input table of  $LR(\leq 50)$  pairs of numbers,  $PR(J)$  and  $RP(J)$ , representing the relative fissioning density as a function of radial position (independently of axial position), from  $R = 0$  to  $R = RP(LR)$ . Linear interpolability of  $PR$  in  $RP$  is assumed. Since the input values of  $(PR)$  represent probability of fissioning per unit volume (or per unit area at a specified axial location), the probability that a given source arises at a radius  $R$  between  $R_1$  and  $R_2$  is

$$\Delta P = P(R_1 \leq R \leq R_2) \sim \int_{R_1}^{R_2} P(r) dA = \int_{R_1}^{R_2} (PR) 2\pi r dr \quad (33)$$

$$\Delta P = 2\pi \int_{R_1}^{R_2} (Ar + B)r dr = 2\pi \left[ \frac{A}{3} R^3 + \frac{B}{2} R^2 \right]_{R_1}^{R_2} \quad (34)$$

where  $A$  and  $B$  are coefficients in a local linear fit, and  $R_1$  and  $R_2$  are consecutive entries in the input table  $RP$ . Subroutine PWRPAT computes, accumulates, and normalizes the values of  $\Delta P$  (Eq. 34) for later use in subroutine TAPGEN.

The main program (VANGEN) also computes, and stores in portions of a common array RJ360, the coefficients A and B for each of the LR-1 radial bins, and the maximum value of PR·R within each of these bins.

A radial source location is selected in TAPGEN as the R satisfying

$$\frac{\int_0^R P(r)r \, dr}{\int_0^{R_{\max}} P(r)r \, dr} = \xi \quad (35)$$

The R-selection is done in two steps. First a random number is located in the table of cumulative  $\Delta P$  to pick a radial bin, then the rejection technique shown in Fig. 6 is used to select a radius within that bin.

(A similar two-step procedure is followed in the selection of an axial location.)

The sine and cosine of a random azimuth  $\phi$  about the Z-axis is chosen in subroutine PHI; x and y coordinates are then set equal to  $R \cos \phi$  and  $R \sin \phi$ . The last step in the spatial selection is the identification of the tracking region containing the selected (Z,R).

The main program (VANGEN) examines the tracking-cylinder input once, and verifies that (1) the active core is occupied only by cobasal-cylinder clusters, and (2) the largest cylinder in a given axial zone has a radius  $\geq RP(LR)$ , the edge of the radial power pattern. (A problem with input not meeting these specifications will be rejected.) Subroutine CYLCOR later orders (in array RJ360) the tracking cylinders by zone and by radius within a zone, and sets up in array KCMIN(26) the initial addresses in array RJ360 of the ordered-radius lists corresponding to each of the ( $\leq 26$ ) axial zones; elsewhere in this array (equivalenced to J360) are the corresponding region numbers. TAPGEN, having access

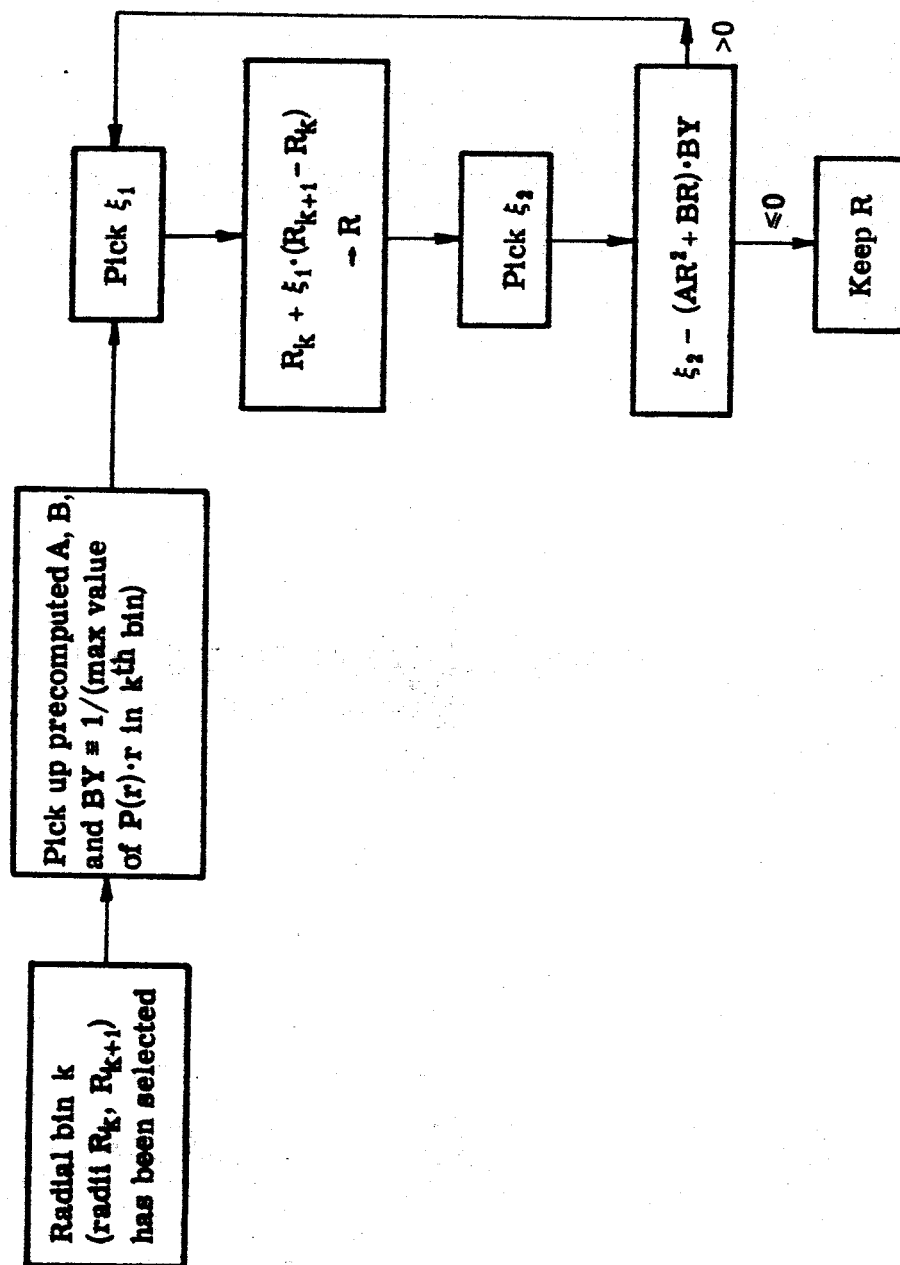


Fig. 6 — Selection of Radius  $R$  within a Radial Bin (360° Geometry)

to the previously determined axial zone (KAX), searches in one of the ordered-radius portions of RJ360 to locate the radial bin containing R, then picks up the integer identifier of the pertinent tracking region from a corresponding entry in J360.

### 5.1.2 30-Degree Geometry

The particles are generated within an "imaginary" or implied configuration of  $\leq 3900$  "micro" fuel cylinders, arranged in coaxial packets of  $\leq 10$  fuel cylinders (20 radii) per stage,  $\leq 26$  stages per fuel rod,  $\leq 15$  fuel rods per problem. The locations of the fuel rods are understood to satisfy the general restrictions discussed under Fig. 3, Chapter 4. Source particles are selected at random from the whole configuration, following input-specified distributions as follows.

1. Each fuel rod is assigned an a priori number PV representing its relative fissioning rate. The program selects locations from the fuel cylinders in the  $K^{\text{th}}$  fuel rod with probability proportional to  $PV(K)$ , and rejects points which lie outside the 30-degree tracking space between the reflection planes.
2. The axial distribution is defined exactly as in the 360-degree geometry, via a table of  $\leq 50$  (PZ,ZP) pairs. Source generation is suppressed in the gaps between stages.
3. The relative numbers of fissions in each of the  $\leq 10$  fuel cylinders is specified by a "micro-radial" distribution  $PFC(10,3)$ ; there may be three different micro-radial distributions in a given problem. All of the stages in a given axial zone must have the same micro-radial distribution.

An important automatic feature of the program is the identification of "macro" or tracking-geometry regions corresponding to the various generated particle locations. This identification proceeds primarily via a micro-to-macro assign-



ment procedure in subroutine CYLCOR. To aid in the discussion of this procedure, we next describe the macro-cylinder input and the limitations imposed thereon by VANGEN (these restrictions apply only to the geometry input to VANGEN, which is a subset of the entire problem geometry; in particular, only cylinders in the source regions need be included in this subset).

Fig. 7(a) illustrates the detailed structure of a fuel stage for a problem with four micro-cylinders per stage [signaled in the input as NACTIV ( $\equiv$  number of active radii) = 8]. Figs. 7(b) through 7(f) are also based on this number of fuel cylinders per stage; the figures and their captions illustrate the following restrictions on the dimensions of the macro-cylinders within which sources may be generated.

1. Radii of macro-cylinders may coincide with the active radii, or lie in the inactive regions between fuel cylinders; they may not be intermediate between the two radii  $R(2n-1)$ ,  $R(2n)$  defining the  $n^{\text{th}}$  fuel "micro" cylinder. This ensures that no micro-cylinder will be only partially contained radially.
2. Macro-cylinders may contain other macro-cylinders with which they are cobasal (top and bottom) and coaxial.
3. Macro-cylinders may enclose several stages and their separations [Fig. 7(d)]; but to ensure proper recognition of the containment there must be some geometric clearance between the end-stages and the cylinder bases (these clearances can be automatically set equal to  $\epsilon/4$  by means of the special cylinder input format described below).
4. Cobasal cylinder-clusters can run the length of several stages [Fig. 7(e)] provided that rules 2, 3 are satisfied.

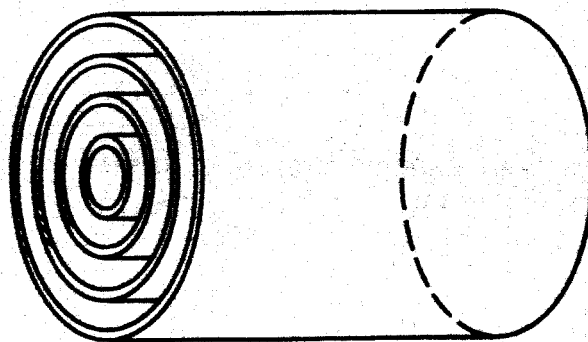


Fig. 7(a) — Fuel Stage with Four Fuel Cylinders; "Active" Radii Are  $R(1)$ ,  $R(2)$ ...,  $R(6)$

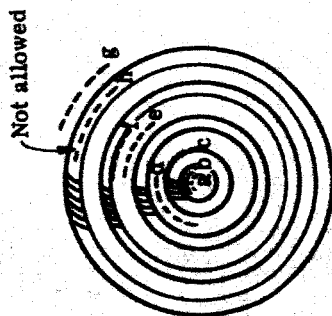


Fig. 7(b) — Top View. Dotted Area a-g Illustrate Some Permissible Macro-Cylinder Radii; h Is Not Permitted.

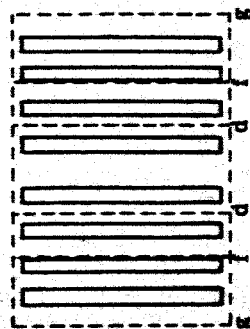


Fig. 7(c) — Illustrating Cobasal Macro Cylinders d, f, and g, enclosing 1, 1, and 2 Micro Cylinders, Respectively

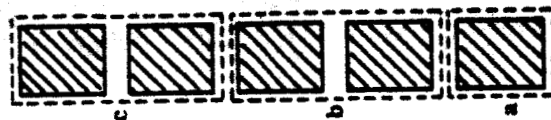


Fig. 7(d) — Macro Cylinders a, b, and c Enclose 4, 8, and 8 Micro Cylinders, Respectively (four cylinders/stage)

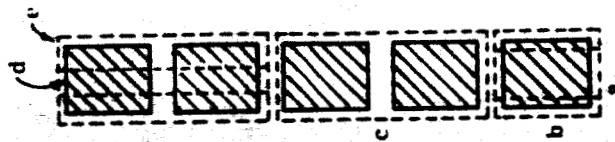


Fig. 7(e) — Macro Cylinders a, b, c, d, e Enclose 3, 1, 8, 2, and 6 Micro Cylinders, Respectively

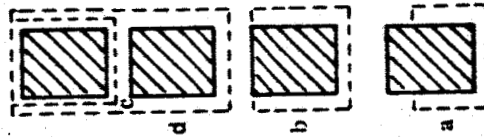


Fig. 7(f) — Macro Cylinders a, b, and d Are Not Permitted, because:  
a — a base intersects stage  
b — a base coincides with stage base  
d — contains another macro cylinder, with which it must be coaxial and coaxial

## 5.2 DIGRESSION ON CYLINDER-INPUT FOR VANGEN AND EZGEOM

The quantity of macro geometry data supplied to VANGEN (a subset of the total problem geometry) is first described by integers NBOX, NCYL, NREG, meaning the number of ordinary boxes, the number of pertinent cylinders, and the number of regions (for this program NREG may be the total number to be considered in the ATHENA problem, or merely the highest region-number in which a source particle may be generated). NCYL must be  $\geq 1$  for a  $360^\circ$  problem, but it may be zero in a  $30^\circ$  problem, in which case all generated particles are located in the appropriate ordinary boxes for proper labeling on the source tape.

Other quantities read in are: a list of radii  $R(K)$ ,  $K = 1, 2, \dots, \text{NRADII}$ ; base locations  $Z\text{BASE}(K)$ ,  $K = 1, 2, \dots, \text{NZBASE}$ ; heights  $HT(K)$ ,  $K = 1, 2, \dots, \text{NHT}$ ; and vertex coordinates  $XV(K)$ ,  $YV(K)$ ,  $K = 1, \dots, \text{NVERT}$ . Then if  $\text{NCYL} \geq 1$ , cards are read containing (for the  $K^{\text{th}}$  cylinder in the deck) the following six integers:

<u>Integer</u>	<u>Meaning</u>	<u>Value</u>
NEXT(K)	Number of the region external to this cylinder	$\geq 0$
JV(K)	Vertex index	$> 0$
JB(K)	Base index	$\neq 0$
JH(K)	Height index	$\neq 0$
JR(K)	Radius index	$> 0$
IREG(K)	Tracking region number	$> 0$

If NEXT = 0, this means the cylinder is straddling several regions, and a follow-up card is required (needed if this type of cylinder input is used in EZGEOM, card called for but its contents ignored in VANGEN).

The other integers in the list are used by the program as follows; let L in each case be the value of the pertinent integer.

**JV:** The cylinder's axis has coordinates  $XV(L)$ ,  $YV(L)$ . (36)

**JB:** (a) If  $L > 0$ , the base of the cylinder is at  $Z = ZBASE(L)$ ; (37a)

(b) If  $L < 0$ , the base of the cylinder is understood to lie  $\frac{1}{4}\epsilon$  below the  $|L|^{th}$  stage, i.e.,

$$Z = (Z_{\min} \text{ of stage } 1) + (|L| - 1) \cdot (H + \epsilon) - \frac{1}{4}\epsilon, \quad (37b)$$

where  $H$  is the active height of a stage, and  $\epsilon$  is the gap between stages.

**JH:** (a) If  $L > 0$ , the height of the cylinder is  $HT(L)$  (38a)

(b) If  $L < 0$ , the height of the cylinder is such as to enclose

$|L|$  stages plus  $(|L| - 1)\epsilon$  (gaps) plus  $\frac{1}{2}\epsilon$ :

$$\text{height} = |L| \cdot (H + \epsilon) - \frac{1}{2}\epsilon. \quad (38b)$$

All cylinder-input to **VANGEN** must be in this six-integer format, accompanied by appropriate lists of radii, vertex coordinates, etc. The program **EZGEOM** will accept cylinder input in **VANGEN** format and/or **EZGEOM** format (Section 7.3) with the restriction that all data in **VANGEN** format be in a single packet immediately following the ordinary-region input. Other cylinder input to **EZGEOM** can appear anywhere in the nonordinary-region deck. Parameters of cylinders described in **VANGEN** format for **EZGEOM** must be within a specified range (see p. 97).

The macro-cylinder input (if any) to a 30-degree **VANGEN** problem is processed in subroutine **CYLCOR**. The principal computation done here is the assignment of each of the  $\leq 3900$  micro fuel cylinders to an enveloping macro-cylinder, for use in later assignment (in subroutine **TAPGEN**) of tracking regions. For each micro-cylinder not so assignable, a flag is set up to direct **TAPGEN** to localize a generated point in the appropriate input ordinary region.

The micro-to-macro assignment proceeds via a single scanning of all the micro-cylinders, each of which is labeled with three indices: LV ( $\leq 15$ , vertex location); LS ( $\leq 26$ , axial stage location); and LF ( $\leq 10$ , fuel-cylinder order within a stage). The fuel cylinder (LV,LS,LF) is determined to be wholly contained within a macro-cylinder N (or what is the same thing, to lie in the space between macro-cylinder N and N's internal cylinder N', if any); or else it is found to be not so contained in any of the input macro-cylinders. In the first instance, the appropriate element of a triply subscripted array, JCOR(LV,LS,LF), is set equal to N; otherwise it is equal to zero.

Other functions performed by CYLCOR for this geometry are:

1. Test that according to the geometry supplied for VANGEN no cylinder contains anything other than a coaxial, cobasal cylinder;
2. Test against multiple definition of a cylinder;
3. Test against larger radius of contained cylinder;
4. On option, count up and print out (a) the numbers of micro-cylinders which have been assigned to each macro-cylinder of the input, (b) the number of unassigned micro-cylinders.

Errors found in any of the four items described above lead to diagnostic print-outs and problem termination.

Prior to the generation of source particles, the input quantities PV(K), (K = 1, 2, ..., NFVERT = number of fuel-rod vertices) are normalized in subroutine PWRPAT to yield PVN(K), where

$$\sum_{K=1}^{NFVERT} PVN(K) = 1.0.$$

Similarly, each of the NMDIST ( $\leq 3$ ) micro-radial distributions is normalized, yielding NMDIST groups of NFCYL ( $\leq 10$ ) entries each, with

$$\sum_{J=1}^{NFCYL} PFN(J,I) = 1.0,$$

for  $I = 1, \dots, NMDIST$ . These normalized tables are used in TAPGEN to make selections of fuel rod and fuel cylinder for each source history in accordance with the input power patterns.

The sequence for picking a source location in 30-degree geometry is as follows:

1. Pick a z-coordinate as described for the 360-degree geometry, above.
2. Determine the stage index (LS) and axial zone (KAX) corresponding to this z.
3. Pick a random number  $\xi$ ; select a vertex location (LV) such that

$$\sum_{j=1}^{LV-1} PVN(j) \leq \xi < \sum_{j=1}^{LV} PVN(j). \quad (39)$$

4. Retrieve (from input) the micro-radial distribution type MDIST (=1,2, or 3) corresponding to axial zone KAX.
5. Pick a random number  $\xi$ ; select a fuel cylinder index (LF) such that

$$\sum_{j=1}^{LF-1} PFN(j,MDIST) \leq \xi < \sum_{j=1}^{LF} PFN(j,MDIST). \quad (40)$$

6. Pick a location uniformly in the annular area centered at XV(LV), YV(LV), between radii  $R(2*LF-1)$  and  $R(2*LF)$ .

7. If the location so selected lies within the  $30^\circ$  tracking region, keep it; otherwise pick a new vertex (step 3).

### 5.3 ENERGY SELECTION AND REGION SPLITTING

Once a particle location (x,y,z, and region number) has been selected for a given history in either geometry, a neutron energy is chosen (if neutron sources are called for in the input), and NN source "particles" are generated and entered in a neutron buffer array in core. The value of NN may be  $\geq 0$ ; it is computed as

$$NN = [1/WTN + \xi], \quad (41)$$

where WTN is the region-dependent weight to be used in the associated ATHENA problem,  $\xi$  is a random number, and the brackets imply taking the integral part of the contained expression. The complete description of a source particle is a set of nine numbers, viz., history number, x, y, z,  $w_x$ ,  $w_y$ ,  $w_z$ , energy, and region number;  $w_x$ ,  $w_y$ ,  $w_z$  are the direction cosines of the particle velocity, chosen isotropically. If NN for a given history is zero, no particles are generated and the pertinent history number does not appear in the neutron buffer nor on the resulting neutron source tape. If  $NN > 1$ , several particles will appear bearing the same location and history number; however, the additional particles will have independently selected energies and directions.

Since the spatial distribution of the source neutrons and the primary (fission-related) gammas is assumed to be the same, the same location is used for generating gamma sources, which are stored in a separate buffer array and written out on a separate source tape. Region splitting is carried out as for neutrons, here using the gamma region-dependent weights.

#### 5.3.1 Neutron Energy Selection – Energy Importance Sampling

Neutrons are normally selected from a portion of the fission spectrum as approximated by Cranberg,<sup>6</sup> i.e., in which



$$N(E) dE = 0.453 e^{-E/0.965} \sinh \sqrt{2.29E} dE, \quad (42)$$

where  $E$  is the energy in Mev. The selection is made via subroutine PFISPC, using a rejection technique due to Kalos:<sup>7</sup>

Pick an  $x$  from a truncated exponential distribution, i.e., so that

$$p_1(x) dx = \frac{e^{-x} dx}{e^{-x_1} - e^{-x_2}}, \quad x_1 \leq x \leq x_2, \quad (43)$$

and a  $y$  from an exponential distribution,

$$p_2(y) dy = e^{-y} dy, \quad 0 \leq y < \infty. \quad (44)$$

If  $-ax + (y-bx-c)^2 \leq 0$ , choose  $E = \gamma x$ ; otherwise reject and repeat from Eq. 43.

To obtain the distribution (Eq. 42) and ensure a maximum efficiency for the rejection technique, the parameters  $a$ ,  $b$ ,  $c$ ,  $\gamma$  have been evaluated as follows, and used in PFISPC:

$$a = 4.572573$$

$$b = 1.069179$$

$$c = 1.069179$$

$$\gamma = 1.99675$$

and in Eq. 43,  $x_1 = E_L/\gamma$ ,  $x_2 = E_U/\gamma$ . The call to PFISPC with arguments  $E_U$ ,  $E_L$  results in selecting an energy  $E$  from the truncated fission spectrum,  $E_L \leq E \leq E_U$ .

Since ATHENA permits energy importance sampling, the source generator is equipped to modify the a priori fission spectrum appropriately. This is done by defining in the VANGEN input as many as 20 neutron energy bins ( $\leq 21$  energy limits) with corresponding energy weights  $WEN(J)$ ,  $J = 1, 2, \dots, NNBINS \leq 20$ .

VANGEN computes the fission fractions, corresponding to each neutron bin, by interpolation in stored tables\* of energies EFF(K), K = 1, 2, ..., NEFF ≤ 75 and the cumulative fission spectrum FABOVE(K), K = 1, ..., NEFF.

$$F = \text{FABOVE}(K) = \frac{\int_{\text{EFF}(K)}^{18.5 \text{ Mev}} N(E) dE}{\int_{9 \times 10^{-4} \text{ ev}}^{18.5 \text{ Mev}} N(E) dE} \quad (45)$$

The interpolation in F is semilogarithmic, i.e., it is assumed that between consecutive entries F<sub>1</sub>, F<sub>2</sub> in the table

$$F(E) = F(E_1) e^{-c(E-E_1)}, \quad (46)$$

$$\text{where } c = \frac{\ln(F_1/F_2)}{E_2 - E_1}.$$

The a priori fission fraction between E<sub>a</sub> and E<sub>b</sub> is then |F(E<sub>a</sub>) - F(E<sub>b</sub>)|. VANGEN computes the a priori fission fractions, then the modified fission fractions FFMOD(J) = FFRAC(J)/WEN(J). These are then normalized by division by Σ FFMOD(J), and the normalized modified fission fractions are stored as a monotonically increasing array

$$\text{PNL}(J) = \sum_{n=1}^J (\text{normalized modified fission fraction})_n.$$

---

\*These tables are compiled into the program. They are consistent with Eq. 42. On option, different tables of EFF and FABOVE can be read in to override the program data.

Hence  $PNL(1)$  = fraction of times that a neutron will be selected from bin 1,  
 $[PNL(2) - PNL(1)]$  = fraction of times that a neutron will be selected from bin 2,...,  
 $PNL(NNBINS) = 1.0$ .

Because the rejection technique may be slow if  $E_U \approx E_L$ , energies within a bin having a fission fraction  $< 0.01$  are selected from a truncated exponential having a slope determined by the local slope of the cumulative fission spectrum. Thus if neutron bin  $J$ , bounded by energies  $E_J$  and  $E_{J+1}$ , is this narrow, the quantity

$$BF(J) = \frac{\ln[F(J)/F(J+1)]}{E_{J+1} - E_J}$$

is stored; for wider bins  $K$ ,  $BF(K) = 0$ . In the neutron-selection portion of TAPGEN, a neutron bin  $L$  is chosen as that satisfying

$$PNL(L-1) \leq \xi < PNL(L). \quad (47)$$

Then if  $BF(L) = 0$ , PFISPC is used to select an energy; otherwise  $c = BF(L)$ , and the energy is selected as

$$E = -(1/c) \ln \left\{ (1-\xi) e^{-cE_1} + \xi e^{-cE_2} \right\}, \quad (48)$$

where  $E_1$  and  $E_2$  are the limits of neutron bin  $L$ .

This is one device which may be used to generate an almost monoenergetic neutron source tape. Its use (i.e., implicit specification of a fission fraction  $< 0.01$ ) is not permitted for energies lower than 1.0 Mev, since the local representation of the cumulative fission spectrum as a pure exponential does not reflect accurately the low-energy shape of the fission spectrum. However, monoenergetic particle source tapes with arbitrary energy can be generated by appropriate use of the gamma branch of the code, described next.

### 5.3.2 Gamma Energy Selection – Energy Importance Sampling

VANGEN computes the instantaneous gamma spectrum corresponding to an instant following an arbitrary reactor operating history. This history will be denoted as  $P(t)$ , representing total fissioning rate as a function of time; it is specified in input via tables of  $P(t)$  and  $t$ , with linear interpolability assumed. The data describing delayed-gamma emission rates following  $U^{235}$  fissioning are embodied in tables specified here as  $\Gamma(\tau, E_j^\gamma)$ , denoting the gamma emission rates in photons/(sec-fission) as functions of time and gamma energy. Such tables [called  $G(I, J)$ ,  $I \leq 80$ ,  $J \leq 15$ ] are at present compiled as program data; they can be printed out on option. The sources of these data, and discussions thereof, can be found in Reference 8. The present data cover 78 post-fission  $\tau$ 's from  $10^{-18}$  sec to 10 hr, and 13 gamma energies representing the fission-gamma source from 0.02 Mev to 7.5 Mev. On option, input data can be read in to override the internal program data.

Given tables describing  $P(t)$  (fissions/sec) and  $\Gamma(\tau; E_j^\gamma)$  (photons/sec-fission), subroutine DELGAM computes

$$\dot{\gamma}_j = \int_{t_i}^{t_f} P(t) \cdot \Gamma(t_f - t; E_j^\gamma) dt, \quad (49)$$

with the quantities in the integrand approximated as

$$P(t) = a_n \cdot t + b_n \quad (50)$$

over the  $n^{\text{th}}$  time-bin in the reactor history, and

$$\Gamma(\tau; E_j^\gamma) = g_{sj} \tau^{-c_{sj}} \quad (51)$$

for the  $j^{\text{th}}$  energy, in the  $s^{\text{th}}$  time-bin of the delayed-gamma tables. The number of delayed-gamma energies present in the  $G(I, J)$  matrix is called NCOL. Thus

NCOL integrals of the type (Eq. 49) are computed in a single pass through the time-range from  $t_1$ , the first input reactor-power time, to  $t_f$ , the input-specified instant for which sources are required. The time-mesh for the reactor history can be arbitrary, provided that consecutive instants in the table are nondecreasing; discontinuities in the reactor power are permitted. If neutron histories are also called for,  $t_f$  must not exceed the last time specified in the reactor history. If in the integrations a delay-time  $\tau_g$  is encountered, greater than the last time-entry in the matrix for  $\Gamma(\tau; E^\gamma)$ , then to compute the  $\Gamma$ 's the program extrapolates (linearly on a log-log scale) to  $\tau_g$ , using the power fits (Eq. 51) valid for the last two time-entries in each  $E^\gamma$  column.

Let  $\dot{\gamma}_j$  denote the results of the integrations (Eq. 49). Their relative magnitudes represent the a priori primary-gamma spectrum at  $t_f$ . Given a table of gamma energy bins and corresponding weights, VANGEN computes modified sources  $\dot{\gamma}'_j = \dot{\gamma}_j / \text{WEG}$ , where WEG is the energy weight corresponding to  $E_j^\gamma$ . The  $\dot{\gamma}'_j$  are then normalized so that

$$\sum_{j=1}^{\text{NCOL}} \dot{\gamma}'_j = 1.0,$$

and the results stored in a table of cumulative, normalized modified source intensities, PGL(K),  $K = 1, \dots, \text{NCOL}$ ;  $\text{PGL}(\text{NCOL}) = 1.0$ . In the source-generation, the  $J^{\text{th}}$  of the NCOL discrete energies is selected, by choosing a random number  $\xi$ , then determining J such that

$$\text{PGL}(J-1) \leq \xi < \text{PGL}(J). \quad (52)$$

Region-dependent particle splitting and Russian roulette are done for gammas as for neutrons; zero, one, or several particles may be generated with a given history number and location. If several particles are generated, their energies are selected (from the modified spectrum) independently, as are their isotropic directions.

#### 5.4 NOTE ON ENERGY-BIN IDENTIFICATION FOR WEIGHT ASSIGNMENTS

Since particle generation (in VANGEN), tracking and scoring (in ATHENA), secondary-gamma production (in GASP), and neutron-interaction editing (in NATALE) are all dependent upon energy weights, these programs should all use weights which are the same function of energy. The programs are generally compatible in this respect, but it is possible to set up a pathological case based on a difference in the handling of exact equality in an energy-bin search. The pertinent subroutines are called BINLOC in VANGEN, and SEEK in the other programs. Their operation is illustrated in Fig. 8, (a) and (b).

Because of this difference, VANGEN must not be set up to generate (with finite probability) source particles having energies exactly coinciding with energy-weight-bin boundaries.

When a 100-particle buffer has been filled, or when particles for the required numbers of both neutron and gamma histories have been generated, 100-particle records are written out on the appropriate source tapes. Printer output, listing the particle parameters, is also available on option for a specified number of groups of 100-particles; any unfinished group of this specified output is also printed.

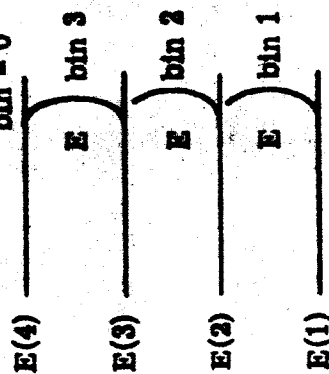
Finally on option subroutine TALLY reads back the just-generated source tapes and prints out the numbers of neutrons and/or gammas generated, by tracking region and by energy-importance bin, along with theoretically equivalent quantities to provide checks on the spatial and energy importance sampling.

#### 5.5 TRANSMISSION OF FLUX-AT-A-POINT DATA TO COMMON DUMP TAPE

Primary-gamma ATHENA calculations of flux-at-a-point (Section 11.5.1) require an analytic representation of the spatial power distribution (360-degree geometry). In particular, the fissioning density per unit volume, normalized to unit

E\* Subroutine returns:

bin = 0



E\* Subroutine returns:

bin = -1

Fig. 8(a) — Subroutine BINLOC.

$E = E(n)$  is assigned to bin  $n$ ;  
exception: highest bin includes  
highest energy.

E\* SEEK gives error diagnostic  
"VALUE EXCEEDS TABLE,"  
prints E and array, and stops.

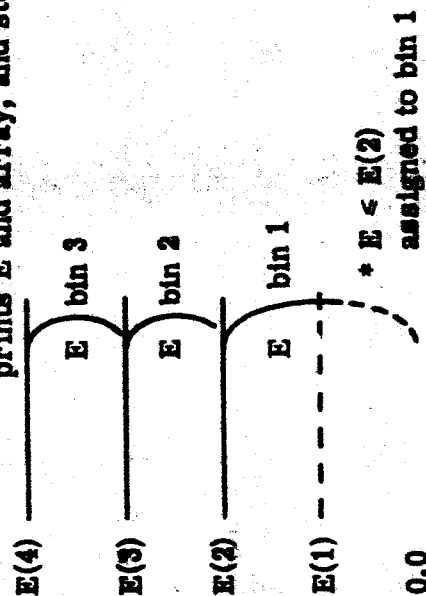


Fig. 8(b) — Subroutine SEEK.  
 $E = E(n)$  is assigned to bin  $n-1$ .

integral over the active volume of the core, is required. Since the nonnormalized power pattern is supplied as input for VANGEN, the required preprocessing is done in this program, and the results are transmitted via a dump tape for later use in ATHENA.

The transmitted tables are generated in subroutine PWRPAT. The axial range from ZMINC to ZU[-ZMINC + NSTAGE·(H+ε) - ε] is divided into 100 equal steps DELZ. A table of 101 values TZ(K) is then computed where

$$TZ(K) = \frac{P[ZMINC + (K-1) \cdot DELZ]}{\int_{ZMINC}^{ZU} P(z) dz} ; \quad K = 1, 2, \dots, 101. \quad (53)$$

(excluding ε's)

The P(z) are obtained by interpolation in the (nonnormalized) input table of the axial power pattern.

Similarly, a table of 101 values TR(K) is set up, representing the normalized radial power pattern at radial points separated by DELR = 0.01 R<sub>max</sub>:

$$TR(K) = \frac{P[(K-1) \cdot DELR]}{2\pi \int_0^{R_{max}} P(r) \cdot r dr} ; \quad K = 1, 2, \dots, 101. \quad (54)$$

Here the P(r) are obtained from the input radial power pattern. For an arbitrary point (R,Z) in the reactor core, TZ·TR ΔV represents the probability that a particle born in the core is born in the volume ΔV cm<sup>3</sup>, if the TZ and TR are obtained by interpolation in Z or R, and TZ is made zero for Z in any of the inter-stage gaps ε.



The following quantities, denoted as labeled common FAPC, are transmitted for later use (subroutine ADJ of ATHENA): TZ(101), TR(101), DELZ, DELR, NSTAGE, ZMINC, H, EPS, and DMMY(434). The last array serves to make the length of this labeled common agree with that in the other programs.

## 5.6 DESCRIPTION OF THE INPUT DATA FOR VANGEN

Integer and E-format floating numbers must be right-adjusted in the indicated fields.

### Card 1 (Format 3I10, E15.4, I15)

<u>Column</u>	<u>Item</u>
8-10	IGEOM = 30 or 360 (geometry type)
11-20	NNH = number of neutron histories
21-30	NGH = number of gamma histories
31-45	FNU = neutrons/fission ( $\approx 2.46$ )
46-60	LRN = starting random number (must be odd; if no input, code uses LRN = 1).

### Card 2 (Format 10I1, 10I5) Option Card

<u>Column</u>	<u>Option</u>
1	1: Print out delayed-gamma tables used; 0: omit printout
2	1: Print micro geometry input (30°) or radial power pattern (360°); also NSTAGE, ZMINC, H, EPS; 0: omit printout
3	1: Print macro geometry input; 0: omit printout
4	1: Print micro-to-macro assignments (30°) or ordering of core cylinders (360°); 0: omit printout
5	1: Call TALLY to read back and edit source tapes; 0: omit TALLY
6	2: Delayed-gamma data present, are to be read in to override program data; #2: no such data; program to use its own
7	2: Cumulative-fission-spectrum data present; #2: no such data; program to use its own
8	1: Print out fission-spectrum tables; 0: omit printout
9,10	Not used
11-15	Number of groups of 100-neutron printouts wanted
16-20	Number of groups of 100-gamma printouts wanted. N.B.: the last two items are right-adjusted to columns 15 and 20. A 3 in column 15 calls for 300 lines of printout.
21-60	Not used.

Delayed-Gamma Data (to be provided only if entry in column 6 of card 2 equals 2)

1. Dimensions of Matrix: NROW, NCOL (Format 2I5)

NROW = number of times in delayed-gamma table ( $\leq 80$ )

NCOL = number of gamma source bins [see (3) below] ( $\leq 15$ )

2. Post-fission times (in seconds, increasing):  $T(J)$ ,  $J = 1, \dots, NROW$  (Format 7E10.4)

3. NCOL + 1 bounding energies for source bins (in ev; bin-order increasing)  $E(K)$ ,  $K = 1, \dots, NE = NCOL + 1$  (Format 7E10.4)

Note: The output gamma energy for the  $K^{\text{th}}$  bin is  $EG(K) = \sqrt{E(K) \cdot E(K+1)}$ .

4. Delayed-gamma intensities, photons/(sec-fission), corresponding to 1st gamma bin and times  $T(1)$ ,  $T(2) \dots, T(NROW)$ . (Format 6E12.4).

Repeat (4), starting on a new card, for each additional gamma bin.

Cumulative Fission Spectrum Data (to be provided only if entry in column 7 of card 2 equals 2)

1. Number of energies in fission table, NEFF ( $\leq 75$ ) (Format I5)
2. Neutron energy (ev, lowest first) and fraction of neutrons above this energy (Format 2E20.8). One card per pair; No. of cards = NEFF.

Reactor Operating History

1. Number of instants for which reactor power is specified, LT ( $\leq 50$ ) (Format I5)
2. Time (seconds, increasing) and corresponding relative power (fissions/sec, not necessarily normalized. (Format 2E20.8.) One card per pair; LT cards.

3. Time (seconds) TF, for which sources are to be generated. (Format E20.8.)

Note: If NNH (card 1) is  $> 0$ , TF must be  $\leq$  last time listed above, and power at TF must be  $> 0$ .

Neutron Energy-Importance Data (to be supplied only if NNH  $> 0$ )

1. Number of neutron energy bins, NNBINS ( $\leq 20$ ) (Format I5)
2. Minimum energy (ev) of each bin, and corresponding energy weight (Format 2E20.8). One card per bin (lowest first); NNBINS cards. Lowest energy must be  $> 0.0009$  ev if internal fission-spectrum table is used.
3. Maximum energy (ev) of last bin (Format 1E20.8). Must be  $\leq 18.01E + 6$ .

Note: Fission fraction  $< 0.01$  requires bin  $E_{\min} \geq 1.0E + 6$ .

Gamma Energy-Importance Data (to be supplied only if NGH  $> 0$ )

1. Number of gamma energy bins, NGBINS ( $\leq 20$ ) (Format I5)
2. Minimum energy (ev) of each bin, and corresponding energy weight (Format 2E20.8). One card per bin (lowest first); NGBINS cards
3. Maximum energy (ev) of last bin (Format 1E20.8). ( $\geq 10.E + 6$ ).

Axial Power Pattern

1. Number of axial points specified, LZ ( $\leq 50$ ) (Format I5)
2. Z-coordinate (cm, lowest first), and corresponding relative reactor power (fissions/cm<sup>3</sup>) (Format 2E20.8). One card per pair, LZ cards.

Notes: (a) Minimum Z specified should be  $\leq$  ZMINC, minimum Z of stage 1. (b) Maximum Z specified should be slightly  $>$  maximum Z of highest stage. (c) Input table need not reflect the suppression of sources

in the gaps between stages; program overrides input tables to put zero sources there.

Axial Dimensions (Format I5,3E15.8). All dimensions in cm

<u>Columns</u>	<u>Item</u>
4,5	Number of stages, NSTAGE ( $\leq 26$ )
6-20	Minimum Z of stage 1, ZMINC
21-35	Height of one active stage, H
36-50	Gap between stages, EPS (Note: Should not be less than 0.0004 cm in any problem with NSTAGE > 1.)

Axial-Zone Indices (Format 14I5)

1. Number of zones, and first stage index in each zone (through zone 13)

<u>Columns</u>	<u>Item</u>
4,5	Number of axial zones, NAXZON ( $\leq 26$ )
10	Minimum stage index in 1st zone (=1)
14,15	Minimum stage index in 2nd zone
19,20	Minimum stage index in 3rd zone
Etc.	Etc.

2. Continuation (14I5) if NAXZON > 13.

Distinct Vertex (Axis) Locations for Cylinders

1. Number of fuel-rod vertices (NFVERT,  $\leq 15$ ), and total number of vertices (NVERT,  $\leq 50$ ) to be specified. (Format 2I5.)
2. x-coordinate and y-coordinate of each vertex (Format 6E12.4). Sequence XV(1), YV(1), XV(2), YV(2), XV(3), YV(3), etc; three vertices per card. List fuel-rod vertices first.

Notes: (a) For 360° problem, XV(1) = 0.0, YV(1) = 0.0. (b) For 360° problem, in-core cylinders are to have vertex type 1; a vertex type n, (n≠1) may also have XV = 0, YV = 0 (for specification of out-of-core cylinders on same axis).

**Distinct Radii (same list serves micro and macro geometry descriptions)**

1. Number of active radii, NACTIV ( $\leq 20$ ; in  $30^\circ$  problem, NACTIV must be even, and  $= 2 \times$  number of fuel cylinders in stage), and total number of radii, NRADII ( $\leq 50$ ) (Format 2I5).
2. Radii R(J), J = 1, ..., NRADII (Format 6E12.5).

**Note:** List active radii (those defining the micro fuel cylinders) first, in increasing order; then all others.

**Fuel-Rod Power Data ( $30^\circ$  problems only)**

1. Relative power per fuel vertex, PV(J), J = 1, ..., NVERT (Format 6E12.4).  
Enter values in order corresponding to vertex locations.  
**Note:** Assume each fuel rod is complete, i.e., do not modify a priori power if rod is cut by reflecting plane(s).
2. Number of micro-radial distributions ( $\leq 3$ ) (Format I5)
3. Relative power (fissions/sec) in each fuel cylinder, according to micro-radial distribution 1. PFC(J,1), J = 1, ..., NACTIV/2 (Format 6E12.4).  
Entry for innermost cylinder first. Repeat (3), starting on a new card, for each additional micro-radial distribution.
4. Micro-radial distribution type (1, 2, or 3) corresponding to each axial zone: MDIST(K), K = 1, ..., NAXZON (Format 36I2).

**Radial Power Pattern ( $360^\circ$  problems only)**

1. Number of radial points specified, LR ( $\leq 50$ ) (Format I5).
2. Radial position and corresponding power, RP(J), PR(J), J = 1, ..., LR (Format 2E20.8). 1 card per pair, LR cards.

**Note:** If  $RP(1) > 0$ , no particles will be generated in  $R < RP(1)$ .

## Macro Geometry Input

1. Numbers of regions described in VANGEN input (Format 3I5).

<u>Column</u>	<u>Item</u>
1-5	Number of ordinary regions, NBOX ( $\leq 80$ )
6-10	Number of cylinders, NCYL ( $\leq 127$ ); NCYL must $> 0$ for 360° problem
11-15	Maximum region-number, NREG ( $\leq 200$ ).

2. Bounding planes for each ordinary region (to be supplied only if NBOX  $> 0$ ).

One card per region: XMIN(J), XMAX(J), YMIN(J), YMAX(J), ZMIN(J), ZMAX(J); (J = 1, ..., NBOX) (Format 6E12.5). Region numbers implied by order in which cards appear.

3. Number of distinct cylinder-base z-coordinates (NZBASE), and number of distinct cylinder-height values (NHT). (Format 2I5).

4. Values of distinct cylinder-base z-coordinates (supply only if NZBASE  $> 0$ ). ZBASE(J), J = 1, ..., NZBASE (Format 6E12.4).

5. Values of distinct cylinder heights (supply only if NHT  $> 0$ ). HT(J), J = 1, ..., NHT (Format 6E12.4).

6. Macro-cylinder input (supply only if NCYL  $> 0$ ) (Format 6I5, 47X, I3).

Note: See discussion of Eqs. 36 through 38 in Section 5.2.

<u>Column</u>	<u>Item</u>
1-5	External macro region number, NEXT (=0 for straddling cylinder)
6-10	Vertex index, JV ( $> 0$ )
11-15	Base index, JB ( $\neq 0$ ); $< 0$ for 360° in-core
16-20	Height index, JH ( $\neq 0$ ); $< 0$ for 360° in-core
21-25	Radius index, JR ( $> 0$ )
26-30	Number of regions straddled (= 0, 2, or 4)
31-77	Not used
78-80	Tracking region IREG ( $> 0$ )

Straddling-Regions Card (supply only if NEXT, column 5 above, is zero)

(Format 4I5). Region numbers of the two or four regions straddled, in any order.  
(This card, needed in EZGEOM, is read but ignored in VANGEN.)

Neutron Region Weights (supply only if NNH > 0)

1. Number of distinct region-dependent neutron weights, NWRN ( $\leq 20$ )  
(Format I5).
2. Distinct region-dependent neutron weights, WRN(J), J = 1, ..., NWRN  
(Format 6E12.5).
3. Neutron-weight index for each region, KWRG(L), L = 1, ..., NREG  
(Format 14I5).

Gamma Region Weights (supply only if NGH > 0)

Note: Same format as for neutron region weights.

1. Number of region gamma weights, NWRG ( $\leq 20$ ) (Format I5).
2. Distinct region gamma weights, WRG(J), J = 1, ..., NWRG (Format 6E12.5).
3. Gamma-weight index for each region, KWRG(L), L = 1, ..., NREG  
(Format 14I5).

Logical Input-Output Assignments for VANGEN

	<u>IBM-7094</u>	<u>CDC-1604-A</u>	
Logical	5	5	Input medium (e.g., card reader)
Logical	6	6	Output medium (e.g., printer)
Logical	1	1	Inter-program dump tape
Logical	3	7	Neutron source tape
Logical	4	8	Gamma source tape.

## **6. THE INPUT SEQUENCER PROGRAM, MEZDA**

**MEZDA** is an overlay program which facilitates the execution, in sequence, of programs **EZGEOM**, **TESTG**, **DATORG**, and **INPUTD**. The end result is a dump tape containing all of the processed geometry, composition, and problem-parameter input needed to run an **ATHENA** problem.

The sequence of the required processing of the dump tape is as follows.

1. (a) Write on dump tape via operation of real **VANGEN** program (required if primary-gamma problem with point detectors);  
or  
(b) Write on dump tape via operation of simulated **VANGEN** routine in **MEZDA**.
2. Run **EZGEOM**.
- 3., 4. Run **TESTG** (optional) and **DATORG**, in either order.
5. Run **INPUTD**.

**EZGEOM** must precede **DATORG**, which must precede **INPUTD**; **TESTG** can be run at any time after **EZGEOM**. A fully processed tape can have a new (e.g., corrected) **DATORG** written onto it, which then would necessitate repeating **INPUTD**. If **EZGEOM** is written over, all subsequent programs must be repeated.

The input to **MEZDA** consists of a series of program-name cards, each followed by the appropriate program input. Thus supposing option 1(b) above were chosen,



the MEZDA input would be:

1. VANGEN name card: Hollerith VANGEN, columns 13-18 (no data)
2. EZGEOM name card (columns 13-18)  
EZGEOM data (see Chapter 7)
3. TESTG name card (columns 13-17)  
TESTG data (see Chapter 8)
4. DATORG name card (columns 13-18)  
DATORG data (see Chapter 9)
5. INPUTD name card (columns 13-18)  
INPUTD data (see Chapter 10).

Logical Input-Output Assignments for MEZDA

<u>IBM-7094</u>	<u>CDC-1604-A</u>	
5	5	Input medium (reader)
6	6	Output medium (printer)
1	1	Dump tape
7	2	Scratch tape (on CDC) or Disk (on IBM)
-	3	MEZDA program tape (CDC version only)
8	13	Element Data Tape.

## 7. THE ORGANIZATION OF THE GEOMETRY DATA (EZGEOM)

Monte Carlo programs track simulated particles through a specified geometrical configuration, undergoing all the interactions that an actual particle is expected to undergo. The particle flight may pass through media having different properties. Therefore, it is of primary importance to know at all times in which medium the particle is, when the particle leaves the medium, and which medium it will be entering. Different media may be described as containing given material compositions in three-dimensional geometrical figures.

However, it is necessary to decompose these figures into particular geometrical forms which can be handled by the ATHENA program, i.e., nonintersecting rectangular parallelepipeds, right cylinders, spheres, and right wedges.

The EZGEOM program processes the input which consists of the description of the desired configuration by means of these elementary geometrical forms and stores the information into tables for rapid data access in subsequent Monte Carlo programs.

### 7.1 DEFINITIONS AND NOTATION

The three-space coordinate system used in describing the geometry is a Cartesian right-handed coordinate system. The  $x$ ,  $y$ ,  $z$  directions will be described as  $x_1$ ,  $x_2$ ,  $x_3$ .

The entire three-dimensional space is initially decomposed into a set of rectangular parallelepipeds whose bounding planes are parallel to the coordinate axes. These parallelepipeds are called ordinary regions and are described by the coordinates of their six bounding planes:  $x_1^\alpha, x_1^\beta$  with  $i = 1, 2, 3$ , and  $x_1^\alpha \leq x_1^\beta$ .

Any elementary geometrical form which is completely described in the input by a vertex  $V(x_1, x_2, x_3)$  and a set of vectors and scalars is called a nonordinary region. Nonordinary regions presently handled by EZGEOM and geometry-tracking routines are spheres, right cylinders, rectangular parallelepipeds, and right wedges.

Due to storage restrictions and word length requirements, the following rules must be observed when preparing EZGEOM input.

1. Nonordinary regions (other than straddling cylinders, cf. Chapter 4) must be wholly contained in either an ordinary or a nonordinary region. Due to possible round-off errors, it is suggested that no surface of a contained region be closer to any surface of the containing region than  $10^{-6}$  times the maximum coordinate found on the surface of the containing region. Note that the geometry is first decomposed into ordinary regions. Hence, a nonordinary nonstraddling region may contain a set of nonordinary regions, but must eventually be itself part of a set of regions which are wholly contained in an ordinary region.
2. The total number of ordinary regions must be  $\leq 80$ .
3. The total number of regions must be  $\leq 200$ .
4. At most, 127 nonordinary regions may be used.
5. A nonordinary nonstraddling region I must be wholly contained in another region E. Let region E be defined as the region external to I. At the most, seven such regions may have E as an external region. We will say that any region may see only seven regions. In turn, each of

these regions may see, at most, seven regions. A straddling cylinder partially contained in an ordinary region is counted as one of its  $\leq$  seven internal regions.

6. The geometry input must be submitted as follows: first, specify the integers NBOX, NCYL, NREG, denoting the number of ordinary regions, the number of cylinders to be described using the VANGEN-type format (cf. Chapter 5), and the total number of regions in the problem. Then define the ordinary regions, which must be entered in order and numbered from 1 to NBOX. Then (if  $NCYL > 0$ ) define NSTAGE, ZMINC, and all other data pertinent to the VANGEN-type cylinder input, this to be followed by the appropriate description of NCYL cylinders. The order of these tracking-region numbers is immaterial. Finally, enter the data for the remaining  $NREG - (NBOX + NCYL)$  regions in any order.
7. The data required to describe the cylinders in VANGEN format have been described in Chapter 5. For other type regions, and cylinders in EZGEOM format, the data required for each type are the region number, the external region number, and the following information.

**a. Spheres**

(x,y,z) coordinates of the center, and the radius.

**b. Right Cylinders**

The (x,y,z) coordinates of the center of the axis, the radius, the half-height, and either the external region number, or (if straddling), the number -2 or -4, followed (in this case) by a follow-up card bearing the 2 or 4 external-region numbers.

**c. Rectangular Parallelepipeds**

Specify the coordinates of the vertex V (one of the corners) and a set of three mutually perpendicular vectors,  $\underline{a}_1$ , representing the vectors

radiating away from the vertex. The bounding planes need not be parallel to the coordinate planes.

#### d. Right Wedges

The input is the same as for the nonordinary rectangular parallelepipeds. However, the first two vectors describe the two legs of the right triangle of the wedge.

## 7.2 TECHNICAL DESCRIPTION

Subroutine RDDTA reads the geometry input and copies each region description onto a scratch tape, accumulating the total number of straddling regions necessary for computing the length of Table 2 in advance. RDDTA converts the cylinder input described in VANGEN format to EZGEOM format, i.e., in terms of vertex at center of cylinder, radius, and half-height.

The EZGEOM routine considers first the ordinary regions and proceeds to find the regions adjacent to each side of the ordinary parallelepipeds, starting with region number 1.

Let  $x_{1,m}^{\alpha}, x_{1,m}^{\beta}$  be the coordinates of the six bounding planes of the ordinary region,  $m$  ( $1 \leq m \leq M$ ,  $M$  being the total number of ordinary regions). The routine starts with  $x_{1,1}^{\alpha}$  and compares it to  $x_{1,m}^{\beta}$  for  $m = 2, 3, \dots, M$ .

Suppose that  $x_{1,1}^{\alpha} = x_{1,m}^{\beta}$ , then the  $x_1^{\alpha}$  face of region 1 and the  $x_1^{\beta}$  face of region  $m$  are on the same plane. This case is illustrated by Fig. 9.

It is necessary to determine whether or not the two faces have an area in common. Hence, the program proceeds to test:

1.  $x_{2,1}^{\alpha} \leq x_{2,m}^{\beta}$ . If greater than or equal, there is no overlap and the routine considers the next region (Fig. 9 and Case a of Fig. 10). If less than, then the second test is tried.

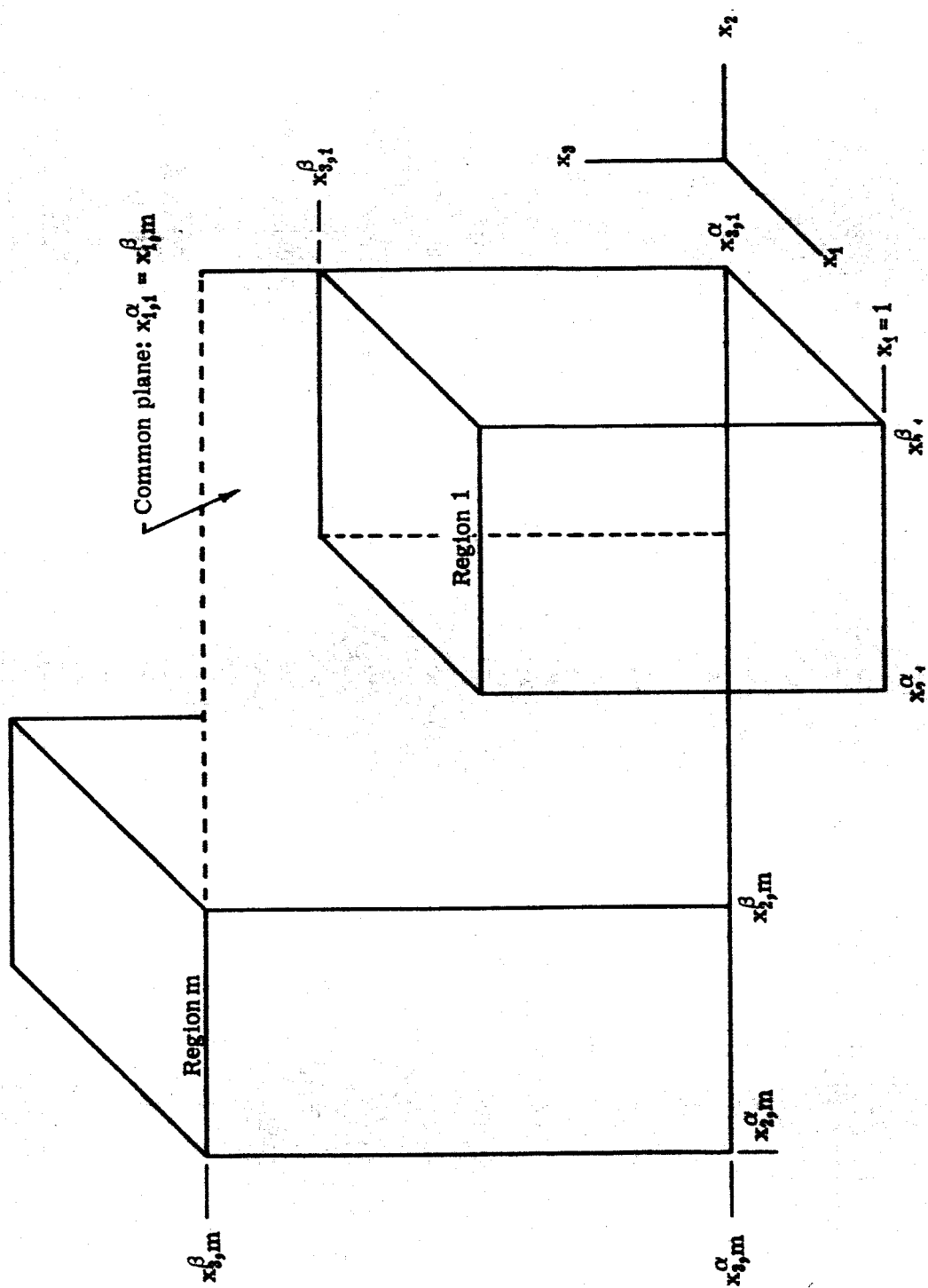
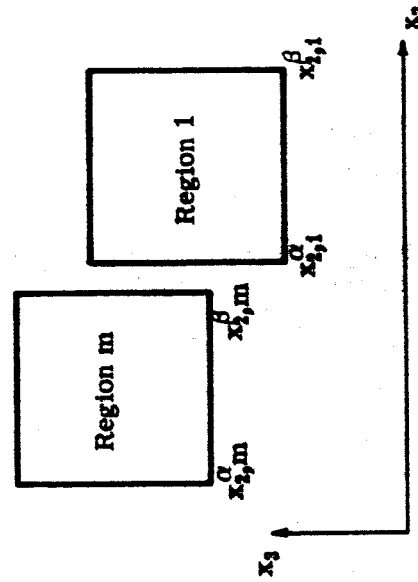


Fig. 9 — Case where Regions 1 and m Have a Face Lying in a Common Plane ( $x_1^{\alpha} = x_1^{\beta}$ ) with No Overlapping

Case a

(No overlapping in the  $x_2$  direction)

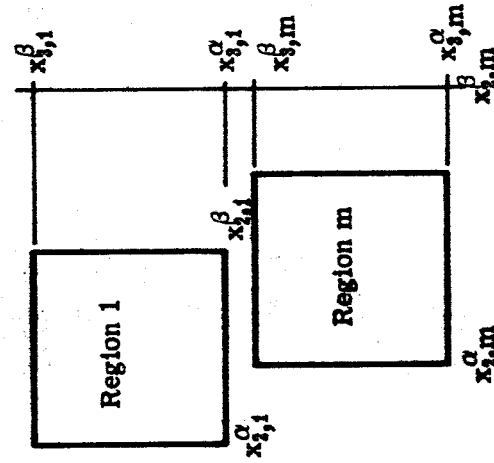
$$(x_{2,1}^{\alpha} \geq x_{2,m}^{\beta})$$



Case b

(Overlapping in the  $x_2$  direction but no overlapping in the  $x_3$  direction)

$$\begin{aligned} x_{2,1}^{\alpha} &< x_{2,m}^{\beta} \\ x_{2,1}^{\beta} &> x_{2,m}^{\alpha} \\ x_{3,1}^{\alpha} &\geq x_{3,m}^{\beta} \end{aligned}$$



Case c

(Overlapping in both the  $x_2$  and  $x_3$  directions)

$$\begin{aligned} x_{2,1}^{\alpha} &< x_{2,m}^{\beta} \\ x_{2,1}^{\beta} &> x_{2,m}^{\alpha} \\ x_{3,1}^{\alpha} &< x_{3,m}^{\beta} \\ x_{3,1}^{\beta} &> x_{3,m}^{\alpha} \end{aligned}$$

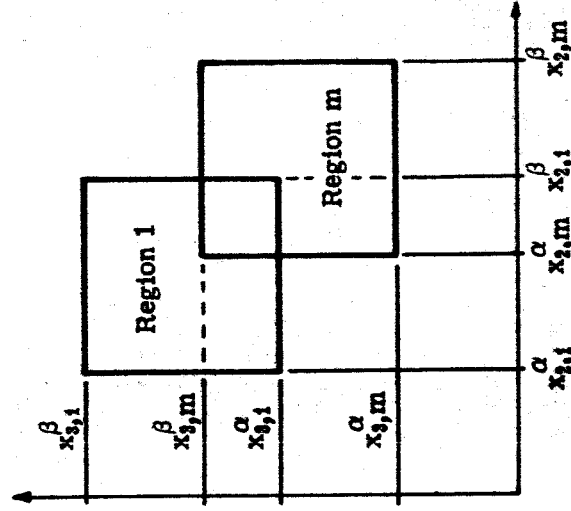


Fig. 10 — Case where Regions 1 and m Have a Face Lying in a Common Plane ( $x_{1,1}^{\alpha} = x_{1,m}^{\beta}$ )

2.  $x_{2,1}^{\beta} : x_{2,m}^{\alpha}$ . If less than or equal, there is no overlap and the routine considers the next region (Case a, Fig. 10). If greater than, then the third test is tried.
3.  $x_{3,1}^{\alpha} : x_{3,m}^{\beta}$ . If greater than or equal, there is no overlap (Case b, Fig. 10) and the comparison to the  $m + 1$  region is considered. If less than, then the fourth and last test is tried.
4.  $x_{3,1}^{\beta} : x_{3,m}^{\alpha}$ . If less than or equal, there is no overlap (Case b, Fig. 10) and the comparison to the  $m + 1$  region is considered. If greater than, then there is an area in common (Case c, Fig. 10). In this case, the region  $m$  is stored in a table in which all regions adjacent to region 1 are recorded.

Once the comparison of  $x_{1,1}^{\alpha}$  to  $x_{1,m}^{\beta}$  for all  $m$  is completed, the number of regions contained in the table is tested.

1. If there is no adjacent region, the coordinate  $x_{1,1}^{\alpha}$  is an extremity for the geometry and the region adjacent to region 1 on the  $x_1^{\alpha}$  face is itself. This coordinate is saved. Then, if in the course of the investigation of the  $x_1^{\alpha}$  coordinate of other regions another extremity is found which is not equal to  $x_{1,1}^{\alpha}$ , it means that the geometry has not been properly defined. This diagnostic is printed, and the program is stopped.
2. If there is only one region, the region number is placed in the proper table as the region adjacent to region 1 on the  $x_1^{\alpha}$  face. Further, a flag is set to denote that region 1 is adjacent to that region, say region  $m$ . Thus, when the  $x_1^{\beta}$  face of region  $m$  will be investigated, there is no need to search for regions in contact with it if their region number is less than  $m$ . The procedure is followed for regions whose number is greater than  $m$  only.



3. If there is more than one region in contact with the  $x_{1,m}^\alpha$  face of a given region, the  $x_{1,m}^\alpha$  face is defined as a complex surface. The EZGEOM program proceeds to decompose the complex surface into a grid of elementary rectangles and assign to each of them the corresponding region number.

Let us consider the complex surface oriented such that the normal to that plane is in the positive direction. The horizontal and the vertical directions are determined, using the right-handed method, i.e., if the  $x_2$ -axis is normal to the complex surface as in the case shown in Fig. 11, then the  $x_1$  and  $x_3$  axes are the horizontal and vertical directions respectively.

The first step performed by the routine is to extract the  $\beta$  coordinates in the horizontal direction of all adjacent regions and place them in increasing order removing duplicated coordinates, say  $H_1, H_2, \dots, H_{\max}$ .

The second step is to test if  $H_{\max}$  is greater than or equal to  $x_2^\beta$  of the region investigated. If it is,  $x_2^\beta$  replaces  $H_{\max}$  in the table. If it is less, this means that there is an area on the right side of the face which has not been accounted for. A diagnostic is printed pointing out that a hole exists and the program is stopped.

The same sequence of operations is performed for the  $\beta$  coordinates in the vertical direction, say  $V_1, V_2, \dots, V_{\max}$ .

These horizontal and vertical sequences determine a two-dimensional matrix. The complex surface is thus decomposed in a grid of rectangles. The EZGEOM program proceeds to place in each of these rectangles the corresponding region number. It must be noted that several rectangles may belong to a given region. This is done as follows: let  $x_{1,m}^\alpha, x_{1,m}^\beta$  be the coordinates in the horizontal direction of the adjacent region  $m$ . The program determines the number of inter-

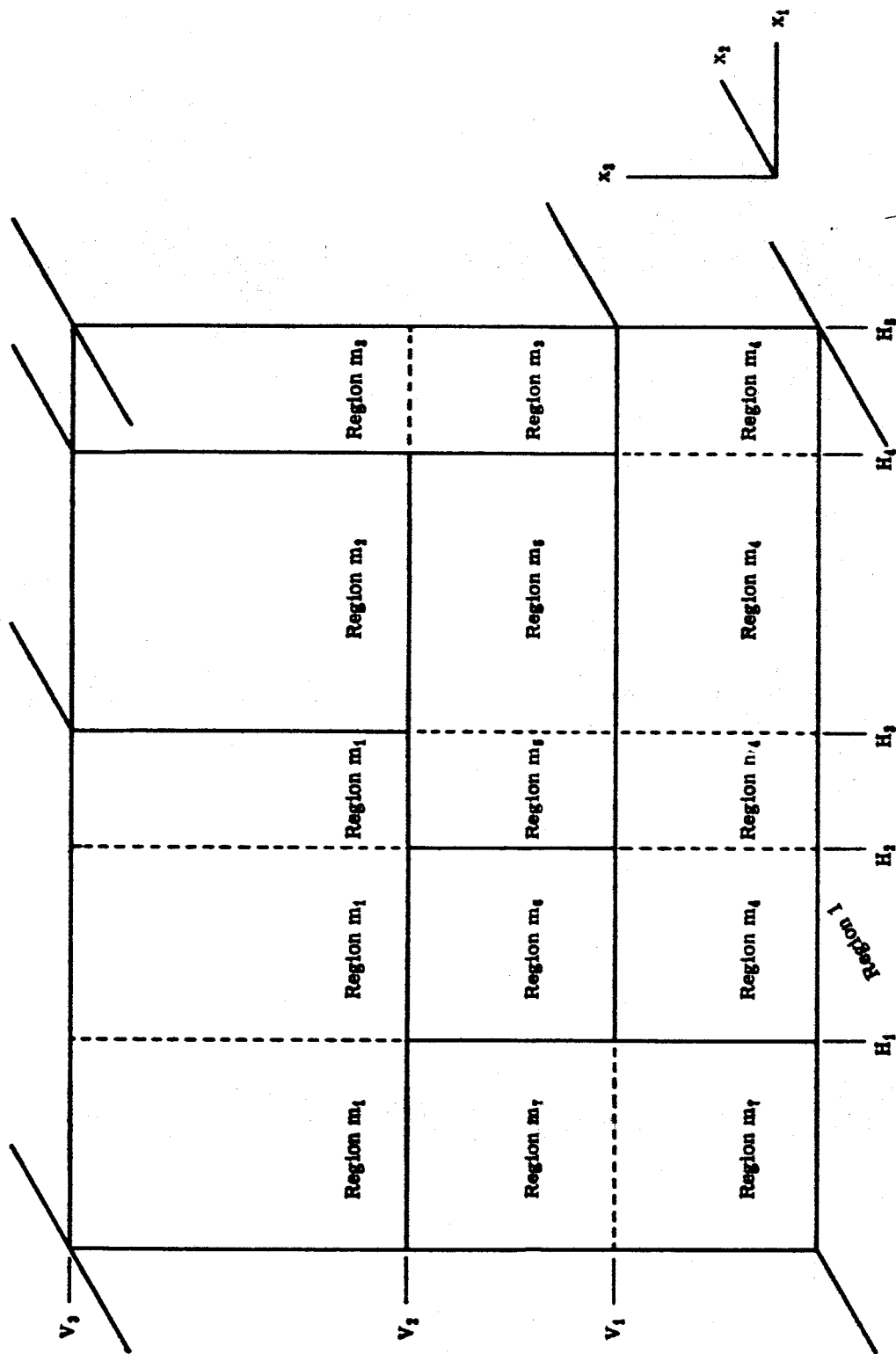


Fig. 11 — Illustration of the EZGEOM Decomposition of a Complex Surface

vals  $H_i$  contained in  $[x_2^\alpha, x_2^\beta]$ . Clearly, there must be horizontal coordinates in the horizontal sequence which are equal to  $x_2^\alpha$  and  $x_2^\beta$ . If not, either a hole or an overlap exists and a diagnostic is printed giving the region number under consideration, the plane being searched, the table of adjacent regions found, and the horizontal and vertical tables. From this information, it is possible to construct the complex surface and find the error.

If no error has occurred, the data gathered for the complex surface are placed in Table 3 which is described in Section 7.4.

The same procedure is repeated for each face of each region.

When all the ordinary regions have been processed, the program reads back from the scratch tape (produced by subroutine RDDTA) images of input cards for the nonordinary regions. These data are stored according to the format described in Section 7.4. It is believed that EZGEOM will find most, if not all, errors made in the input data for the ordinary regions.

It is possible for EZGEOM to fail to give a diagnostic when the programmed dimensions of a table for complex surfaces are exceeded. This may occur when a complex surface is defined by a grid of more than  $25 \times 25$  rectangles and the investigated region is located near the end of the ordinary region listing. This is an instance when an incorrect edit can be obtained. In this case, all the regions adjacent to region 1 will be called 1, showing that the geometry was handled incorrectly. In general, the situation is improved by assigning a very low region number to that region.

There is no routine built into EZGEOM to check input data for the nonordinary regions. However, several other routines in the system (TESTG, CYLLOC, VOLUME) perform a variety of tests on the validity of the nonordinary geometry as well as the ordinary. These routines are all normally called in the operation of MEZDA.

In conclusion, it is believed that with reasonable care in the input preparation, the geometric tests performed in VANGEN, EZGEOM, TESTG, CYLLOC, and VOLUME practically ensure that no faulty configuration will go undetected to the main Monte Carlo tracking phase.

### 7.3 DESCRIPTION OF THE INPUT DATA FOR EZGEOM

These data follow the EZGEOM card in the MEZDA input deck.

1. Integers NBOX ( $\leq 80$ ), NCYL ( $\leq 127$ ), NREG ( $\leq 200$ ) (Format 3I5).
2. Ordinary-region input (NBOX cards): XMIN(J), XMAX(J), ..., ZMIN(J), ZMAX(J) (Format 6E12.4).

Optional: columns 73-75: BPO; columns 78-80: region number.

Notes: (a) irrespective of the entry in columns 78-80, the  $J^{\text{th}}$  card in the deck will define the  $J^{\text{th}}$  ordinary region,  $J \leq \text{NBOX}$ . (b) In a  $30^\circ$  problem, set the maximum y-coordinate to a value large enough to enclose any cylinders whose axes are on the  $30^\circ$  reflecting plane (if TESTG is to be used; see Chapter 8).

3. Data required for VANGEN-format (cf. Chapter 5) cylinder input (supply only if NCYL  $> 0$ )
  - a. NSTAGE, ZMINC, H, EPS (Format I5, 3E15.8).
  - b. NVERT ( $\leq 100$ ) (Format I10).
  - c. Vertex locations: XV(J), YV(J),  $J = 1, \text{NVERT}$  (Format 6E12.5) (three vertices per card).
  - d. NRADII ( $\leq 200$ ) (Format I10).
  - e. Radii: R(J),  $J = 1, \text{NRADII}$  (Format 6E12.5).
  - f. NZBASE ( $\leq 100$ ), NHT ( $\leq 100$ ) (Format 2I5).

g. Z-base locations (supply only if NZBASE > 0)

ZBASE(J), J = 1, NZBASE (Format 6E12.4).

h. Heights (supply only if NHT > 0)

HT(J), J = 1, NHT (Format 6E12.4).

i. Cylinder description, 1st card (see Chapter 5 for discussion)

Columns 1-30: NEXT, JV, JB, JH, JR, NSTRAD (= 0, 2, or 4)  
(Format 6I5, ...)

Columns 78-80 (same card), Region number, IREG (Format ....., I3)

Columns 73-75, same card; Optional: CYL

Follow-up card (supply if NEXT, above, is zero):

Straddled-region numbers, in any order (Format 4I5).

Notes: (a) All cylinders described in this format must be in a group immediately following the ordinary-region input. Within this group, however, the sequence of the region numbers is immaterial. (b) Radius, half-height, and X, Y, Z of midpoint of any cylinder in this group must be expressible with adequate precision in format F12.6, e.g., ±1234.123456.

Supply items(s) (i) for NCYL cylinders.

4. Descriptions of all other nonordinary regions (sphere: 1 card; cylinder: 1 or 2 cards; nonordinary box: 3 cards; wedge: 3 cards), as follows.

All locations and coordinates in cm.

a. Sphere

<u>Column</u>	<u>Item</u>
1-12	x-coordinate of center (E12.4)
13-24	y-coordinate of center (E12.4)
25-36	z-coordinate of center (E12.4)
53-55	SPH
58-60	External region number (I3)
(73-75)	SPH (optional)
78-80	Sphere region number (I3)

**b. Cylinder (EZGEOM-format input)**

**1st card**

<u>Column</u>	<u>Item</u>
1-12	x-coordinate of axis (E12.4)
13-24	y-coordinate of axis (E12.4)
25-36	z-coordinate of midpoint of axis (E12.4)
37-48	Radius (E12.4)
53-55	CYL
58-60	External region number (I3) (>0 for nonstraddling; -2 or -4 for straddling)
61-72	Half-height of cylinder (E12.4)
(73-75)	CYL (optional)
78-80	Cylinder region number (I3)

**2nd card**

(Supply only for straddling cylinder)

Columns 1-20: Straddled-region numbers, in any order (4I5)

**c. Wedge**

**Card 1**

<u>Column</u>	<u>Item</u>
1-36	X,Y,Z of vertex of wedge (Format 3E12.4, ...)
53-55	WED
58-60	External region number (I3)
(73-75)	WED (optional)
78-80	Wedge region number (I3)

**Card 2**

1-72	Components, $X_1$ , $Y_1$ , $Z_1$ , $X_2$ , $Y_2$ , $Z_2$ of base vectors from vertex. (Format 6E12.4, ...)
(73-76)	WEDA (optional)
(78-80)	Wedge region number (optional)

**Card 3**

1-36	Components $X_3$ , $Y_3$ , $Z_3$ of length vector of wedge (Format 3E12.4, ...)
(73-76)	WEDB (optional)
(78-80)	Wedge region number (optional)

#### d. Nonordinary Rectangular Parallelepiped (RPP)

##### Card 1

<u>Column</u>	<u>Item</u>
1-36	X,Y,Z of vertex of RPP (Format 3E12.4, ...)
53-55	RPP
58-60	External region number (I3)
(73-75)	RPP (optional)
78-80	Region number (I3)

##### Card 2

1-72	Components $X_1, Y_1, Z_1, X_2, Y_2, Z_2$ of any two vectors from the RPP vertex (Format 6E12.4, ...)
(73-76)	RPPA (optional)
(78-80)	Region number (optional)

##### Card 3

1-36	Components $X_3, Y_3, Z_3$ of 3rd vector from RPP vertex (Format 3E12.4, ...)
(73-76)	RPPB (optional)
(78-80)	Region number (optional)

#### 7.4 EZGEOM OUTPUT

The output edit gives a complete description of each region and is self-explanatory.

EZGEOM generates and stores three tables which completely describe the geometry specifications for the problem. The data in these tables are arranged so that they are rapidly accessible to the Monte Carlo routines.

##### Table 1

There is an entry in Table 1 corresponding to each region of the problem. (The  $i^{\text{th}}$  entry corresponds to the  $i^{\text{th}}$  region.) Each entry to Table 1 is packed into 35 bits as follows.

1. The first three high-order bits contain the number of internal regions that the region sees (see Section 7.1). The maximum number of such regions for any given region is seven.
2. The next three bits describe the type of region
  - 0 = ordinary parallelepiped
  - 1 = sphere
  - 2 = cylinder
  - 3 = wedge
  - 4 = nonordinary parallelepiped.
3. The next eight bits contain the number of the region external to the region. This only applies to nonordinary regions (types 1-4). For straddling cylinders, this entry is zero.
4. The next nine bits contain a location relative to Table 2 where the regions whose external region is the region considered are listed. The entry is zero when there are no such regions.
5. The last 12 bits contain the location relative to Table 3 where the region data are listed.

**Table 2**

This table contains an entry for each of the nonordinary regions (types 1-4), and these entries are grouped corresponding to their external region. Each entry is packed into 25 bits as follows.

1. The first three high-order bits (25 through 23) contain the type of the region (same as Table 1, item 2, but 0 type is excluded).
2. Bits 22, 21 are not used.
3. Bits 20 through 13 contain the region number of the nonordinary region.
4. The low-order 12 bits contain the location relative to Table 3 where the region data are listed.



**Table 3**

This table contains the parameters that define each region. The first location is referenced from Table 1 or Table 2.

**1. Ordinary Parallelepipeds**

The first six entries contain the six bounding planes ( $x_i^\alpha, x_i^\beta, i = 1, 2, 3$ ). The next six entries contain the adjacent region numbers for each of the corresponding six sides.

a. If a side sees more than one region this side is defined as a complex surface. The entry contains the negative of the location relative to Table 3 where the data for the complex surface may be found. At this location relative to Table 3 the following information is recorded:

- (1) A word containing the number of horizontal and the number of vertical intervals for the complex surface packed 18 bits apart.
- (2) Following this word appear the upper limits of each of the horizontal intervals.
- (3) Then the upper limits of each of the vertical intervals appear.
- (4) Finally, packed four to a word, nine bits apart, are the regions on the complex surface. The region numbers along the horizontal, from the first to the last horizontal interval, are listed for the first vertical interval; then for the second vertical interval, etc., as shown in Fig. 11.

b. If the side sees only one region, then the region number of this region appears.

**2. Nonordinary Regions (Types 1-4)**

**a. Spheres**

The first three entries contain the coordinates of the center of the sphere. The next entry is the square of the sphere radius.

**b. Cylinders**

The first three entries contain the coordinates of the center of the cylinder axis. The 4th entry contains the square of the radius. The 5th entry contains the half-height of the cylinder. The 6th entry does not apply if entry 3 of Table 1 is nonzero (indicating a nonstraddling region, with a single external region). For a straddling cylinder, the 6th entry is 2, 3, or 4, with these meanings:

2 – the two straddled boxes have a bounding plane

$y = y_a$  in common;

3 – the two straddled boxes have a bounding plane

$x = x_b$  in common;

4 – the cylinder straddles four boxes.

Finally, the next two or four entries are the external-region numbers, in the following order:

(Previous entry was 2) – region above, region below  $y = y_a$

(Previous entry was 3) – region to left, region to right of  $x = x_b$

(Previous entry was 4) – region numbers in clockwise order  
(in x-y plane) starting from upper left.

**c. Nonordinary Parallelepipeds**

The first three entries contain the coordinates of the vertex of the parallelepiped. The next nine entries contain the x-y-z components of the three vectors which define the parallelepiped.

**d. Wedges**

The description for the wedge is the same as the nonordinary parallelepiped, the two first vectors defining the legs of the wedge right triangle.

Since EZGEOM is run as part of the sequencer program MEZDA, its input-output tapes are included in the list of those needed by MEZDA (Chapter 6).

## **8. THE GEOMETRY TESTING ROUTINE, TESTG**

TESTG is a program which tests a proposed geometric configuration by a Monte Carlo method. Points are chosen at random within the volumes of each pair of uninhabited (innermost) regions in the configuration, and tracking is attempted from one to the other point of each pair. The tracking subroutines used are the same as those in the ATHENA program. If the program gets "lost" at any point in one of these trajectories, a synopsis of the trajectory is printed out, in detail which is generally sufficient to localize the input error. Briefly, the operation of TESTG is as follows. TESTG has access to the EZGEOM-processed geometry data, via the dump tape required by MEZDA. For each pair of innermost regions (I,J), (I=J included), a point is chosen at random within each of the pertinent volumes (using subroutine PIKPT), and the distance and direction from one point to the other are computed. (In a 30-degree problem, no points are chosen with negative x or y coordinates; points above the 30° plane can be chosen however, so that cylinders cut by this plane should be below the maximum y-coordinate of the ordinary geometry.) Subroutine G1 determines which of the following events occurs first along the trajectory: (1) an internal body is struck before the total required track is traversed; (2) the outer edge of the current region is struck; or (3) the total track length occurs in the original region. This output information from G1 is used by subroutine G2 to either bring the particle up to the appropriate boundary (internal body, or surface of initial region) and determine the next region entered, or terminate the track within the current region. As track

lengths are generated in the various regions along a trajectory, these are stored in an array, as well as the coordinates of points at which the trajectory pierces surfaces, next-region identifiers, and the value of an event-flag IFLG at each exit from subroutine G1. On option (Sense Switch 3) this trace is printed out for each trajectory. Otherwise the trace is printed out only for unsuccessful trajectories. Some of the types of input errors and computational anomalies leading to this printout are:

1. Nonordinary region (e.g., sphere) not completely contained in its designated external region; on emerging from the overlapping volume the particle is found in forbidden territory;
2. Illegally overlapping regions in general;
3. Imperfectly rectangular RPP's or wedges;
4. Excessive number of surface crossings ( $>200$ );
5. Next region identical to current one (a condition set in the geometry control routines if a particle leaves the configuration);
6. Particle not brought up to required final point to within a small  $\epsilon$  (symptomatic of geometry input error such as those described in items 1 through 3).

If 20 errors are found in a TESTG problem, the program stops. One complete pass through TESTG is defined as the set of trackings between each pair of innermost regions. The number of desired passes is specified in the input.

#### Description of the TESTG Input and Output

##### Input

The TESTG input, following the program name card in the MEZDA deck, is a single card.

<u>Column</u>	<u>Item</u>
1-10	NMAX, Number of TESTG passes to be attempted
19-20	Geometry type (30 for 30°, ≠30 for 360°)

### Output

Without Sense Switch 3 on, and with no errors detected in the tracking, TESTG prints out **PASS 1 COMPLETED**, and the time in seconds for that pass; it prints similarly for all subsequent successful passes.

With Sense Switch 3 on, or as a result of a tracking error, a trace of the trajectory is printed, including: regions containing initial and attempted final points; coordinates of these points; length and direction cosines of connecting vector; and, for each segment of the track, the coordinates of its terminus, its length, the next region encountered, and IFLG upon returning from subroutine G1.

The quantity IFLG has the following meanings:

- IFLG = 1      Total remaining track length has not been exhausted, and some region surface (other than the flat face of a cylinder) is encountered
- IFLG = -1     The flat face of a cylinder is encountered
- IFLG = 0      No surface is struck; the flight path has been exhausted.

If errors are indicated by TESTG, the geometry input should be corrected, and EZGEOM rerun until several successful passes through TESTG can be made.

## 9. THE DATA ORGANIZATION PROGRAM, DATORG

The GENDA and GENPRO programs are used to generate an Element Data Tape (EDT) which contains microscopic cross sections and probability tables for all nuclides of interest. This EDT can be considered as a library tape for any subsequent Monte Carlo problems.

For a specific problem, however, the system is divided into regions which contain given nuclide compositions. Each composition may be described by a set of nuclides and their respective concentrations. When a particle enters a region of a given composition, the Monte Carlo program has to have access to the region's macroscopic cross section as a function of energy, as well as the concentrations and the various microscopic cross sections. Thus when a collision occurs in the region, the program can select the nuclide with which the collision occurs, and finally the type of collision.

The probability that a particle with energy  $E$  will interact with nuclide  $k$  of the composition  $m$  is given by

$$P(k,m) = \frac{C_{k,m} \sigma_T(k,E)}{\mu_{T,m}(E)} \quad (55)$$

where  $\mu_{T,m}$  is the total macroscopic cross section ( $\text{cm}^{-1}$ ) of the composition, and  $C_{k,m}$  is the concentration of nuclide  $k$  in composition  $m$ . DATORG calls for the  $C_{k,m}$  expressed in units of (atoms/barn-cm), or  $(\text{atoms}/\text{cm}^3) \times 10^{-24}$ .

## 9.1 TECHNICAL DESCRIPTION

The DATORG program searches and reads from the appropriate (neutron or gamma) EDT all information concerning the nuclides called for in the various compositions specified in the input. It computes the total macroscopic cross sections of each composition at each final energy,  $\mu_{T,m}(E_j^G)$ ,

$$\mu_{T,m}(E_j^G) = \sum_{\substack{\text{k's in} \\ \text{composition} \\ \text{m}}} C_{k,m} \sigma_{T,k}(E_j^G), \quad (56)$$

using the concentration data supplied as input. The output energy mesh for DATORG is that given by the fixed lethargy interval used to generate the EDT.

For gamma problems only, there is in addition a computation of composition-dependent (macroscopic) gamma-heating response functions, which are used in ATHENA to estimate heat deposition, corresponding to computed gamma track lengths, in the various regions. For a medium with macroscopic energy-absorption coefficient  $\mu_a(\text{cm}^{-1})$ , the expected quantity of energy deposited along a track length  $TL(\text{cm})$  is  $(TL \times E \times \mu_a)$  joules, where  $E$  is the photon energy in joules. The  $E\mu_a$  for a mixture  $m$ , at energy  $E$ , is computed as

$$E \cdot \mu_{a,m}(E) = E \cdot \sum_{\substack{\text{nuclides k in} \\ \text{composition m}}} \{C_{k,m} \sigma_{T,k}(E) [p_{a,k}(E) + p_{s,k}(E) \cdot G(E)]\}, \quad (57)$$

where  $C_{k,m}$  = concentration in atoms/barn-cm

$\sigma_{T,k}(E)$  = total cross section, barns/atom

$p_{a,k}(E)$  = probability of absorption for nuclide  $k$ , at energy  $E$

$p_{s,k}(E)$  = probability of scattering for nuclide  $k$ , at energy  $E$

$G(E)$  = average fraction of photon energy lost in a Compton scattering at energy  $E$ .



The fraction  $G(E)$  is equal to

$$G(E) = 1.0 - \frac{3}{8\sigma_c(E)} \left[ \frac{\ln(1+2E)}{E^3} + \frac{2(1-E)(2E^2-2E-1)}{E^2(1+2E)^2} + \frac{8E^2}{3(1+2E)^3} \right], \quad (58)$$

where  $E = (\text{photon energy, ev}) / (0.511 \times 10^6)$ , and

$\sigma_c(E)$  = the total Klein-Nishina cross section, in Thomson units per electron:

$$\sigma_c(E) = \frac{3}{4} \left\{ \frac{1+E}{E^3} \left[ \frac{2E(1+E)}{1+2E} - \ln(1+2E) \right] + \frac{1}{2E} \ln(1+2E) - \frac{1+3E}{(1+2E)^2} \right\}. \quad (59)$$

The quantities transmitted to the dump tape from this portion of DATORG are the heating response functions  $E\mu_a$  (joules/cm) for each composition and at each output energy of the EDT mesh.

Finally, for both neutron and gamma problems, DATORG stores and transmits to the dump tape the microscopic total, elastic scattering, and absorption cross sections for each nuclide and at each energy, and the data describing inelastic and anisotropic elastic scattering.

#### Nuclide Identifiers in Neutron and Gamma DATORG Problems

The integer identifying a nuclide in the ATHENA system is a 5-digit integer ZZABC, where ZZ must be the atomic number, and ABC any arbitrary numbers. A given nuclide should have the same identifier in GENDA, GENPRO, DATORG, GASP, and NATALE. In neutron problems, the entire 5-digit number is used for comparison, whereas in gamma problems only the first two digits (ZZ) are considered (gamma cross sections, etc., functions of atomic number only). For example, if a DATORG input deck called for nuclides 74382 and 74383 (identifiers for tungsten isotopes  $W^{182}$  and  $W^{183}$ ), a neutron DATORG problem would search the EDT for two nuclides; a gamma DATORG problem would treat each as 74000, and would effectively combine their concentrations. Thus, the main portion of a DATORG input deck can be used for either type of problem.

## 9.2 DESCRIPTION OF THE INPUT FOR DATORG

(Each card may have the optional identifier XSDAT in columns 73-77, and may be numbered serially in columns 78-80.)

Following the DATORG program-name card in MEZDA:

### Card 1 - Problem Identification Card

<u>Column</u>	<u>Item</u>
6-10	Problem number
11-43	Blank
44-45	Number of distinct compositions ( $\leq 32$ )
50	Problem type: 0 = neutron, 1 = gamma
55	Option to print out entire cross-section array (unedited) including inelastic-scattering data.
	IBM-7094 version: 0 = suppress printout; 1 = print.
	CDC-1604-A version: 0 = print; 1 = suppress

### Card 2

<u>Column</u>	<u>Item</u>
9,10	Composition number
19,20	Number of nuclides in this composition ( $\leq 15$ for neutron, $\leq 20$ for gamma)

### Card 3

Nuclide cards for above composition, one card per nuclide (Format I5, E15.8)

<u>Column</u>	<u>Item</u>
1-5	5-digit identifier ZZABC
6-20	Concentration (atoms/barn-cm)

Repeat card 2 and card(s) 3 for each additional composition.

## 9.3 DATORG OUTPUT

The DATORG output is a printed edit, and a number of tables transmitted to the dump tape.

The printed edit includes:

1. A listing of the input.
2. The number of energies on the EDT mesh.
3. For each composition,  $\mu_T$  (and  $E\mu_a$ , if gamma problem), also NORG (=location relative to origin of XSECT table of  $\mu_T$ ) and (if gamma problem) NORGH (=same, for  $E\mu_a$ ); all vs E(ev).

(Note: for a neutron problem, the length of the cross section table, D (which is one factor limiting the size of problem which can be run, cf. Eq. 81) is the highest printed value of NORG. For a gamma problem, D = highest printed value of NORGH.

4.  $4\pi$  times the electron density (e/barn-cm)

$$4\pi \sum_k C_{k,m} Z_k,$$

for each composition m.

5. A list of the energies on the EDT mesh.
6. A table of KPHYS, NEL, and MUTORG for each composition (defined below).
7. A table of IATWT and CONCT for each nuclide of each composition; if IATWT = 4 for a particular nuclide, this means that at its first appearance in the DATORG input, the pertinent nuclide identifier represented the 4th distinct nuclide to appear; the CONCT entries are the corresponding concentrations.

(Note: in a gamma problem, all different ZZABC with the same ZZ are treated as the same nuclide, but their concentrations are printed out separately.)

8. NEVAT, NSECT, and EVAT (defined below) for each distinct nuclide, in the order of first input appearances of the nuclides.
9. Tables of microscopic cross sections for each nuclide. The heading **ATOMIC WEIGHT** is followed by a 5-digit identifier and a floating number. For neutron problems, the floating number is the atomic weight; for gamma problems it is the floated atomic number; and
10. (unless suppressed on card 1) a printout of the entire XSECT table, unedited.

The data stored internally by DATORG contains the following items in their order of listing.

<u>Symbol</u>	<u>No. of Locations</u>	<u>Definition</u>
<u>Counters</u>		
NORG	1	Counter denoting relative address in the array XSECT
NELEM	1	Counter denoting number of distinct nuclides ( $\leq 15$ for neutron, $\leq 20$ for gamma)
NR	1	Counter denoting number of compositions ( $\leq 32$ )
NENERG	1	Counter denoting number of energies ( $\leq 149$ )
JK	1	Counter denoting the sum of all nuclides in every composition ( $\leq 165$ ).
<u>Tables</u>		
NEL	NR	Number of nuclides for each composition
NEVAT	NELEM	5-digit identifier ZZABC for nuclides. These are ordered in the order in which the distinct nuclides (distinct ZZ for gamma) first appear in the DATORG input.
EVAT	NELEM	Corresponding to each nuclide in NEVAT the atomic weight is entered in EVAT.

<u>Symbol</u>	<u>No. of Locations</u>	<u>Definition</u>
<u>Tables</u>		
IATWT	$\sum_{i=1}^{NR} NEL_i$	For each composition in the order of composition number, IATWT contains the nuclide-order number of each nuclide of the composition.
CONCT	$\sum_{i=1}^{NR} NEL_i$	Corresponding to each entry in IATWT the concentration of the nuclide is entered in CONCT.
KPHYS	NR	Initial address, in table IATWT or CONCT, of data for pertinent composition.
XSECT	(Variable dimension)	Contains the cross section and the probabilities for each prescribed nuclide. They are given in the order in which they are obtained in GENPRO (and appear in the EDT). Also contains macroscopic cross sections for each composition in the order of composition number.
NSECT	NELEM	Contains the origin relative to start of XSECT for each nuclide (in the order specified by NEVAT).
MUTORG	NR	Contains origin of location of the tables of total cross sections, $\mu_T$ , in XSECT which are written in the order of composition number.
MHTORG	NR	Contains origin of the locations (relative to XSECT) of the heating-response-function table for each composition, in order of composition.

Logical tape assignments for DATORG are included in the list for MEZDA.

## 10. THE PARAMETER-INPUT PROGRAM, INPUTD

This last program in the MEZDA overlay reads in a variety of data needed to complete the specification of an ATHENA problem. In addition, certain minor calculations are performed to check some of the geometry input, and compute parameters relating to point detectors and sectorized cylinders.

### 10.1 TECHNICAL DESCRIPTION

INPUTD and subroutine MPINP read in problem parameters as described in Section 10.2. The input is printed out by MPINP, in a self-explanatory format. If sectorized cylinders are called for, MPINP stores, as part of entry IRSC(IR) for each such cylinder IR, the required number of sectors, plus the initial address, ISC, of the sector-heating answers for this cylinder in the answer-array S.

For each region IR for which tracklength fluxes are called for, there is stored the initial address ISC, in array S, of the fluxes for this region [also as part of IRSC(IR)].

For use in primary-gamma flux-at-a-point, each detector I is classified as in-core [IKD(5,I) = 1], or out-of-core [IKD(5,I) = 0]. A detector is classified as out-of-core if it is distant by more than 2 mm from the nearest point on the core (the core described via data communicated by VANGEN).

For 30° problems, INPUTD calls subroutine CYLLOC, which checks the legality of vertex locations for all cylinders in the problem, classifies each legally situ-

ated cylinder, and records the classification as a portion of **IRSC(IR)**. This is later converted by subroutine **COVOL** into the argument **KCYL** for subroutine **VOLUME**. **KCYL** = 1, 2, 3, or 4 according as the cylinder is cut by neither plane, the  $0^\circ$ , the  $30^\circ$ , or both reflecting planes (see Fig. 12).

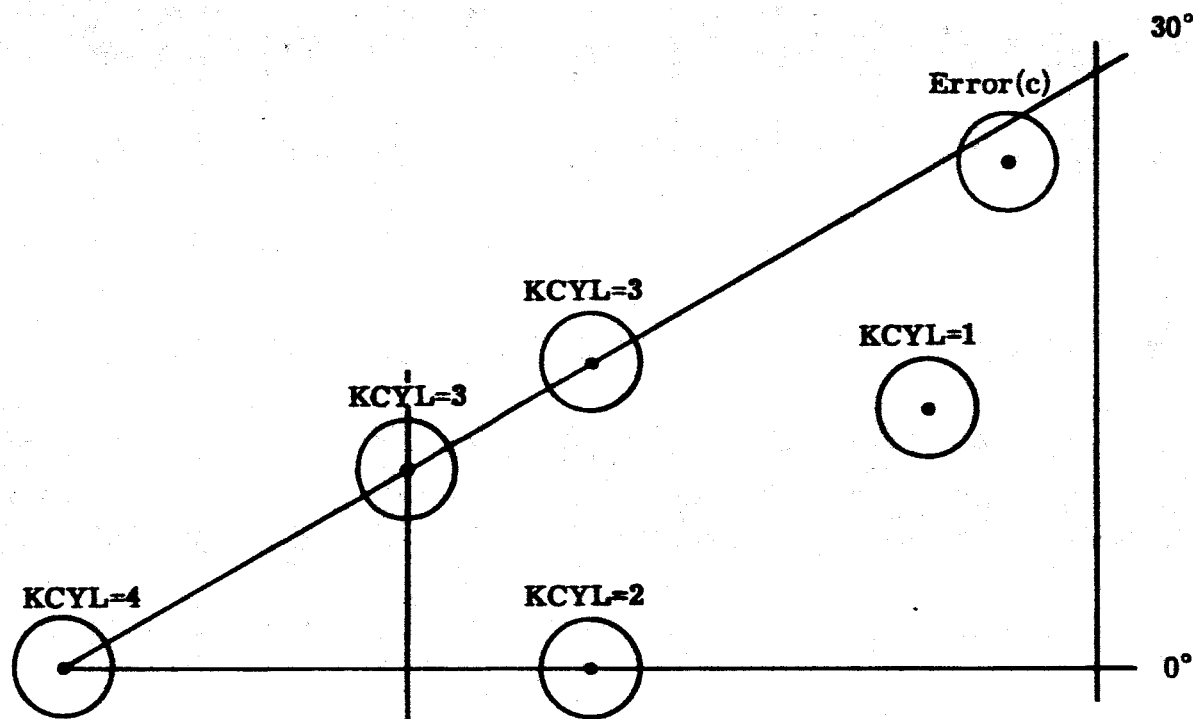


Fig. 12 — Cylinder Location Types. For a  $360^\circ$  Problem, Each **KCYL** = 1.

Illegal vertices caught by **CYLLOC** are:

1. negative  $x$  or  $y$  of vertex;
2.  $y - x/\sqrt{3} > 0.01 y$ ;
3.  $|y - x/\sqrt{3}| > 0.01 y$ , and cylinder intersecting a reflection plane ( $|y - x/\sqrt{3}| \leq 0.01 y$  classified as **KCYL** = 3).

Next the volumes of all regions are computed via subroutines COVOL and VOLUME. VOLUME is called again in the final Monte Carlo edit; its use in INPUTD is mainly for the purpose of detecting geometry errors. Error flags are set and diagnostic printouts occur for a number of types of error:

1. Illegal sphere locations, in 30° geometry;
2. Imperfectly rectangular wedge or RPP;
3. Negative volume of region, before or after subtraction of internal regions;
4. Sector volumes wanted for noncylinder, or cylinder with other than one internal body (a coaxial cylinder).

In the 30-degree geometry, the volumes computed pertain only to those portions of the regions in which track lengths can be generated, i.e., the portions included between the reflecting planes. Thus, in the final edit of the Monte Carlo problem, true volumetric fluxes and heating are computed.

Volumes of regions completely outside the trackable geometry are not computed; for regions which are partly trackable, but which have some pertinent dimension  $\geq 10^9$  cm, the volumes are not computed, and division by the pertinent volumes is suppressed in the final edit.

Finally, via subroutines TANTAB and INITIA, INPUTD sets up tables of tangents, initial-sector locations, etc., needed in the sector-cylinder scoring routines, REPART and SECTID.

## 10.2 DESCRIPTION OF THE INPUT FOR INPUTD (See Chapter 11 for Discussion)

Following the INPUTD program name card in MEZDA, supply:

1. Title card: any 80 Hollerith characters
2. Problem Information Card (Format 2I10, 10I5)



<u>Column</u>	<u>Item</u>
1-10	First history number
11-20	Last history number
21-25	Number of histories per statistical group (usually $\approx 20$ )
26-30	Problem type: $\pm 30$ or $\pm 360$ (primary = +, secondary = -).
31-35	Transmission region
36-40	Number of sectorized cylinders
41-45	Number of distinct region-dependent weights
46-50	Number of importance-sampling energy bins
51-55	Number of flux energy bins
56-60	Number of point detectors ( $\leq 75$ ; in practice, $\leq 5$ recommended; = 0 for $30^\circ$ problem)
61-65	Number of regions for which <u>fluxes</u> are required
70	Original or restart: 0 = original, 1 = restart.

### 3. Low-Energy Specification (Format 2E14.5)

(Note: This and subsequent cards may be omitted on a restart problem.)

<u>Column</u>	<u>Item</u>
1-14	Cutoff energy ( $\geq$ lowest energy on EDT mesh)
15-28	Neutron thermal option (0 = no thermal group; 1 = thermal group to be tracked).

[Notes: (a) In gamma problems, a particle degrading below the cutoff energy has its final energy (heat) deposited at the collision point; (b) in neutron problems, with thermal option  $\neq 0$ , degradation below cutoff energy puts the neutron at the lowest energy on the EDT, and tracking continues. With option = 0, a neutron absorption is forced.]

### 4. Energy Importance Sampling Data (n.b. same as VANGEN Format)

- a. Minimum energy (ev) of each bin, and corresponding energy weight (Format 2E20.9). One card per bin, lowest first.
- b. Maximum energy (ev) of last bin (Format 1E20.9).

**5. Flux Energy-Bin Limits (Format 5E14.5)**

Number of entries = 1 plus number of flux bins, five to a card. Values in ev, ascending; first value should be 0.0.

**6. Distinct Region-Dependent Weights**

(For appropriate particle type, neutron or gamma; particle type communicated from DATORG.)

Five entries per card (Format 5E14.5), in the order in which they will be referenced in item 7.

**7. Region-Weight Index for Each Region (Format 14I5)**

Fourteen entries per card.

**8. Composition Number for Each Region (Format 14I5)**

Fourteen entries per card.

**9. Identification of Sectorized Cylinders**

(Supply only if entry in columns 36-40, card 2, is > 0.)

One pair of integers, region number followed by number ( $\leq 12$ ) of sectors, for each sectorized cylinder. Regions in any order. Seven pairs per card (Format 14I5).

**10. Identification of Flux Regions**

(Supply only if entry in columns 61-65, card 2, is > 0.)

Flux-region numbers, in any order; 14 entries per card (Format 14I5).

### 11. Locations of Point Detectors

(Supply only if entry in columns 56-60, card 2, is > 0.)

<u>Column</u>	<u>Item</u>
1-14	x-coordinate
15-28	y-coordinate
29-42	z-coordinate
43-45	Region containing detector.

(Note: Check input carefully; there is no built-in check that the specified coordinates and region number for a detector are compatible.)

### 12. Macro-Gamma Cross Sections

(Supply only if neutron problem with point detectors.)

Representative (for  $E_\gamma \approx 1.0$  Mev) gamma cross sections ( $\text{cm}^{-1}$ ) for each composition, in order of compositions (see gamma DATORG output). Five entries per card (Format 5E14.5).

Logical tape assignments for INPUTD are included in the list for MEZDA.

## **11. THE MONTE CARLO TRACKING AND SCORING PROGRAM, ATHENA**

With access to the processed geometry, cross-section, and problem-parameter input via the inter-program dump tape, and a source-particle tape, one is ready to run a main Monte Carlo problem with program ATHENA.

The Monte Carlo calculation is basically the analog of an actual experiment, the stochastic behavior of the actual particles and the relative probabilities of competing events being simulated, as closely as possible, for a large number of computed histories. The total accumulated scores (fluxes, heating, etc.) tend to approximate the corresponding physical results more closely as the number of histories increases.

### **11.1 IMPORTANCE SAMPLING**

Depending upon the nature of the physical problem and the types of answer required, it is advisable not to run an exact analog calculation, but to employ some techniques to reduce the variance in the scores of interest.

The ATHENA system allows for the use of spatial and energy importance sampling, via splitting and Russian roulette. By appropriate use of these devices, one may effectively "direct" the computer to spend more of its time computing in regions and at energies of interest than it would in a purely analog calculation. This is accomplished by the assignment of low weights to the pertinent regions

or energy bins. A low weight corresponds to a high "importance" of the phase-space region to the answer desired.

A typical application of spatial importance sampling is the assignment of decreasing region weights to regions farther removed from the source, in shield-penetration calculations. For gamma-heating calculations with delayed-fission-gamma spectrum, it has been found efficient to assign higher energy weights to the lower energy sources, thereby:

1. Selecting from a modified gamma spectrum, with fewer low energy gammas, and
2. Tending to kill off particles by Russian roulette as they degrade.

As a general rule, the region or energy weights specified should not vary abruptly; the ratio of contiguous values is usually between 1.5 and 4.0. Exceptions are the very high weights ( $\sim 10^{20}$ ) used to define "killing" regions.

## 11.2 STATISTICAL ESTIMATION

In addition to applying splitting and Russian roulette to reduce the variance, ATHENA has options to employ routines for computing gamma heating and fluxes at point detectors. These flux-at-a-point routines implement statistical-estimation procedures devised by Kalos (see Section 11.5 for description).

## 11.3 THE MAIN TRACKING AND SCORING SEQUENCE

1. ATHENA calls subroutine D360, which reads in particles in groups of 100 from a source tape, such as that produced by VANGEN or GASP, and sequences their tracking and scoring. The description of each source particle includes nine words, normally containing the history number, three spatial coordinates, three direction cosines, the energy, and region number. Each particle is further identified as either a

"real" particle or a "fake" particle, the latter describing a special secondary-gamma particle generated by the FAP (flux-at-a-point) routine in a neutron problem, specifically for estimating uncollided secondary-gamma flux-at-a-point. A fake particle, identified by a pertinent nonzero detector number included in its source-tape description, is processed by FAP to score at that detector.

2. A real particle is tracked as follows.

If no point detectors are present, normal tracking proceeds (3). If point detectors are present, the new particle is classified as a source particle ( $IS=1$ ), which affects its treatment in FAP. FAP is then called to carry out the first step in a secondary-gamma-flux estimation (if a neutron problem), or the estimation of gamma flux (if a gamma problem); in the first pass of a real gamma through FAP, estimation is made of both the uncollided flux at each detector, and the once-more-collided flux. The particle is then classified as nonsource ( $IS=0$ ) and normal tracking resumes (3). (Just before each subsequent collision of the nonsource gamma, only once-more-collided-flux estimations are made.)

3. Next the program determines which of the following four events occurs first along the particle trajectory (Fig. 13):

- a. A reflection plane is struck;
- b. The particle leaves its current region;
- c. A boundary of an internal region is struck; or
- d. The particle undergoes a collision.

For 30° geometry problems, subroutine GR1 is called to determine which reflection plane (if any) is intersected by the extended trajectory. GR1 returns a distance SR to the pertinent plane (SR set to a large number, PINF, if no plane could be hit; SR initialized and kept = PINF

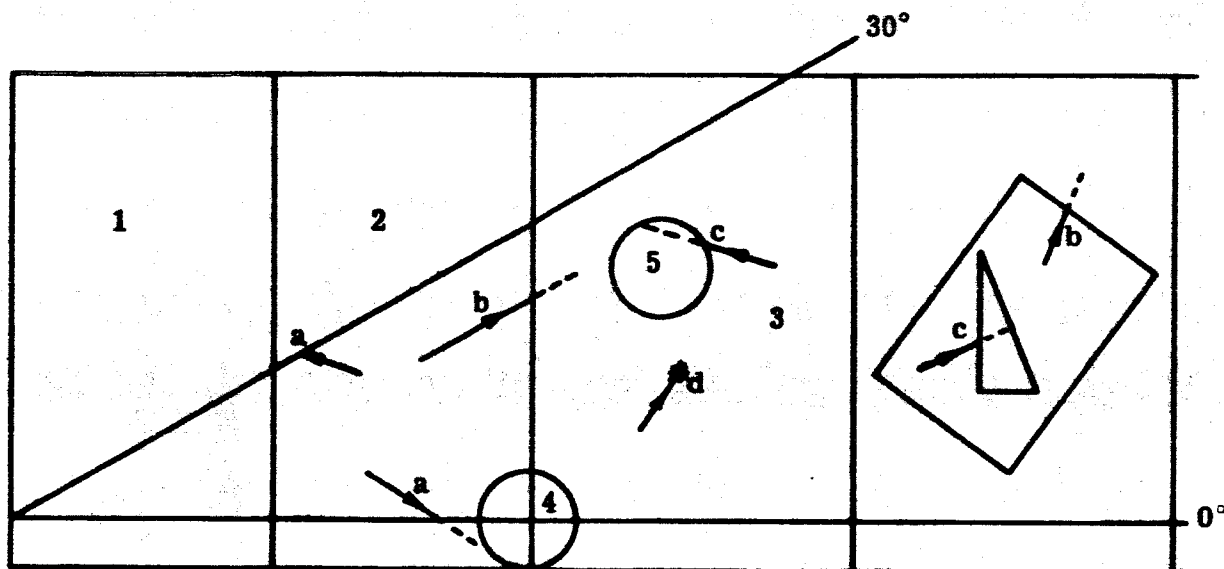


**Fig. 13 — Illustrating Types of Events Occurring during Particle Tracking. If an Ordinary-Region Boundary Coincides with the 0° Reflection Plane, the Reflection Event Takes Precedence.**

for 360° problems), and a flag IRELT = 0, 1, or 2 according as the extended trajectory would strike the z-axis, the lower, or the upper plane, respectively.

4. Next a number of mean-free-paths is selected from  $p(\lambda)d\lambda = e^{-\lambda} d\lambda$ , and allotted to the particle:  $\lambda = -\ln \xi$ , with  $\xi$  a random number.
5. The Data Retrieval subroutine, entry 1 (DR,1), is called to compute the total cross section  $\mu_T$  of the current medium for the particle energy, and the heating response function (if a gamma problem).
6. The distance SP to a collision (i.e., the free path if the current medium were unbounded) is computed as  $SP = \lambda/\mu_T$ ; if  $\mu_T = 0$  (vacuum region), SP is not computed, and the quantity SMP, the minimum of SP and SR, is set to SR.

7. The minimum (= SMP) of SP and SR (distances to collision and reflection plane) is established. It is now known that if an event of type (b) or (c) is to occur, it must occur at a shorter distance than SMP. KCOL is assigned the value 18 or 20 according as the tentative minimum-distance event is collision or reflection.
8. The geometry control subroutine G1 then determines if the particle emerges to the outside of the current region, or strikes an internal region, before traveling the distance SM(= SMP). In computing distances required to reach various internal regions, or to emerge from the current one, G1 calls specific geometry subroutines G1CYL, G1SPH, G1ORP, G1WED, and G1RPP. [Improved efficiency in scanning and tracking out of cylinders and spheres is achieved by updating the minimum (SM) of all distances previously computed, and suppressing the tracking of spheres and curved surfaces of cylinders (costly because of the square roots involved) for which it can be shown that no intersection closer than SM exists.]

G1 returns with IFLG = 0, -1, or +1, denoting: no boundary struck (closer than SMP), the base of a cylinder struck, or some other region boundary struck. Also returned is M = 0, -1, or NE > 0; these have the following meanings (pertinent only if IFLG ≠ 0): M = 0 means that the current region is exited, and that region is not a straddling cylinder; M = -1 means that the current region, a straddling cylinder, is being exited; M = NE means that the internal region NE is struck.

- Finally, G1 returns the actual distance SM traveled in the current region before the next event (collision, reflection, or boundary crossing) occurs.
9. Next, all answers dependent on SM are scored. These include the neutron or gamma track-length (if the current region is specified as a flux region), the gamma heat deposition in the region, and (for sec-



tored cylinders) the gamma heat deposition in each sector traversed by the track SM. Sector-cylinder scoring<sup>11</sup> is done via subroutines FNDANS, REPART, and SECTID.

10. The type of event terminating SM is next considered. If IFLG = 0, the event is collision (KCOL = 18) or reflection (KCOL = 20). If the latter, the reflection subroutine<sup>12</sup> GR2 is called to change the direction cosines of the particle to their post-reflection values, and to compute the new SR and IRELT. The remaining distance and number of mean free paths are updated:

$$SP - SM - SP; \quad \lambda - \mu_T \cdot SM - \lambda,$$

and tracking resumes at step (7).

11. If, on the other hand, KCOL = 18, a collision occurs. (FAP is called prior to the real collision to score for point detectors, if any.) Subroutine DR, entry 3, selects the interacting nuclide and type of interaction, which are identified by returned quantities IWT and NCDB, respectively. The values given NCDB have the following meanings: 1-4, elastic scattering; 1 = isotropic in C.M. system, 2 = hydrogen scatter, 3 = anisotropic scattering, 4 = isotropic in lab system, no energy degradation; 5, not used; 6 = absorption; 7 = inelastic discrete-level; 8, not used; 9 = inelastic continuum; 10 = beryllium inelastic, discrete; 11, not used; 12 = beryllium inelastic, continuum.

Depending on the value of NCDB, the particle is absorbed or scattered into a new direction and energy computed by subroutine ELAST or INELAS (for neutrons), or NIKI (for gammas). If absorption occurs, a particle-absorption counter for the pertinent region is incremented; also, for neutrons, the energy and location of the event are recorded [via (TAP,1)] in a neutron-interaction buffer, which is periodically

dumped on the interaction tape. If scattering occurs, the energy  $E'$  upon emerging is compared to the input cutoff energy, ECUT. If  $E' \leq$  ECUT, the particle (if a gamma) is counted as a degradation in the region, and its energy  $E'$  is added to the heat deposition in the region (and sector if applicable); if a neutron falls below ECUT, and a thermal group is specified ( $ETH \neq 0$ ), the particle assumes the value ETABLE(1) (the lowest energy in the EDT table), and tracking resumes (3); if no thermal group, a neutron absorption is forced, via (DR,5), at either  $E'$  or (if too low) at ETABLE(1). Upon death or absorption of any particle, a new particle is obtained from the latent list or (if this list is empty) from the source buffer [via subroutine (TAP, 3)] and tracking commences as for the first particle.

If  $E' > ECUT$ , Russian roulette or splitting is done if the energy weights ( $W$  and  $W'$ ) before and after the collision are different: the emergent particle is converted into NN1 particles, computed as

$$NN1 = \left[ \frac{W}{W'} + \xi \right], \quad (60)$$

where the brackets denote integral part.  $NN1 = 0$  means a death by Russian roulette;  $NN1 = 1$  continues the particle (step 12);  $NN1 > 1$  causes the storing of a latent "bundle" of  $NN1 - 1$  identical particles having the emergent energy  $E'$  and direction  $\underline{\omega}'$ , and the location of the collision; the one particle not stored away is then tracked from step (12).

12. Before tracking continues, the new direction cosines  $\omega'_1, \omega'_2, \omega'_3$  in the laboratory system are computed by subroutine DIREC, described in Section 11.4. Tracking then resumes from (3).
13. If, upon exiting G1 (step 10), IFLG  $\neq 0$ , then the event terminating SM is intersection with a region boundary.  $\lambda$  and SR are updated:

$\lambda - \mu_T \cdot SM \rightarrow \lambda$ ,  $SR - SM \rightarrow SR$ ; subroutine G2 updates the particle coordinates:  $x_i + \omega_i \cdot SM \rightarrow x_i$ ,  $i = 1, 2, 3$ . G2 also determines the next region entered; various branches of this subroutine handle the next-region identification on (a) emerging from an ordinary region, (b) emerging from a straddling cylinder, (c) emerging from the base of a cylinder (uses subroutine CMPRCD), (d) entering the base of a cylinder (uses subroutine CMPRS).

14. The next region entered is tested to determine if it is the input-specified transmission region, in which case a record of the particle transmission is made (TAP, 4), and the transmitted-particle counter IPT incremented, or, if the particle escapes from the overall ordinary geometry (indicated by  $IR' = IR$ ), in which case an escaped-particle counter IRR is incremented. If either occurs, a new particle is started. If latents are present, the last one stored is picked up and tracked, and the latest list is decreased accordingly. If the list is empty, a new source particle is started. If neither escape nor transmission occurs, the old and new region weights (RW) and (RW)' are compared; if they differ,

$$NN1 = \left\lceil \frac{(RW)}{(RW)'} + \xi \right\rceil \quad (61)$$

and  $NN1 - 1$  latents are stored (if  $NN1 > 1$ ) or the particle is killed (if  $NN1 = 0$ ).

15. Finally, if a particle survives into the next region,  $\mu_T$  is computed via (DR, 2) and the next event is determined (3).
16. The problem terminates with a dump of answers onto the dump tape when:
  - a. A source-particle is picked up with a history number greater than the last history number called for INPUTD; or

- b. A negative history number is encountered, signaling the end of the source tape; or
- c. Sense switch 6 is on (IBM-7094 version), or sense switch 7 is on (CDC-1604-A version).

Communication between the dump tape and ATHENA or the MEZDA programs (cf. Fig. 1) is accomplished via subroutine RSTRT(N,M), where  $N = 1, \dots, 8$  and  $M$  is a logical tape number. If  $N$  is odd, RSTRT(N,M) writes data from core onto logical  $M$ . If  $N$  is even, it reads data from  $M$  into core. From one to four groups of data are written for  $N$  odd, as indicated in the schematic flow diagram (Fig. 14). A similar sequence is followed for  $N$  even: in Fig. 14, replace "Write" by "Read," and (1, 3, 5, 7) by (2, 4, 6, 8).

#### 11.4 THE DATA RETRIEVAL AND INTERACTION ROUTINES

Subroutine DR(N,  $A_1$ ,  $A_2$ ) has entries for  $N = 1, 2, \dots, 10$ ; it returns various quantities  $A_1$ ,  $A_2$ , and data to common arrays. Calling DR(N, ...) will be denoted here as (DR, N); a synopsis of the operations for different  $N$  is given in Table 1.

The interaction experienced by the particle is determined in two steps. First the interacting nuclide is chosen; second, the specific event is chosen. If the event is scattering, the energy and direction of the scattered particle are evaluated.

The interacting nuclide is chosen by comparing the product of a random number and the total macroscopic cross section of the region composition,  $\xi \mu_T(E, R)$ , with the total macroscopic cross section of each nuclide in that composition,  $\mu_T(E, e_j)$ , where  $e_j$  denotes the  $j^{\text{th}}$  nuclide in the composition of region  $R$ ,  $j = 1, 2, \dots, l, \dots, L$ . If

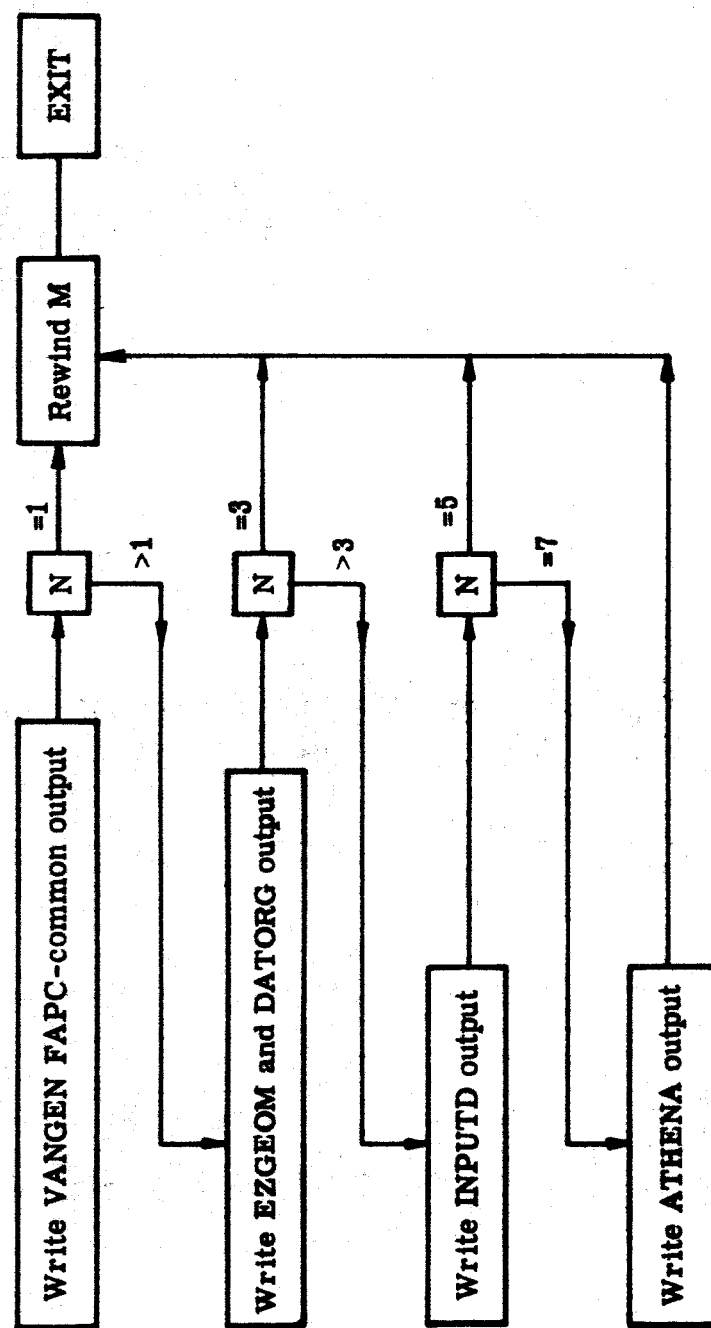


Fig. 14 — Operation of Subroutine RSTRT (N,M) for Odd N;  
Tape Writing Operations on Logical M

**TABLE 1 — FUNCTIONS OF THE DATA RETRIEVAL  
(DR,N) BRANCHES**

<u>N</u>	<u>Function</u>
1	Compute energy-interpolation factor
2	Compute composition total cross section (and gamma heating response function if applicable)
3	Select a nuclide and interaction type
4	Compute basic lethargy interval and initial address (IMY) of cross-section table in array of geometry and cross-section data
5	Pick a nuclide in which capture is to be forced (following neutron degradation with no thermal group)
6	Select $(\cos \theta)_{CM}$ in anisotropic elastic scattering
7	Select energy $E'$ in discrete inelastic scattering
8	Select energy $E'$ in continuum inelastic scattering
9	Given the cosine of a C.M. scattering angle, compute $G$ = twice the probability per unit $(\cos \theta)_{CM}$ of reaching such an angle, in anisotropic elastic scattering (used in FAP)
10	Select a nuclide with which to interact, and find the probabilities of absorption and elastic scattering, given that the interaction occurs with this nuclide (used in FAP)

$$\sum_{j=1}^{\ell-1} \mu_T(E, e_j) \leq \xi \mu_T(E, R) < \sum_{j=1}^{\ell} \mu_T(E, e_j), \quad (62)$$

then the interacting nuclide is  $e_{\ell}$ .

The type of interaction is similarly determined by comparing a random number to the probabilities that a given event takes place. These probabilities have been tabulated for each nuclide by the GENPRO program.

The selection of the nuclide and interaction type is done via the DR routine, as follows.

The incident energy,  $E$ , is referenced with respect to the output mesh energies  $E_j^G$  in an energy interval  $(E_j^G, E_{j-1}^G)$  by (DR,1). For each nuclide, at each  $E_j^G$ , GENPRO has supplied tables of total microscopic cross sections, scattering probabilities, absorption probabilities, and a scattering index. This index is given the type of scattering, if any, e.g., elastic, discrete, or continuum inelastic. If elastic scattering is indexed, it gives the type of elastic scattering that the particle suffers. For anisotropic elastic scattering, discrete inelastic, or continuum inelastic scattering, the scattering index gives the location of the tables of probabilities supplied by GENPRO: CHI, PLEV, and ENN tables (see Chapter 3). (DR,3) computes the microscopic total, elastic scattering, and absorption cross sections separately by linear interpolation in energy, using an interpolation factor computed in (DR,1). Then by comparing  $\xi \sigma_T$  successively with  $\sigma_{el}$  and  $(\sigma_{el} + \sigma_{abs})$ , it determines if the event is elastic scattering, absorption, or inelastic scattering. (DR,3) also returns the integer NCDB further identifying the interaction. (See Section 11.3, item 10.)

#### 11.4.1 ELAST Routine

The control digit NCDB has been set in (DR,3) to 1, 2, 3, 4 for the following cases: (1) isotropic in center-of-mass system, (2) hydrogen scatterer, (3) anisotropic

scattering, and (4) isotropic in laboratory system – no energy degradation. (Note: the present version of GENPRO does not output any scatter index implying NCDB = 4.)

### 1. Isotropic Scattering in Center-of-Mass System

It can be shown that if  $\xi$  is random in (0,1)

$$\chi = \frac{1 - \cos \theta_c}{2} = \xi \quad (63)$$

where  $\theta_c$  is the scattering angle in the center-of-mass system.  $E'$  and  $\cos \theta$  are then obtained by the standard relations

$$E' = E \left[ 1 - \frac{4A\chi}{(1+A)^2} \right], \quad \cos \theta = \frac{A + 1 - 2A\chi}{(A+1) \left[ 1 - \frac{4A\chi}{(A+1)^2} \right]^{1/2}}, \quad (64)$$

where  $A$  is the atomic weight and  $E$  is the incident energy.

### 2. Hydrogen Scatterer

Upon collision with hydrogen, particles are scattered in the forward direction only. It can be shown that the probability distribution function for  $\cos \theta$  is given by  $2 \cos \theta$ .

To pick a  $\cos \theta$  from the distribution  $2 \cos \theta$ , two random numbers are selected<sup>13</sup> and the larger of the two is retained as  $\cos \theta$ . Then

$$E' = E (\cos \theta)^2.$$

The control digit NCDC is set equal to one; this tells subroutine DIREC to apply the standard equations (Eq. 70) in computing the direction cosines in the laboratory coordinate system.



### 3. Anisotropic Scattering

The cosines of angles between which elastic scattering is equally probable for the specified energy mesh points,  $E_j^G$ , are supplied in the CHI tables referenced by the scattering index.

If the incident neutron energy,  $E$ , lies in the interval  $(E_j^G, E_{j+1}^G)$ , the CHI table relative to  $E_j^G$  is selected. This tabulation consists of

$$\chi_n = \frac{1 - \cos \theta_n}{2} \text{ for } n = 0, 1, 2, \dots, N; \quad \chi_0 = 0, \chi_N = 1.$$

In ATHENA,  $N$  is restricted to 10. The proper  $\chi$  is selected in (DR,6) by choosing a random number,  $\xi$ , and comparing the product  $10\xi$  with the numbers 1, 2, ...,  $N = 10$  successively.

If  $n < 10\xi < n+1$ , this means that  $\chi_n < \chi < \chi_{n+1}$ .

The integral part of the product  $10\xi$  is rejected and the remainder is taken as the interpolation factor,  $f$ . [This assumes a uniform probability distribution of  $\chi$  in each interval  $(\chi_n, \chi_{n+1})$ .]

Then

$$\chi = \chi_n + f(\chi_{n+1} - \chi_n), \quad (65)$$

and  $E'$  and  $\cos \theta$  are obtained using Eqs. 64.

### 4. Isotropic in Laboratory System, No Degradation

If the scatterer atomic weight is large, Eqs. 64 show that

$$E' \approx E, \quad (66)$$

and

$$\cos \theta \approx 1 - 2\chi = \cos \theta_c. \quad (67)$$

Thus, the scattering is approximately isotropic in the laboratory system and the particle energy remains unchanged by the collision. Therefore, a random number,  $\xi$ , is chosen and  $\cos \theta = 1 - 2\xi$ ; NCDC is set to 2. (This branch is not used in the present system since GENPRO does not output NCDB = 4.)

For all NCDB < 4, ELAST sets the control digit NCDC equal to one.

#### 11.4.2 INELAS Routine

Subroutines (DR,7) and (DR,8) are entered for discrete and continuum scattering, respectively (overlapping is included in the continuum spectrum), to select  $E'$ .

If  $E$  lies in  $(E_j^G, E_{j+1}^G)$ , the PLEV and ELEV tables\* for discrete scattering or the ENN table\* for continuum scattering relative to  $E_j^G$  are selected.

To select from the ENN table, (DR,8) uses the same technique as (DR,6).

To select from the PLEV table, (DR,7) uses the same technique as (DR,3) in the selection of the interacting element.

Using the inequality (Eq. 62) in which the nuclide cross sections are replaced by the level-excitation probabilities, one obtains the appropriate energy level  $E''$  to which the particle scatters, and  $E' = E - E''$ .  $\cos \theta = 1 - 2\xi$ , and NCDC is set = 2, implying that DIREC is to direct the emergent particles isotropically in the laboratory system.

#### 11.4.3 The NIKI Routine

It is assumed that  $\gamma$ -scattering results from the Compton effect. A  $\gamma$ -ray of energy  $\alpha$  (in  $mc^2$ ) traversing matter has a probability,  $p(\chi/\alpha) d\chi df$ , of having a collision in the distance  $df$  (cm) and emerging from this collision with an energy

---

\*See Chapter 3.

$\alpha' = \chi\alpha$ . For  $\chi$  satisfying  $1 \leq \chi \leq 1 + 2\alpha$ ,

$$p(\chi/\alpha) d\chi = \frac{A}{\chi^2} (\cos^2 \theta - 1 + \chi + \frac{1}{\chi}) d\chi, \quad (68)$$

where  $A = n\pi a_e^2/\alpha$

$n$  = the number of electrons per  $\text{cm}^3$

$a_e$  = the classical radius of the electron =  $2.81833 \times 10^{-13}$  cm

$\theta$  = the scattering angle which is related to  $\alpha$  and  $\chi$  by the Compton relation

$$\cos \theta = \frac{1}{\alpha} - \frac{\chi}{\alpha} + 1. \quad (69)$$

$p(\chi/\alpha)$  is called the Klein-Nishina probability distribution function. To pick a  $\chi$  from  $p(\chi/\alpha)$ , a rejection technique devised by H. Kahn is used in ATHENA.<sup>13</sup>  $p(\chi/\alpha)$  is broken up into the sum of two probability distribution functions. A random number,  $\xi_1$ , is compared to  $(2\alpha+1)/(2\alpha+9)$ .

If  $\xi_1 < (2\alpha+1)/(2\alpha+9)$ ,  $y$  is set equal to  $1 + 2\alpha\xi_2$  (where  $\xi_2$  is a second random number), and another random number,  $\xi_3$ , is compared to  $4 [(1/y) - (1/y^2)] = m$ . If it is less than  $m$ ,  $\chi = y$ . If it is greater than  $m$ ,  $y$  is rejected and the procedure is repeated.

If  $\xi_1 > (2\alpha+1)/(2\alpha+9)$ ,  $y$  is set equal to  $(2\alpha+1)/(1+2\alpha\xi_2)$ , and  $\xi_3$  is compared to

$$\frac{1}{2} \left( \cos^2 \theta + \frac{1}{y} \right),$$

where

$$\cos \theta = \frac{1}{\alpha} - \frac{y}{\alpha} + 1.$$

If it is less than  $(1/2) [\cos^2 \theta + (1+y)]$ ,  $\chi = y$ . If it is greater than  $(1/2) [\cos^2 \theta + (1/y)]$ ,  $y$  is rejected and the procedure is repeated.

Once  $\chi$  has been selected, NIKI computes  $E' = \chi E$ , and  $\cos \theta$  (Eq. 69).

#### 11.4.4 The DIREC Routine

The interaction routines compute and transmit to the main program the energy after scattering,  $E'$ , and the cosine of the scattering angle,  $\cos \theta$ . What is required is to evaluate the direction cosines of the new particle direction in the Cartesian coordinate system, given  $\cos \theta$  and the initial direction cosines. The DIREC routine computes these cosines as follows.

1. A rejection technique is used to choose the sine and cosine of an azimuth  $\phi$  with respect to the initial direction,  $\phi$  equidistributed in  $(0, 2\pi)$ .
2. (a) If the argument NCDC (supplied by the interaction routines) is 1, the new direction cosines are computed as

$$\begin{aligned}\Omega'_x &= \sqrt{\frac{1-\mu^2}{1-\Omega_z^2}} (\Omega_y \cos \phi + \Omega_z \Omega_x \sin \phi) + \Omega_x \mu \\ \Omega'_y &= \sqrt{\frac{1-\mu^2}{1-\Omega_z^2}} (\Omega_y \Omega_z \sin \phi - \Omega_x \cos \phi) + \Omega_y \mu \\ \Omega'_z &= -\sqrt{(1-\mu^2)(1-\Omega_z^2)} \sin \phi + \Omega_z \mu\end{aligned}\tag{70}$$

where  $\mu = \cos \theta$ , and

$\underline{\Omega} = (\Omega_x, \Omega_y, \Omega_z)$  is the given initial direction.

- (b) If NCDC = 2, the new direction cosines are chosen isotropically [given as input a  $\cos \theta_z$  equidistributed in  $(-1, +1)$ ].
- (c) If NCDC = 3, DIREC chooses an isotropic direction independent of the input  $\cos \theta$ .

## 11.5 THE FLUX-AT-A-POINT ROUTINES

In the CDC-1604-A version and one of the IBM-7094 versions of ATHENA there is available the option of specifying a number of point detectors at which gamma fluxes and volumetric heating are to be computed. Several statistical-estimation procedures are used to effect the scoring. Different branches treat: (1) the primary-gamma uncollided fluxes for in-core and out-of-core detectors; (2) the secondary-gamma uncollided fluxes (here the estimation starts in the neutron ATHENA problem, is continued in GASP, and is completed in the secondary-gamma ATHENA); and (3) the collided gamma fluxes.

The principal routines in ATHENA which implement the method are subroutines FAP, ADJ, and TRACK.

Brief descriptions and flow charts of the procedure follow.

### 11.5.1 Primary-Gamma Estimations

The method employed here is essentially that described by Kalos<sup>14,15</sup> for the estimation of once-more-collided flux. A modification, devised by the same author, has been made in the procedure for selecting the intermediate points at which virtual collisions are made in the estimations for the point detectors.

The new procedure for selecting intermediate points is designed to ensure that, when a real collision occurs close to a detector (say within a small optical path  $\lambda_0$ ), with finite probability the intermediate point will be chosen within a radius of  $\lambda_1 \sim \lambda_0$  mean free paths (mfp) from the collision or detector point. \* Taking the probability density per mfp as

$$\frac{dp}{d\lambda} = \frac{dp}{dH} \frac{dH}{d\lambda} = e^{-H(\lambda)} H'(\lambda), \quad (71)$$

---

\*Such a condition was found to be necessary for finite-variance estimations.

where the function  $H(\lambda)$  is yet to be determined, then the probability ( $P_0$ ) that a selected point be within  $\lambda = \lambda_0$  is

$$P_0 = \int_0^{\lambda_0} \frac{dp}{d\lambda} d\lambda = \int_0^{\lambda_0} H'(\lambda) e^{-H(\lambda)} d\lambda = e^{-H(0)} - e^{-H(\lambda_0)}. \quad (72)$$

If now we let

$$H(\lambda) = \lambda + \frac{\lambda}{\lambda + \lambda_0}, \quad (73)$$

then

$$H(0) = 0, \quad H(\lambda_0) = \lambda_0 + \frac{1}{2},$$

and

$$P_0 = 1 - e^{-(\lambda_0 + \frac{1}{2})}; \quad \text{hence } P_0 \approx 0.4 \text{ as } \lambda_0 \rightarrow 0, \quad (74)$$

and Eqs. 71 and 73 define a spatial distribution function with the required property for collision points with small  $\lambda_0$ . Also  $H'(\lambda) = 1 + \lambda_0/(\lambda + \lambda_0)^2 \rightarrow 1$  for large  $\lambda_0$ , and  $H(\lambda) \rightarrow \lambda$ ,  $dp/d\lambda \rightarrow e^{-\lambda}$ , so that for distant collisions the intermediate points will effectively be chosen from  $e^{-\lambda}/4\pi r^2$  by the following procedure.

1. Compute the number of mfp ( $\lambda_0$ ) from collision to detector;
2. Pick  $H_1$  from  $e^{-H}$ :  $H_1 = -\ln \xi$ ;
3. Track (isotropically, from collision or detector point) through  $\lambda$  mfp (at the incident energy  $E$ ), where  $\lambda$  satisfies

$$\lambda + \frac{\lambda}{\lambda + \lambda_0} = H_1; \quad (75)$$

i.e.,

$$\lambda = -\frac{T}{2} + \frac{1}{2} \sqrt{T^2 + 4H_1\lambda_0}, \quad T \equiv \lambda_0 + 1 - H_1. \quad (76)$$

This procedure is used in the estimation of all but the uncollided fluxes. The intermediate point is located by tracking from either the collision or the detector point, with equal probabilities. The probability distribution function corresponding to this method of sampling is

$$(\text{pdf}) = \frac{\mu_I(E)}{8\pi} \left[ \frac{H'(\lambda_1) e^{-H(\lambda_1)}}{r_1^2} + \frac{H'(\lambda_2) e^{-H(\lambda_2)}}{r_2^2} \right] \quad (77)$$

where  $\mu_I(E)$  is the macroscopic cross section at the intermediate point, and subscripts 1 and 2 refer to quantities computed from collision or detector point, respectively, to the intermediate point. The estimated once-more-collided flux at a given detector, based on the a priori pdf of the intermediate point and the probability of the second scattering, is divided by the sampling pdf (Eq. 77). Further details of the calculation are indicated in the FAP flow chart (Fig. 15).

For the uncollided primary-gamma fluxes (estimated for each detector at the beginning of each particle history), the method of calculation depends on whether the pertinent detector is in-core or out-of-core. (This detector classification has been done in program INPUTD.)

For out-of-core detectors, a direct estimate is made of the uncollided flux:

$$\phi_0 = \frac{e^{-\lambda}}{4\pi r^2} \cdot Wt,$$

where  $Wt$  = the product of the region and energy weights of the source particle.

For in-core detectors, the method of direct estimation has infinite variance, hence an adjoint calculation is made: a location  $\vec{r}$  is selected from

$$\frac{\mu e^{-\lambda}}{4\pi|\vec{r}-\vec{r}_D|^2},$$

and the quantity  $S(\vec{r})/\mu(r)$  is scored, where  $S(\vec{r})$  is the probability per unit volume that a given source particle originates in the vicinity of the position  $\vec{r}$ . This calculation is done in subroutine ADJ (Section 11.5.6); the  $S(\vec{r})$  is computed by interpolation in the normalized source-density tables which have been communicated by VANGEN.

### 11.5.2 Secondary-Gamma Estimations

Neutron absorptions and inelastic scatterings are recorded on an interaction tape, and the information on this tape is used by the GASP program (Chapter 13) to produce a secondary-gamma source tape. ATHENA tracks and scores these particles as in a primary-gamma problem, with the exception that, in FAP, the estimation of uncollided secondary-gamma fluxes is suppressed for "real" particles, but scored for the "fake" particles generated during the neutron problem specifically for this portion of the answer. (The adjoint method, used in primary-gamma calculations, is not convenient here since there is no a priori information to provide an analytic representation of the secondary-gamma spatial distribution.)

The method<sup>16,17</sup> is similar to that used in the calculation of once-more-collided gamma fluxes. What is required is to estimate for each source neutron or neutron going into collision the flux of gammas after one more neutron collision. Apart from factors which relate to scattering probability for neutrons and production cross sections for gammas, the flux of gamma rays at a detector following one more flight as neutron plus one flight as gamma is



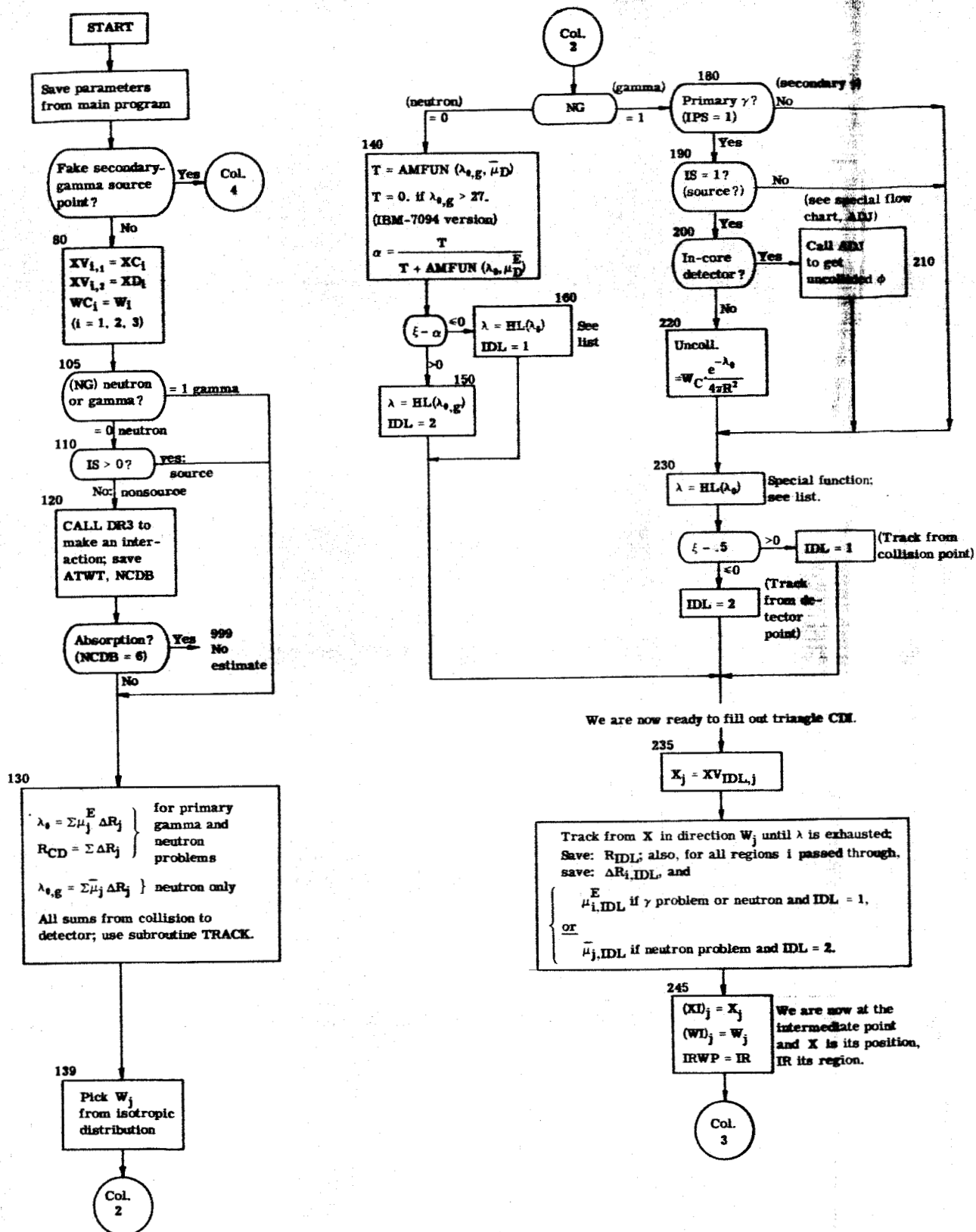
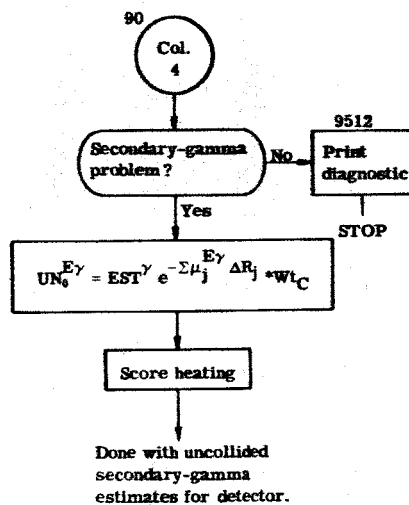
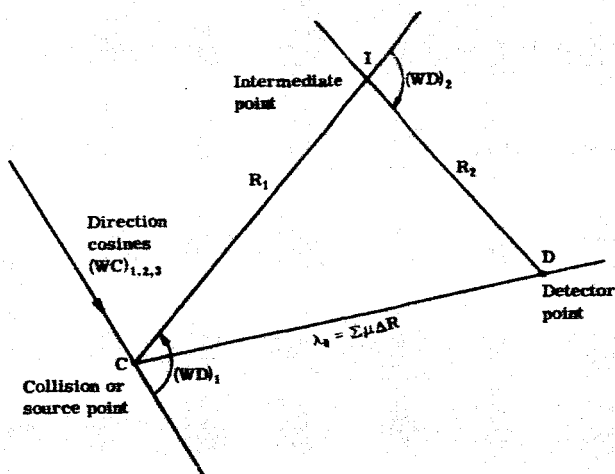
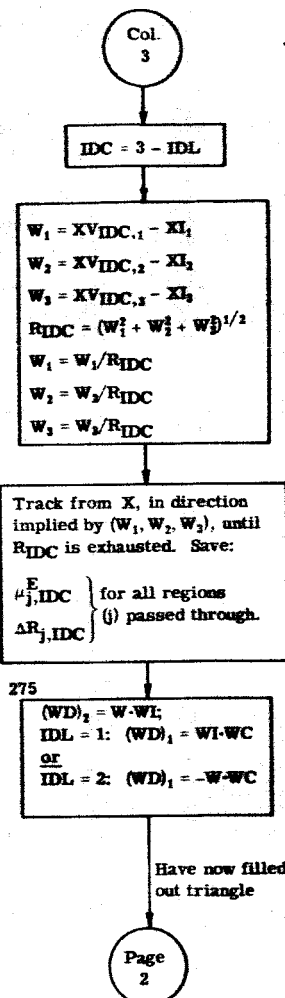


Fig. 15 — Flux at a Point, Tracking Part



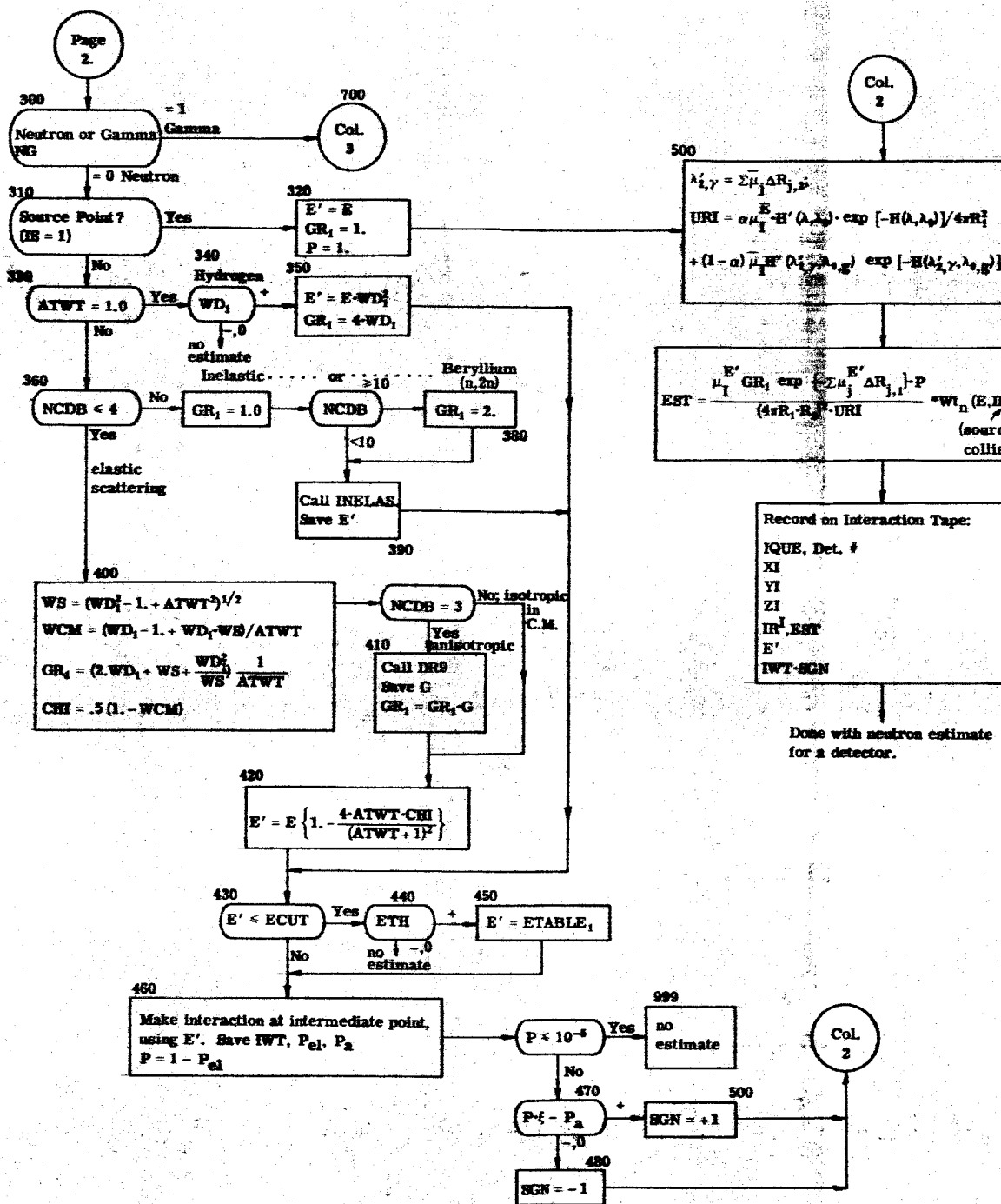
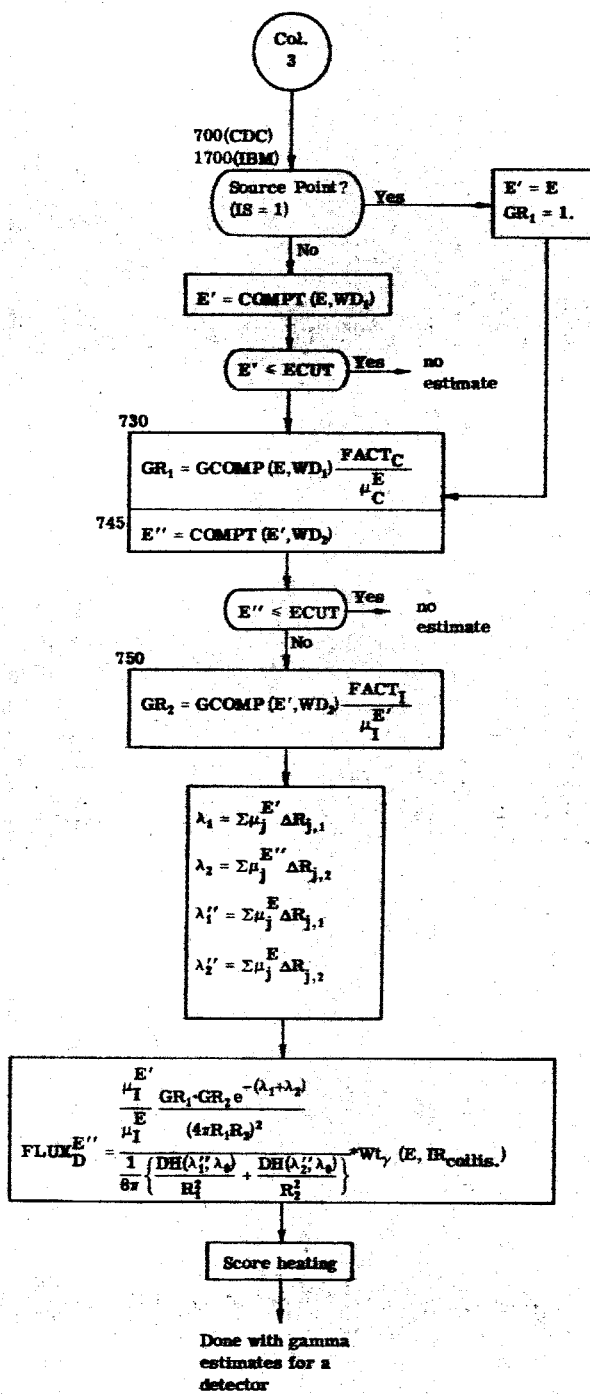


Fig. 15 — (Continued) — Estimation Phase



$$\phi(r_D) = \frac{\mu_n(r_I) e^{-\lambda_{1n}} e^{-\lambda_{2\gamma}}}{(4\pi r_1 r_2)^2}; \quad (78)$$

here  $\mu_n(r_I)$  is the attenuation coefficient for the scattered neutron at the intermediate point (where the gamma is produced),  $\lambda_{1n}$  is the optical depth (total mean free paths) for the scattered neutron evaluated between collision (or source) point and the intermediate point,  $\lambda_{2\gamma}$  is the optical depth for secondary gamma between intermediate and detector points evaluated for an appropriate energy, and  $r_1, r_2$  are distances from intermediate to collision or detector point.

In sampling to select an intermediate point, the method leading to Eq. 76 is used. In the present application, tracking to locate the intermediate point proceeds from the collision point with probability  $\alpha$  (defined below), using the attenuation coefficient  $\mu_n(r)$  for the original neutron energy, and with probability  $(1-\alpha)$  from the detector point, using representative gamma cross sections ( $E_\gamma \sim 1.0$  Mev) for the various compositions supplied as input for the neutron problem. These are called  $\mu_\gamma(r)$  below.

The pdf for the intermediate point is

$$U(r_I) = \alpha \mu_n(I) H'(\lambda_{1n}, \lambda_{0n}) \exp[-H(\lambda_{1n}, \lambda_{0n})/4\pi r_1^2] + (1-\alpha) \mu_\gamma(I) H'(\lambda_{2\gamma}, \lambda_{0\gamma}) \times \exp[-H(\lambda_{2\gamma}, \lambda_{0\gamma})/4\pi r_2^2], \quad (79)$$

where  $H(\lambda, \lambda_0) = \lambda + \lambda/(\lambda + \lambda_0)$ ,

$$H'(\lambda, \lambda_0) = (\partial/\partial\lambda) H(\lambda, \lambda_0) = 1 + \lambda_0/(\lambda + \lambda_0)^2,$$

$\lambda_{0n}$  = the optical depth for a neutron at the unscattered energy, evaluated between collision and detector,

$\lambda_{0\gamma}$  = the optical depth for a gamma at the representative energy, evaluated between collision and detector.

These procedures ensure that  $U(r_1)$  is large in the neighborhood of the collision point and of the detector point. It is desirable to arrange that the relative magnitudes of  $U(r_1)$  in each neighborhood match those of the expected contributions to  $\phi_\gamma$  (i.e., track preferentially from collision point if resulting  $\phi_\gamma$  is large). This is accomplished by determining  $\alpha$ , the probability of tracking from the collision point, prior to each estimation.

$$\text{As } r_1 \rightarrow 0, \phi_\gamma = \phi_\gamma(r_C) - \mu_n(r_C) e^{-\lambda_{en}/(4\pi r_1 R)^2},$$

$$U = U(r_C) - \alpha \mu_n(r_C) (1 + 1/\lambda_{en}) / 4\pi r_1^2;$$

$$\text{as } r_2 \rightarrow 0, \phi_\gamma = \phi_\gamma(r_D) - \mu_n(r_D) e^{-\lambda_{en}/(4\pi r_2 R)^2},$$

$$U = U(r_D) - (1 - \alpha) \mu_\gamma(r_D) (1 + 1/\lambda_{e\gamma}) / 4\pi r_2^2.$$

When the ratio  $U(r_C)/U(r_D)$  is set equal to  $\phi_\gamma(r_C)/\phi_\gamma(r_D)$  (and  $\mu_n$  replaces  $\mu_\gamma$ ) we find

$$\alpha = \frac{\mu_\gamma(r_D) (1 + 1/\lambda_{e\gamma}) e^{-\lambda_{e\gamma}/(4\pi r_D R)^2}}{\mu_\gamma(r_D) (1 + 1/\lambda_{e\gamma}) e^{-\lambda_{e\gamma}/(4\pi r_D R)^2} + \mu_n(r_D) (1 + 1/\lambda_{en}) e^{-\lambda_{en}/(4\pi r_D R)^2}} \quad (80)$$

The flux-at-a-point procedures are embodied in subroutine FAP, for which a flow diagram is given (Fig. 15).

This subroutine handles both the neutron and gamma calculations. There is a subdivision into a Tracking Phase, which is concerned with selecting an intermediate point (for neutrons or real gammas) or completing the estimation (for a fake gamma), and an Estimation Phase, which, given an intermediate point, generates an estimate of the flux (for real gammas), or produces a fake interaction (for neutrons) which includes an incompleted estimate of uncollided secondary-gamma flux.

### 11.5.3 Tracking Phase

The parameters of the particle in the main program are saved, for restoration on exiting from FAP. If a fake particle, no further selection of intermediate points is made; the completion of neutron to uncollided secondary gamma flux is made for the pertinent detector (statement 950).

If a real particle, the neutron branch at (105) calls for DR(3) to select a neutron interaction at the collision point (bypassed if a source neutron). Then the collision-to-detector optical depth  $\lambda_0$  and distance  $R_{CD}$  are computed, also the effective  $\lambda_{0,g}$  (based on the representative  $\mu_\gamma$  of Eq. 79) if a neutron problem.

Isotropic direction cosines  $W_j$  are selected for use in tracking to the intermediate point (137).

At column 2 a decision is made to track from collision point (IDL = 1) or detector point (IDL = 2). The neutron branch follows the procedure explained in Section 11.5.2 (Eq. 80); in the gamma branch tracking proceeds for nonsource particles from either point with equal probability. If the gamma is in a secondary-gamma problem, the uncollided-flux estimate is bypassed because it is computed via the generation and scoring of the fake particles. If a primary source particle, the uncollided flux is estimated as  $e^{-\lambda_0}/4\pi R_{CD}^2$  for an out-of-core detector, or via the adjoint-calculation subroutine ADJ, described below; then a once-more-collided estimate is made as usual.

In column 3, the length of the last leg of the triangle containing collision, detector, and intermediate points is computed, as well as the segments  $\Delta R_j$  in the various regions traversed by this leg.

With the determination of point I and the angles whose cosines are  $(WD)_1$  and  $(WD)_2$ , the Tracking Phase of FAP is completed.

#### 11.5.4 Estimation Phase

Virtual events are forced at C and I, implying that:

1. For gammas, a collision (or emergence of source particle) at C and energy E caused a deflection (or initial motion) through  $\cos^{-1} (WD)_1$ , a free flight at energy E' (or E) for the distance  $R_1$ , a collision at energy E' (or E) at I resulting in a deflection through  $\cos^{-1} (WD)_2$ , and a free flight (at energy E'') at least as far as  $R_2$ ; or
2. For neutrons, a collision (or emergence of source particle) at C and energy E caused a deflection (or initial motion) through  $\cos^{-1} (WD)_1$ , a free flight at energy E' (or E) for the distance  $R_1$ , and a secondary-gamma-producing event (absorption or inelastic scattering) at I and energy E' (or E).

We next enter the Estimation Phase (p. 2 of Fig. 15). If the particle is a gamma, at this point we have only to compute the estimate for once-more-collided flux (column 3, p. 2), since uncollided fluxes are computed via the procedures of column 2 or column 4 of page 1. The estimate depends upon quantities  $GR_1$  and  $GR_2$ ;  $GR_1$  is  $4\pi$  times the probability per steradian at  $\cos^{-1} (WD)_1$  that a collision (or source particle) at E will result in a scattering (or first flight) through the angle  $\cos^{-1} (WD)_1$ ; similarly for  $GR_2$ , where the pertinent quantities are E' and  $\cos^{-1} (WD)_2$ . The estimate also depends upon the distances  $R_1$  and  $R_2$ , the optical thicknesses  $\lambda_1(E')$  and  $\lambda_2(E'')$ , and finally on the factors

$$8\pi [\mu_I(E')/\mu_I(E)] / \left[ \frac{DH(\lambda_1'', \lambda_2)}{R_1^2} + \frac{DH(\lambda_2'', \lambda_2)}{R_2^2} \right],$$

which compensate for the difference between the forced density of collision points I and the density with which collisions would naturally occur at I. For the computation of the differential scattering probabilities and the degraded energies E'



and  $E''$ , functions GCOMP and COMPT compute the Klein-Nishina differential cross section and Compton-scattering emergent energies, respectively.

For neutrons, the determination of  $GR_1$  requires entry into the ATHENA interaction routines to select a forced interaction at C, and appropriate calculations based on the outcome. If the particle is a source particle,  $GR_1 = 1.0$  (as is also done for gammas); this implies isotropicity of the sources. As indicated on the flow chart, the computations for  $GR_1$  and  $E'$  distinguish among hydrogen scatter, isotropic (C.M.) elastic scattering, anisotropic elastic scattering, inelastic scattering, and the (n,2n) reaction in beryllium. If, as a result of the virtual interaction at C, the neutron degrades below a cutoff energy ECUT (input), the estimation is terminated unless the problem calls for a thermal group (ETH $\neq$ 0). Since considerable calculating effort has been expended to arrive at this point in the neutron-to-gamma estimate, the neutron interaction at I is forced to be other than elastic scattering (which would produce no gamma), and the estimate is multiplied by an extra factor  $(1-p_{el})$ , where  $p_{el}$  is the probability of elastic scattering for the nuclide selected, at energy  $E'$ . If  $1 - p_{el} \leq 10^{-5}$ , the estimation is terminated; otherwise an inelastic scattering or absorption is forced, with the appropriate relative probabilities. The output from this pass through the subroutine is an array of numbers recording the description of the estimation thus far completed; the array includes the neutron history number, the detector being scored, coordinates of I, region of I, the quantity EST (representing differential scattering probabilities, geometric and material attenuation factors, and the forced-interaction distribution function URI implied by the method of locating I), the intermediate neutron energy  $E'$ , and  $\pm IWT$ , identifying the nuclide involved at I and the type of interaction (- for absorption, + for inelastic scattering). This array is kept in a buffer area in core which is periodically dumped on magnetic tape or disc (interaction tape).

Special functions referred to in Fig. 15 are presented in Table 2.

TABLE 2 — SPECIAL FUNCTIONS REFERRED TO IN THE  
FLUX-AT-A-POINT FLOW CHARTS

<p>Function HL(<math>\lambda</math>)</p> $H_1 = -\log \xi$ $T = 1 + \lambda - H_1$ $HL = \frac{-T + \sqrt{T^2 + 4H_1\lambda}}{2}$
<p>AMFUN(<math>\lambda, \mu</math>) = <math>\mu^{\mu}(1+1/\lambda) e^{-\lambda}</math></p> $H(\lambda, \lambda_0) = \lambda + \lambda/(\lambda + \lambda_0)$ $HP(\lambda, \lambda_0) = \frac{\partial}{\partial \lambda} [H(\lambda, \lambda_0)] = 1 + \lambda_0/(\lambda + \lambda_0)^2$
<p>COMPT(<math>E, \omega</math>) = <math>\frac{E}{1 + \frac{E(1-\omega)}{0.510984 \times 10^6}}</math></p>
<p>GCOMP(<math>E, \omega</math>) = <math>\frac{1}{4\pi} \left\langle \left( \frac{1+\omega^2}{2} \right) \left[ \frac{1}{1 + \alpha(1-\omega)} \right]^2 \left\{ 1 + \frac{\alpha^2(1-\omega)^2}{[1 + \alpha(1-\omega)][1+\omega^2]} \right\} \right\rangle ; \left( \alpha = \frac{E}{m_0 c^2} \right)</math></p>
<p>FACT = <math>4\pi \sum_A Z_A C_A</math>, sum over elements in region;</p> <p>= <math>4\pi \times \text{No. of electrons/(barn-cm)}</math></p> <p>DH(<math>\lambda, \lambda_0</math>) = HP(<math>\lambda, \lambda_0</math>) * expf [-H(<math>\lambda, \lambda_0</math>)]</p>

This completes the discussion of the flux-at-a-point routine proper. The calculation of the uncollided secondary-gamma fluxes at detectors, begun in the neutron problem, is completed via processing of the neutron interaction tape (which also has records of real inelastic scatterings and absorptions) by the GASP program to produce a gamma source tape, which is input for the gamma ATHENA program.

#### 11.5.5 Adjoint Calculations

To avoid the infinite variance associated with a direct inverse-square estimation of uncollided flux at detectors located in a source region, an adjoint calculation is made of this quantity for in-core detectors. For each direct estimate bypassed, a call is made to subroutine ADJ (see flow chart, Fig. 16). Here the number of mfp,  $\lambda$ , is selected from  $e^{-\lambda}$ , and a ray is tracked from the detector in a direction chosen from an isotropic distribution until  $\lambda$  is exhausted (evaluated at the energy  $E$  of the original primary source particle). A number of tests are made, leading to zero estimates if the end-point of the ray is (1) above or below the core, (2) outside the core radially, or (3) in a gap between stages. If none of these occurs, the contribution to the uncollided flux at the pertinent detector is computed as the product of the values of TR and TZ at the terminal point, divided by the gamma attenuation coefficient for the terminal region at the source energy. TR and TZ are tables, transmitted from VANGEN, of the source densities per unit core area and axial length, respectively; the required values of TR(R) and TZ(Z) are obtained in ADJ by linear interpolations in the arguments. It can be shown that the expected flux per trial using this procedure is the same as in a direct estimation.

### 11.6 DESCRIPTION OF THE ATHENA INPUT AND OUTPUT

#### 11.6.1 Input

All of the data and problem parameters needed by ATHENA are supplied by the dump and source tapes. To restart a problem which has been terminated via a

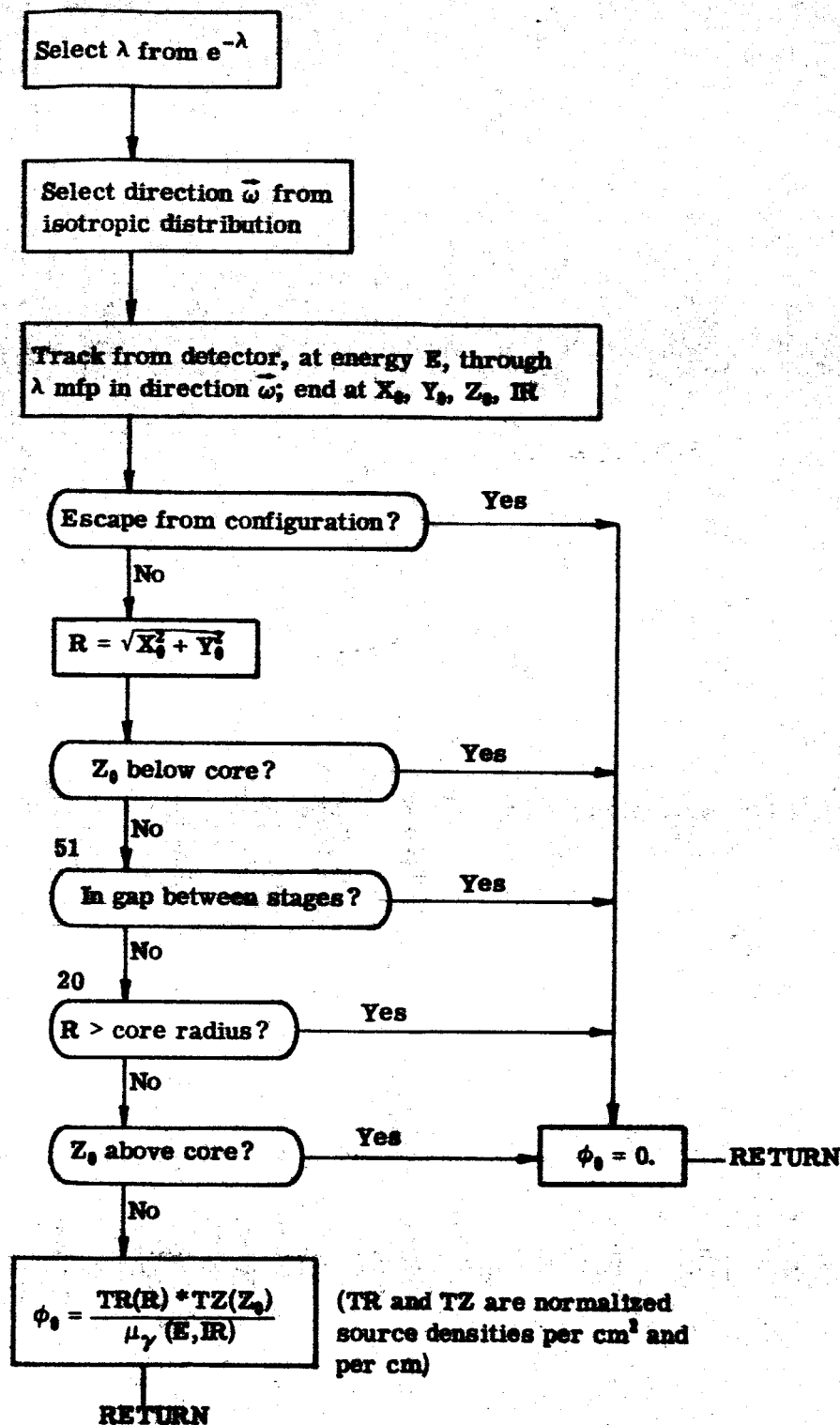


Fig. 16 — The ADJ Routine

sense-switch option, it may be necessary to rerun INPUTD with appropriate changes (see Section 11.7.1).

### 11.6.2 ATHENA Output

#### Dump Tape

ATHENA communicates to the dump tape\* the results of the tracking and scoring, including:

1. An answer array *S* containing all region heats (if a gamma problem), sector heats, track lengths by energy bin in each flux region, fluxes by energy bin for each point detector (gamma problems), and the squares of the corresponding answers as accumulated in statistical groups;
2. Tables of absorptions, deaths by importance sampling, ~~births~~ by (importance sampling + source introduction), and degradations, all vs region number, and of deaths and births by energy importance sampling [and particles arising from the (n,2n) reaction in beryllium].

#### Transmission Tape

The data on the transmitted-particle tape are in the standard format for a source tape; the energy, history number, positions, and direction cosines describe the particles as they struck the transmission region in the ATHENA problem. The region number attached to each particle is the region from which the particle struck the transmission region.

#### Interaction Tape (Neutron Problems)

A seven-word record of each real neutron absorption and inelastic scattering is written out; each record contains:

---

\*There is also an unedited printout of the accumulated answers and particle counts.

1. the neutron history number;
- 2.,3.,4. x,y,z coordinates of the interaction;
5. region;
6. energy;
7.  $\pm$ IWT, the nuclide identifier [(+) = inelastic; (-) = absorption].

Also on the interaction tape (if point detectors were present) are records of "fake" interactions. These are intermixed with the real interactions, as they occur in the neutron problem. Format is the same as above, except for the following items:

1. Packed into word 1 is a pertinent detector number;
2. Packed into word 5 is a floating number EST, the result of the incomplete estimate of uncollided secondary-gamma flux-at-a-point.

### 11.6.3 Error-Tracing Printout

Subroutine DPRIN is called (1) to provide a trace of a faulty trajectory arising from a number of causes, such as a tracking error, or an incorrectly-defined source particle; (2) to trace the completion of the last history when a sense-switch 6 or 7 termination is effected; or (3) to trace without terminating, via sense-switch 3 (CDC version only).

In case (1) the program recomputes from the start of the trajectory of the pertinent particle.

DPRIN prints out the contents of a number of labeled-common arrays, at all points on the trajectory at which significant changes occur, such as source-particle origins, region crossings, and exits from collisions. The printout occupies one page per event; by examining successive pages one can reconstruct the details of the trajectories traced. The items are printed out with minimal identification, hence we identify them below.

<u>Label</u>	<u>Items in Order of Printout</u>
(None)	N = integer identifying location in program from which DPRIN was called; its meanings are as follows.
<u>N</u>	<u>Location in program; status of calculations</u>
1	D360, statement 8540; $\lambda$ , SM, SR, SP, and SMP have been computed; XSB (q.v.) is the random number whose negative logarithm is $\lambda$ ; FMUTOT (q.v.) applies
2	D360, statement 119; have come out of collision; NCDB, ATWT apply
3	D360, statement 1010; source particle has been acquired; GR1 has been called (30° problem) and energy-weight bin JS has been computed; E is now the source energy or the energy after collision
4	D360, statement 6; source particle has been acquired
5	D360, statement 111; statistical grouping has just been done
6	Not used
7	FAP, statement 609; FAP about to be exited; labeled-common FAPC applies
8	D360, statement 8537; G2 has just been exited (region boundary met); IR, IRPRIM apply.
BLANK	INERR, ≠0 if error has occurred; ND = size of answer array (see Section 11.7); IEORG = origin of geometry data, relative to TAB 3; IORG3 = length of geometry data; IRMAX = number of regions; NBOD = number of external regions.
PARAM	IE2, number of energy-weight bins; IE3, number of flux bins (for regions and/or FAP); IPROB = 1 for 30°, 2 for 360°; NARG5 = 0 for original problem, 1 for restart; NFIRST, first history number; NLAST, last history number; IETAG, number of histories per statistical group; IRT, transmission region; LSECF, number of sectorized cylinders; NRDW, number of region-dependent weights; ITLFF, number of flux regions.

<u>Label</u>	<u>Items in Order of Printout</u>
<b>PAREM</b>	<p> <b>IQUE</b>, current history number;  <b>JDUM</b>, latest index in interaction buffer (<math>\leq 36</math>);  <b>LWRI</b>, number of groups of interactions that have been written;  <b>MIB</b>, latest index in source-particle buffer (<math>\leq 100</math>);  <b>IREC</b>, number of 100-particle source groups that have been read from tape;  <b>MOB</b>, latest index in transmitted-particle buffer (<math>\leq 100</math>);  <b>IP3</b>, number of 100-particle transmission groups that have been written onto tape. </p>
<b>ITAPS</b>	<p>Six integers, of which only the first five have meanings, viz: logical number assignments for Element Data Tape, dump tape, source tape, transmission tape, and interaction tape, respectively.</p>
<b>SSS</b>	<p>Seven integers, representing the states of sense switches 1-7; 0 = off, 1 = on.</p>
<b>GEDEP</b>	<p> <b>M</b> = number of the nonordinary region struck, if any;  <b>IFLG</b> (<math>\neq 0</math> if G1 finds region boundary is struck; cf. Section 11.3);  <b>IR</b>, current region;  <b>IRPRIM</b>, next region (when applicable);  <b>SM</b>, distance to next event;  <b>SMP</b>, minimum of distances to collision and reflection;  <b>SR</b>, distance to pertinent reflection plane;  <b>SP</b>, distance to a collision assuming unbounded medium;  <b>NEXT</b>, external-region number;  <b>IM</b>, applies to ORP; = 1, 2, or 3 if an x, y, or z face is struck;  <b>KM</b> (= 1, 2, ..., 6) applies to ORP;              (1,2) - (min, max x-face struck);              (3,4) - (min, max y-face struck);              (5,6) - (min, max z-face struck);  <b>The current x, y, z, <math>\omega_x</math>, <math>\omega_y</math>, <math>\omega_z</math>.</b> </p>
<b>XSDEP</b>	<p> <b>E</b>, energy (in ev);  <b>EPRIM</b>, energy after the collision;  <b>CSTHT</b>, cosine of scattering angle;  <b>NCDB</b>, <b>NCDC</b> (see Section 11.3);  <b>ATWT</b>, atomic weight of interacting nuclide;  <b>NREG</b> = composition number;  <b>FLMDA</b>, number of mfp chosen;  <b>FMUTOT</b>, total cross section;  <b>RSF</b>, heating response function (joules/cm);  <b>JS</b>, index of energy-weight bin. </p>



<u>Label</u>	<u>Items in Order of Printout</u>
<b>RDEP</b>	Last random number used (octal).
<b>MAINP</b>	LAT, index of current latent-particle bundle; NN1, number of particles left in this bundle; IRR, number of transmissions due to particles which have reached boundaries of the over-all rectangular configuration; IPT, number of transmissions due to particles striking the transmission region; IQT, upper-limit history number in current statistical group; JR, current region-dependent weight index; JSP, index of energy-weight bin for EPRIM; JRP = JR for IRPRIM (next region); IANS = index in answer array S denoting where the sector-heating answers for the particular region start (nonzero if region is a sectorized cylinder); MSEC, used as initial address in answer array S for track-length flux answers for particular region; LSEC, number of sectors; KCYL, cylinder classification (1, 2, 3, or 4) established by CYLLOC; IRELT, reflection plane along trajectory (= 1, 2, 0, or undefined); NLR, problem type (30 or 360); IORG1T, origin of TAB1, relative to TAB3; XSI, last random number; XSB, random number last used to compute number of mfp.
<b>FAPC</b>	NSTAGE, number of stages; ZMINC, minimum z of stage 1; H, height of one stage; EPS, gap between stages; IS = 1 for source particle, 0 for nonsource; IPS = 1 for primary gamma, 2 for secondary gamma; IDET, number of the detector being scored; EST, incomplete secondary-gamma estimate.

### 11.7 OPERATING INSTRUCTIONS FOR ATHENA, RESTART OPTION, LIMITS ON PROBLEM SIZE

Specify (via INPUTD, cf. Chapter 10) first and last history numbers NFIRST and NLAST; also the number of histories per statistical group (IETAG). ATHENA decreases the value of NFIRST (if necessary) so that NFIRST corresponds to the start of a statistical group.

ATHENA computes until it encounters either (1) a source particle with a new history number in excess of the history number IQT required to complete the current group, at which point it completes the scoring for that group, updates IQT, and checks if the newest history number exceeds NLAST; or (2) a source particle with a negative history number (signaling the end of the source tape). In either case, the floating-point scores (heat, fluxes) in the current (unfinished) group are not included in the edit. Fixed-point counters (particle births, deaths, escapes, transmissions) do however include the events through the last trajectory computed.

Hence for a neutron problem which is to be followed by a corresponding secondary-gamma problem, specify an NLAST which is a few histories in excess of that corresponding to the required number of completed statistical groups in the secondary-gamma problem.

In general, a source tape should contain history numbers larger than needed to complete the last statistical group desired.

#### 11.7.1 Restarting a Terminated ATHENA Problem

An ATHENA problem terminates if:

1. The history number NLAST has been completed (normal termination); or
2. Sense Switch 6 (7 on CDC-1604-A) has been set; or
3. A tracking or interaction error has occurred; or
4. Other accidental termination (time limit exceeded, etc.).

The problem can be restarted (with certain restrictions) from terminations of types (2) and (4). The restart capabilities of the program for all cases are as follows.

1. A problem which has terminated normally (i.e., having completed the history NLAST specified in INPUTD, and/or reached the end of the source tape) cannot at present be restarted. Hence if the ultimate length of the problem is not known at the start, it is advisable to start with a large NLAST, or stop by a sense switch, and increase NLAST via INPUTD.
2. A problem terminated by sense switch 6 or 7 can be restarted with no further input. The appropriate tapes will be automatically repositioned, and the problem will continue. INPUTD need not be rerun unless NLAST is to be changed; in this case, enter a 1 as the restart option. These are the only input changes permitted on a restart; the other INPUTD cards may be omitted.
3. In general, true error stops are not recoverable.
4. On the IBM-7094 version only, ATHENA dumps its answers after every 500 histories (NFIRST + 499, NFIRST + 999, etc.). Hence, if a monitor (time-limit) termination occurs after at least one such dump, the main scoring problem can be restarted (no input required). At present this type of restart will not reposition the transmission or interaction tapes.

#### 11.7.2 Limitations on Problem Size

ATHENA uses variable dimensioning to utilize core storage space efficiently. The size of the answer arrays and the method of storage impose the following additional restrictions on the input parameters.

Let  $D$  = length of the cross-section table (printed out by DATORG; cf. Section 9.3)

$E$  = number of words needed for geometry data (the first item in the EZGEOM printout)

NREG = number of regions in the problem

IFAP = number of point detectors

IEB = number of energy bins for fluxes

NF = number of flux regions

$\Sigma(\text{LSEC})$  = total number of sectors, over all sectorized cylinders

NRDW = number of region-dependent weights

I2 = number of energy bins for energy importance sampling

NM = (NF) · (IEB) for neutron problems

= (NF) · (IEB) + NREG + IFAP · (IEB + 1) +  $\Sigma(\text{LSEC})$  for gamma problems.

Then if these quantities satisfy the following inequality, the ATHENA problem will fit in the machine:

$$D + E + 3 \cdot NM + 6 \cdot NREG + (4I2 + 1) + (IEB + 1) + NRDW \leq ND, \quad (81)$$

where ND = 15700 for CDC-1604-A;

= 15000 for IBM-7094 version without flux-at-a-point routines;

= 9500 for IBM-7094 version with flux-at-a-point routines.

A problem which is too large will be stopped in INPUTD or at the start of ATHENA, with a diagnostic printout; redefine the problem and rerun INPUTD and ATHENA.

As a guide in estimating the effects (on D and E) of simplifying the input, one may assume that each region adds about 12 words to E (14 for ORP, 12 for RPP or wedge, about 8 for cylinder, 6 for sphere). The size of the cross-section array for an 81-energy mesh is given by  $D = 81P + 324E$  for a gamma problem, where E is the number of distinct nuclides, and P is the number of compositions;  $D = 81P + \sum_i N_i$  for a neutron problem, where P is the number of compositions and  $N_i$  is the size of the array for nuclide i.

Table 3 gives the  $N_i$  and identifiers for several nuclides on the ATHENA neutron EDT.<sup>18</sup>

**TABLE 3 — NUCLIDE IDENTIFIERS (ATHENA NEUTRON DATA TAPES) AND SIZES OF NEUTRON DATA ARRAYS**

<u>Nuclide or Element</u>	<u>Identifier</u>	<u>Atomic Weight</u>	<u>N</u>
H	01001	1.000	324
Be	04100	9.013	687
C	06000	12.010	566
O	08000	16.000	500
U <sup>235</sup>	92235	235.0	724
U <sup>238</sup>	92238	238.0	850
Zr	40000	91.0	746
Al	13000	26.98	714
Cd	48000	112.41	324
W-182, dilute	74382	182.01	837
W-183, dilute	74383	183.01	837
W-184, dilute	74384	184.01	837
W-186, dilute	74386	186.01	837
W-182, homogenized	74482	182.01	837
W-183, homogenized	74483	183.01	837
W-184, homogenized	74484	184.01	837
W-186, homogenized	74486	186.01	837

Logical Input-Output Assignments for ATHENA

<u>IBM-7094</u>	<u>CDC-1604-A</u>	
5	5	Input medium (reader)
6	6	Output medium (printer)
1	1	Dump tape
4	8	Interaction tape
2	11	Source tape
3	14	Transmission tape

## 12. THE ATHENA-EDITING PROGRAM, STATC

This program reads back and edits the answers sent to the dump tape by ATHENA. It computes (1) the total number of histories, NHIST, in the completed statistical groups (gamma histories for primary gamma, neutron histories for neutron or secondary-gamma problems), (2) the region and sector volumes, and (3) standard deviations of the flux and heating scores. The region-dependent weights, which were not included in the ATHENA region scoring, are multiplied into all region and sector track lengths and heating.

The volumetric fluxes  $\phi(R,E)$  are computed as track length per unit volume (and per history) in each pertinent region R and energy bin E:

$$\phi(R,E) = \frac{S(R,E)}{V(R)} \cdot \frac{WT(R)}{NHIST}, \quad (82)$$

(for all specified flux regions; in each flux energy bin)

where S = track length

V = volume

WT = region weight.

Also edited (in gamma problems) are the heat deposition and heat deposition per unit volume in each region of the problem, and in sectors of specified cylinders. The accumulation of  $S(R,E) \times H(R,E)$  [where  $H(R,E)$  is the gamma heating response

function  $E\mu_a(E)$  in the appropriate composition] has been done in ATHENA. STATC retrieves these scores and incorporates the weight, volume, and history count as in Eq. 82.

The standard deviation of each track-length and heating answer is computed as follows.

In the ATHENA problem, pertinent scores are accumulated over groups of  $n$  histories each; there are  $G (=NHIST/n)$  groups, each contributing a group-score  $S_g$  to array S1 and  $(S_g)^2$  to array S2. For each score (heat, energy-bin track length) the standard deviation of the score per history is  $1/n$  times the standard deviation per group:

$$STD = \frac{1}{n} \frac{1}{\sqrt{G-1}} \sqrt{S_g^2 - (\bar{S}_g)^2} \quad (83)$$

Absolute and per cent deviations are printed out for all scores except the counters for particle escapes, etc.

In gamma problems with point detectors, for each such detector STATC retrieves and prints out heat per unit volume and energy-bin fluxes, along with their deviations. For neutron problems with point detectors, STATC prints out the detector locations to indicate that neutron-to-secondary-gamma estimation was done.

The printed output is generally self-explanatory; quantities are expressed in the following units.

1. Heat: joules/(neutron or gamma history)
2. Standard deviation: in same units as those of reference quantity (heat or track length)
3. Track length (T.L.): cm/history

4. Volume:  $\text{cm}^3$
5. Heat/v:  $(\text{joules}/\text{cm}^3)/\text{history}$ . Applies to regions and point detectors.
6. Energy: ev
7. Flux:  $(\text{neutrons or photons})/(\text{cm}^2\text{-history})$ . Applies to regions and point detectors.
8. Region particle counts: events (births, deaths, absorptions, or degradations)/region. Notes: (a) total is over all particle histories (may be in excess of last complete statistical group) without regard to weights; (b) source-particles introduced are counted as region births, as are particles generated in region importance sampling.
9. Energy particle counts: events (births or deaths)/(energy-importance bin). Notes: (a) above applies here also; (b) additional neutrons produced in  $(n,2n)$  reactions are counted as energy births.
10. Transmitted-particle count  $(N_1+N_2)$ :  $N_1$  = number of particles leaving the x,y,z limits of the configuration;  $N_2$  = number of particles striking the transmission region.

#### Logical Assignments for STATC

STATC requires the dump tape (as Logical 1) and two scratch tapes. Logical 5 and Logical 6 are reader and printer.



### 13. THE SECONDARY-GAMMA SOURCE PROGRAM, GASP

GASP is a program for generating secondary-gamma sources, given as input a neutron-interaction tape and gamma-production data for the pertinent nuclides. The program reads and recognizes both real and fake interactions (cf. Section 11.5), and converts these into correspondingly labeled source particles.

#### 13.1 REAL INTERACTIONS AND SECONDARY GAMMAS

For real interactions the operation of GASP is as follows. The pertinent nuclide and interaction type (absorption or inelastic scattering) are identified, and the pertinent gamma-production table is consulted (if needed data are absent, the program stops with an error printout). This table is a matrix with columns corresponding to output gamma energies, and rows corresponding to incident interacting-neutron energies; the elements of a row in this matrix represent expected numbers of secondary gammas produced per appropriate interaction of a neutron in the energy bin represented by this row. (These numbers are taken to be piecewise constant over the neutron energy bins.)

For a neutron absorption in a given nuclide, and in energy bin  $k$ , GASP attempts to produce secondary gammas from each column  $j$  of the appropriate matrix. Let a typical matrix element be  $N_{k,j}$ ; then the number of secondary gammas produced at energy  $E_j$  is:

$$\text{secondary } \gamma\text{'s at } E_j = N_{k,j} \cdot \frac{W_n(E_n) \cdot W_n(IR)}{W_\gamma(E_j) \cdot W_\gamma(IR)}; \quad (84)$$

where the W's are the energy and region weights used in the neutron and gamma problems.

The number of secondary gammas produced at  $E_j$  ( $j = 1, 2, \dots, L$ ) from this interaction is computed as the integral part of the above expression, augmented by 1 if a new random number is less than the fractional part. These are written out on the secondary-gamma source tape in VANGEN-compatible format. The history number is that of the original neutron history, and all the directions are chosen independently and isotropically. The particle coordinates and region are those of the neutron interaction.

Different data tables, but the same procedures, are used to process real inelastic-scattering records.

### 13.2 FAKE INTERACTIONS AND SECONDARY GAMMAS

A fake neutron interaction is identified by the nonzero detector number packed into its first word. GASP generates either zero or precisely one fake (detector-labeled) secondary particle as a result of each such interaction. The energy of the fake particle is taken to correspond to the  $j^{\text{th}}$  column of the appropriate GASP data matrix with probability proportional to the element  $N_{k,j}$ , i.e.,

$$p_j = N_{k,j} / \sum_j N_{k,j}.$$

(No particle is generated if the sum is zero.) GASP passes on to the source-particle tape for each fake particle: history number; detector number; coordinates; isotropic direction (not pertinent for fake particle); and the previously-generated neutron estimate (EST) multiplied by the sum  $\sum_j N_{k,j}$ .

The problem terminates when a history number = -1 is encountered, signaling the end of the interaction tape.

GASP prints out the input data and the last 100 generated source particles in format similar to the VANGEN printout; but each history number and region number are printed in octal format to display the detector numbers and EST values, respectively, packed in for fake particles.

Finally GASP prints out a tally of generated real and fake particles, by region and by energy-importance bin.

### 13.3 DESCRIPTION OF THE GASP INPUT

#### 1. Card 1, Columns 4,5

Number of nuclides ( $\leq 15$ ).

#### 2. Nuclide Gamma-Production Data

##### 2a. Nuclide Parameter Card (Format 5I5)

<u>Column</u>	<u>Item</u>
1-5	Nuclide identifier ZZABC
6-10	LA = number of absorption-gamma output energies (=0 if no capture gammas produced)
11-15	KA = number of incident-neutron energies (=number of neutron energy bins + 1). (=0 for no capture $\gamma$ )
16-20	LI = number of inelastic- $\gamma$ output energies
21-25	KI = number of corresponding neutron energy bins + 1.

##### 2b. Capture-Gamma Energies, in ev, ascending (Format 6E12.6) LA entries; six to a card.

##### 2c. Capture Neutron-Bin Energies, in ev, ascending (Format 6E12.6) KA entries; six to a card.

##### 2d. Capture-Gamma Numbers ( $N_{k,L}$ ) for each neutron bin, at each of the LA output energies, and for bins $k = 0, 1, 2, \dots, KA$ (Format 6E12.6). The first LA entries must be 0.0 representing the 0<sup>th</sup> bin. Start a new card for each neutron bin.

} Supply  
only if  
LA > 0

2e.-2f. Repeat items (2b-2d) for inelastic-scattering input (if LI > 0).

Repeat all data under (2) for each additional nuclide.

3. Weight-Parameters (Format 5I5)

<u>Column</u>	<u>Item</u>
1-5	Number of regions ( $\leq 200$ )
6-10	Number of distinct neutron region weights ( $\leq 200$ )
11-15	Number of distinct gamma region weights ( $\leq 200$ )
16-20	Number of neutron energy importance-sampling bins ( $\leq 199$ )
21-25	Number of gamma energy importance-sampling bins ( $\leq 109$ )

4. Distinct Neutron Region Weights (Format 5E14.4)

Five to a card

Note: different format from VANGEN input.

5. Distinct Gamma Region Weights (Format 5E14.4)

Five to a card

Note: different format from VANGEN input.

6. Neutron Region-Weight Indices (Format 14I5)

14 entries to a card, one entry for each region. Index L in the K<sup>th</sup> field of this array assigns to region K the L<sup>th</sup> entry in array (4).

7. Gamma Region-Weight Indices (Format 14I5)

One entry per region, as in (6). Indices refer to array (5).

8. Neutron Energy-Importance Data

8a. Minimum energy (ev) of each bin, and bin weight. (Format 2E20.8).

One card per bin, lowest first.

8b. Maximum energy (ev) of last bin (Format E20.8).

9. Gamma Energy-Importance Data

Gamma bin energies and weights as for neutrons (Format 2E20.8).

Note: since the GASP nuclide data give rise to secondary gammas with  $E \leq 10$  Mev, the highest bin energy should be  $\geq 10^7$ .

### 13.4 LIMITATION ON GASP PROBLEM SIZE

Let LA, KA, LI, and KI denote the quantities on card (2a) of the GASP input, for a given nuclide.

Then if

$$\sum_{\text{nuclides}} [(LA) \times (KA-1) + LA + (KA-1) + (LI) \times (KI-1) + LI + (KI-1)] \leq 10,000$$

the problem can be run.

Logical Input-Output Assignments for GASP

<u>IBM-7094</u>	<u>CDC-1604-A</u>	
5;6	5;6	Reader; printer
2	8	Interaction tape
4	11	Secondary-gamma tape

#### 14. THE NEUTRON ABSORPTION TALLY PROGRAM, NATALE

NATALE is another program designed to extract additional information from the neutron interaction tape. The real absorptions can be tallied (and/or converted via input response functions into tallied estimates of the fissioning density, neutron activation, etc.) in various regions, nuclides, and energy ranges. The output tallies (absorptions, weighted absorptions) may be called for as functions of neutron energy or may be summed over all energies. There may be several response functions  $R_i(E_n)$  in a given problem, each associated with a nuclide; each nuclide may have more than one response function.

Any response is computed as

$$\{ \text{Response}_i \} = \sum_{\{ \text{absorptions} \}} (\text{RWT})_k \cdot (\text{EWT})_j \cdot R_i(E) \quad (85)$$

where  $(\text{RWT})_k$  is the neutron region weight in the pertinent region,  $(\text{EWT})_j$  is the neutron energy weight in the pertinent energy bin, and  $R_i(E)$  is the value of the  $i^{\text{th}}$  response function at the energy of absorption (R obtained by linear interpolation in input table of  $R_i$  vs E). The braces  $\{ \}$  denote either restriction to a limited energy range, or summation over all energies, on both sides of the equation.

For tallies of absorptions (with or without breakdown into energy bins) the factor  $R_i(E)$  is suppressed.

#### 14.1 NATALE OPTIONS (1-4)

Any or all of the following types of output are available, subject to the limitation (Eq. 86).

##### Option 1

For each of a number N1 of specified isotopes, count and print the total absorptions in each region of the problem.

##### Option 2

For each of a number N2 of specified isotopes, count and print the total of response-function-weighted absorptions in each region of the problem.

##### Option 3

For each of a number N3 of specified isotopes, and in each of a specified number NREG1 of regions, count and print the total absorptions on a specified output energy mesh. Note: only one output energy mesh per problem.

##### Option 4

For each of a number N4 of specified isotopes, and with the same region limitations and output energy mesh as in Option 3, count and print total of response-function-weighted absorptions as a function of energy.

Note that each associated pair (isotope + response function) contributes to the count of N1, N2, N3, or N4; i.e., the N2 isotopes counted for Option 2 (or the N4 in Option 4) are not necessarily distinct.

#### 14.2 DESCRIPTION OF THE INPUT FOR NATALE

##### 1. Option Counts: IOP1 ( $\equiv$ N1 + N2), IOP2 ( $\equiv$ N3 + N4); (Format 2I5)

<u>Column</u>	<u>Item</u>
1-5	IOP1 = total number of isotopes, Options 1 and/or 2
6-10	IOP2 = total number of isotopes, Options 3 and/or 4.

Notes: (a) If an isotope is described for both Options 1 and 2, it must appear twice and be counted twice (more times if several response functions in Option 2 pertain to this isotope). Similarly for Options 3 and 4.  
 (b)  $IOP1 + IOP2 \leq 90$ .

## 2. Neutron Weight Data (Format 3I5)

<u>Column</u>	<u>Item</u>
1-5	IRMAX = total number of regions in neutron ATHENA problem ( $\leq 200$ )
6-10	NRDWN = number of distinct neutron region-dependent weights
11-15	IE2 = number of neutron energy-weight bins.

## 3. Distinct Neutron Region-Dependent Weights

WNE(L), L = 1, ..., NRDWN (Format 5E14.5).

## 4. Neutron Region-Weight Indices

IWTN(K), K = 1, ..., IRMAX (Format 14I5).

## 5. Neutron Energy-Importance Data

5a. Minimum energy (ev) of each bin, and bin weight (Format 2E20.9).  
 One card per bin, lowest first.

5b. Maximum energy (ev) of last bin (Format E20.9).

## 6. Option and Response Function Data (Options 1 and 2)

(Supply only if  $IOP1 > 0$ .) There are IOP1 packets of data, packet (6a or 6a, b, c) for each isotope in Options 1, 2.

6a. IDEL, MENG C (Format 2I5); IDEL is the 5-digit isotope identifier, MENG C is the number of energy points at which the response function is tabulated. (MENG C = 0 means Option 1,  $>0$  Option 2 in these data.)

6b. Energy points at which this response function is given:  $E_n(J)$ , J = 1, ..., MENG C (Format 5E14.5).  
 Energies in ev, ascending.

6c. Response function R(J), J = 1, ..., MENG C at corresponding energies. (Format 5E14.5.)

} Supply  
 only if  
 MENG C > 0

Repeat 6a (or 6a-6c) for each succeeding member of the IOP1 group.  
 Packets for Options 1 and 2 may be intermixed, but the edit is clearer if they are not.



### 7. Parameters for Options 3 and 4

Supply items (7) and (8) only if IOP2 > 0.

The following cards (7a-7c) are supplied only once; they limit the output for all the Options 3, 4.

#### 7a. NREG1, IGE2 (Format 2I5)

NREG1 = number of scored regions, and IGE2 = number of output energy bins for scoring.

#### 7b. Scored-Region Numbers

IOUT(J), J = 1, ..., NREG1 (Format 14I5).

#### 7c. Energies Defining Output Bins

GE2(L), L = 1, ..., (IGE2 + 1). In ev, ascending (Format 5E14.5).

### 8. Option and Response Function Data (Options 3 and 4)

IOP2 packets of data; format identical to 6a or 6a-6c. MENG C = 0 means Option 3, >0 means Option 4.

## 14.3 NATALE OUTPUT

The input deck will be printed as it appears, then the statement **LAST SOURCE = XXX**. XXX is the particle number of the last history encountered. The output for Option 1 and/or 2 follows if it has been specified. Next the Option 3 and/or 4 output is edited, if the option has been specified. The output consists of matrices, the columns representing isotopes in the order specified in the input. The rows represent regions. Any row that has a zero response for each isotope will be eliminated.

## 14.4 LIMITATION ON PROBLEM SIZE

The answers tallied by NATALE are stored consecutively in an array of 15,000 words. If

$$2 * \left\{ \sum_{\substack{\text{all} \\ \text{response} \\ \text{functions}}} (\text{MENG C}) \right\} + \text{IOP1} \cdot \text{IRMAX} + \text{NREG1} \cdot \text{IOP2} \cdot \text{IGE2} \leq 15,000 \quad (86)$$

the NATALE problem can be run.

**Logical Assignments for NATALE**

The interaction tape is Logical 2 (IBM-7094) or Logical 8 (CDC-1604-A). Units 5 and 6 are reader and printer.

**FINIS**

## 15. REFERENCES

1. Eisenman, B. and Nakache, F. R.: UNC-SAM: A FORTRAN Monte Carlo System for the Evaluation of Neutron or Gamma-Ray Transport in Three-Dimensional Geometry, UNC-5093 (Aug. 31, 1964).
2. Goldstein, H.: GENDA Li Inelastic Spectrum, UNC internal memo, Phys/Math 2019 (June 30, 1961). (Unpublished.)
3. Troubetzkoy, E. S.: Revision of Inelastic Scattering of Neutrons by Beryllium, UNC internal memo, Phys/Math 1222 (Oct. 19, 1959). (Unpublished.)
4. Goldstein, H. and Mechanic, H.: UNC memo 2092-9 (1958).
5. Lustig, H. and Kalos, M.: UNC internal memo, Phys-657 (1958). (Unpublished.)
6. Cranberg, L. et al.: Phys. Rev., 103:662 (1956).
7. Kalos, M. H.: A Rejection Technique for the Fission Neutron Spectrum, UNC internal memo, Phys. 345 (Feb. 17, 1958). (Unpublished.)
8. Celnik, J. and Spielberg, D.: Gamma Spectral Data for Shielding and Heating Calculations, NASA CR-54794 (UNC-5140) (Nov. 1965).
9. Brysk, H.: Sphere Tracking, UNC internal memo, Phys/Math 4036 (Feb. 10, 1965) and Phys/Math 4175 (Apr. 13, 1965). (Both unpublished.)
10. Brysk, H.: Vertical Cylinder Tracking, UNC internal memo, Phys/Math 4178 (Apr. 13, 1965). (Unpublished.)
11. Brysk, H. and Spielberg, D.: Scoring a Sectorized Cylindrical Shell, UNC internal memo, Phys/Math 4067 (Feb. 25, 1965) and Phys/Math 4176 (Apr. 13, 1965). (Both unpublished.)
12. Brysk, H.: Reflection Subroutines, UNC internal memo, Phys/Math 4112 (Mar. 15, 1965). (Unpublished.)
13. Kahn, H.: Application of Monte Carlo, the RAND Corporation, AECU-3159 (1954).

14. Kalos, M. H.: On the Estimation of Flux at a Point by Monte Carlo, Nuclear Sci. and Eng., 16:1 (May 1963).
15. Ibid. Reference 1, p. 113.
16. Kalos, M. H.: Secondary Gamma Ray Flux at a Point, UNC internal memo, Phys/Math 3241 (Nov. 22, 1963). (Unpublished.)
17. Kalos, M. H.: Further Remarks on Secondary Gamma Ray Flux at a Point, UNC internal memo, Phys/Math 4095 (Mar. 8, 1965). (Unpublished.)
18. Guber, W.: Size of the Cross-Section Tables Used in the Monte Carlo Programs, UNC internal memo, Phys/Math 3805 (Oct. 26, 1964). (Unpublished.)

## **DISTRIBUTION**

### **MANDATORY**

#### **All Reports**

<u>Recipient</u>	<u>Address</u>
Concerned NASA Lewis Research Center program manager (3 & reproducible)	NASA Lewis Research Center 21000 Brookpark Road Cleveland, Ohio 44135 Attention: Walter A. Paulson, MS 49-2
Concerned NASA Lewis Research Center contracting officer (1)	NASA Lewis Research Center 21000 Brookpark Road Cleveland, Ohio 44135 Attention: T. J. Flanagan Contracting Officer, MS 500-210
Concerned NASA Lewis Research Center technical utilization office (1)	NASA Lewis Research Center 21000 Brookpark Road Cleveland, Ohio 44135 Attention: Technical Utilization Office, MS 3-16
NASA Headquarters technical information abstracting and dissemination facility (6 & reproducible)	NASA Scientific and Technical Information Facility Box 5700 Bethesda, Md. Attention: NASA Representative
Lewis Library (2)	NASA Lewis Research Center 21000 Brookpark Road Cleveland, Ohio 44135 Attention: Library
Lewis Technical Information Division (1)	NASA Lewis Research Center 21000 Brookpark Road Cleveland, Ohio 44135 Attention: Report Control Office

### **Reports with Nuclear Content**

**U. S. Atomic Energy Commission (3)  
Technical Reports Library  
Washington, D. C.**

**U. S. Atomic Energy Commission (3)  
Technical Information Service Extension  
P. O. Box 62  
Oak Ridge, Tenn.**

### **APPROPRIATE**

<u><b>Recipient</b></u>	<u><b>Address</b></u>
<b>NASA Headquarters program office (2)</b>	<b>National Aeronautics and Space Admin- istration Washington, D. C. 20546 Attention: NPO</b>
<b>Westinghouse Electric Corp. (1)</b>	<b>Westinghouse Electric Corp. Astronuclear Laboratory Box 10864 Pittsburgh, Pennsylvania 15236</b>
<b>General Dynamics Corp. (1)</b>	<b>General Dynamics Corp. General Atomic Division P. O. Box 608 San Diego, California 92112 Attention: John T. Iles</b>
<b>North American Aviation (1)</b>	<b>North American Aviation, Inc. Atomics International Division 8900 Desota Avenue Canoga Park, California</b>
<b>General Electric Co. (1)</b>	<b>General Electric Company Nuclear Materials &amp; Propulsion Opera- tions P. O. Box 15132 Evandale, Ohio 45215 Attention: E. B. Delson</b>

<u>Recipient</u>	<u>Address</u>
Lewis Research Center staff members (1 copy to each)	NASA Lewis Research Center 21000 Brookpark Road Cleveland, Ohio 44135 Attention: Nuclear Rocket Technology Office, MS 54-1 Mr. Leroy V. Humble, MS 49-2 Mr. Samuel J. Kaufman, MS 49-2 Mr. Edward Lantz, MS 49-2 Mr. Irving M. Karp, MS 49-2 Mr. Leonard Soffer, MS 500-201 Mr. Millard L. Wohl, MS 49-2 Dr. John C. Liwosz, MS 501-2 Mr. Gerald P. Lahti, MS 49-2 Mr. Michael J. Kolar, MS 49-2
Combustion Engineering, Inc. (1)	Combustion Engineering, Inc. Prospect Hill Road Windsor, Conn.
Babcock-Wilcox Research Center (1)	Babcock-Wilcox Research Center P. O. Box 835 Alliance, Ohio Attention: Mr. Blazer
Aerojet-General Nucleonics (1)	Aerojet-General Nucleonics P. O. Box 77 San Ramon, California 94583 Attention: R. W. Durante
United Aircraft Corp. (1)	United Aircraft Corp. Pratt & Whitney Aircraft Division 400 Main Street E. Hartford, Conn. Attention: W. J. Leuckel
Radiation Shielding Information Center (1)	Radiation Shielding Information Center Oak Ridge National Laboratory Post Office Box X Oak Ridge, Tennessee 37831 Attention: Mrs. Betty F. Maskewitz
Argonne National Laboratory (1)	Argonne National Laboratory Argonne, Illinois 60440 Attention: Dr. Marshall Grotenhuis

<u>Recipient</u>	<u>Address</u>
University of California (1)	University of California Los Alamos Scientific Laboratory Post Office Box 1663 Los Alamos, New Mexico 87544 Attention: Mr. R. E. Malenfant
Lewis Office of Reliability and Quality Assurance (1)	NASA Lewis Research Center 21000 Brookpark Road Cleveland, Ohio 44135 Attention: Office of Reliability and Quality Assurance
Ames Research Center (1)	NASA Ames Research Center Moffett Field, California 94035 Attention: Library
Flight Research Center (1)	NASA Flight Research Center P. O. Box 273 Edwards, California 93523 Attention: Library
Goddard Space Flight Center (1)	NASA Goddard Space Flight Center Greenbelt, Md. 20771 Attention: Library
Jet Propulsion Laboratory (1)	Jet Propulsion Laboratory 4800 Oak Grove Dr. Pasadena, California 91103 Attention: Library
Langley Research Center (1)	NASA Langley Research Center Langley Station Hampton, Va. 23365 Attention: Library
Marshall Space Flight Center (1)	NASA Marshall Space Flight Center Huntsville, Alabama 35812 Attention: Library
Western Operations (1)	NASA Western Operations 150 Pico Blvd. Santa Monica, California 90406 Attention: Library